

Universität Konstanz

# **Signaling and Redox Regulation by Nitric Oxide, Superoxide and Carbon Monoxide**

Dissertation

zur Erlangung des akademischen Grades des  
Doktors der Naturwissenschaften (Dr. rer. nat.)

an der Universität Konstanz,

Fachbereich Biologie

vorgelegt von

**Daniel Frein**

Tag der mündlichen Prüfung: 18. Dezember 2006

Referent: Prof. Dr. Volker Ullrich

Referent: Prof. Dr. Peter Kroneck

# Danksagung

Die vorliegende Arbeit wurde zwischen Januar 2003 und August 2006 unter der Leitung von PROF. DR. VOLKER ULLRICH am Lehrstuhl für Biochemie im Fachbereich Biologie der Universität Konstanz angefertigt.

Mein Dank gebührt daher Herrn PROF. DR. VOLKER ULLRICH, der mit seinen zahlreichen Ideen und Anregungen, den fruchtbaren wissenschaftlichen Diskussionen und seiner andauernden Unterstützung deutlich mehr als nur die Rahmenbedingungen für diese Arbeit schuf.

Den Kollegen meiner Arbeitsgruppe, im Besonderen DR. MARKUS BACHSCHMID, danke ich für die wertvolle Unterstützung bei allen Aspekten der wissenschaftlichen Arbeit. Danken möchte ich VERA LORENZ und REGINA HÖLZ, die mir besonders bei der Primärzellkultur eine große Hilfe waren. Bei der Sekretärin des Lehrstuhls, Frau GISELA NASCHWITZ, bedanke ich mich neben ihrer wertvollen Unterstützung für die motivierenden Worte.

Mein Dank gilt auch DR. ANDREAS DAIBER, der mich für das Thema begeisterte und mir auch nach dem Ausscheiden aus der Arbeitsgruppe mit Rat und Tat zur Seite stand.

DR. DENNIS STUEHR von der Cleveland Clinic Foundation (Cleveland, Ohio), der die •NO-Synthesen und sein Fachwissen beisteuerte, danke ich herzlich.

DR. HARRY ISCHIROPOULOS vom Children's Hospital of Philadelphia, danke ich für die Vorarbeiten zur CO-Wirkung.

DR. REINHARD KISSNER und PROF. DR. WILLEM KOPPENOL von der ETH Zürich danke ich für die erfolgreiche Zusammenarbeit und die inspirierenden Gespräche zur Chemie des Peroxynitrits.

An dieser Stelle möchte ich mich auch bei den vielen anderen Menschen bedanken, die durch ihre Hilfe und Unterstützung diese Arbeit ermöglicht haben. Mein größter Dank gilt meinen Eltern – ohne Eure stete Unterstützung und Euer Vertrauen würde diese Arbeit nicht existieren.

CHRISTINA, nicht nur Deine Geduld und der Glaube an mich waren wunderbar – vielen Dank für alles.

Zu guter Letzt gilt mein Dank auch der Deutschen Forschungsgemeinschaft (DFG), die diese Arbeit durch ihre finanzielle Unterstützung ermöglichte.

# Abbreviations

3-NT	3-Nitrotyrosine
ADH	Alcohol dehydrogenase
Ang II	Angiotensin II
Arg	L-Arginine
ALR2	Aldose reductase (aldehyde reductase 2)
ALS	Amyotrophic lateral sclerosis
BAEC	Bovine aortic endothelial cells
BCA	Bicinchoninic acid
BH <sub>4</sub>	Tetrahydrobiopterin
BK <sub>Ca</sub>	Big-conductance Ca <sup>2+</sup> -activated K <sup>+</sup> channel
BSA	Bovine serum albumin
CaM	Calmodulin
CBS	Cystathionine $\beta$ -synthase
cGMP	Cyclic guanosine monophosphate
CSE	Cystathionine $\gamma$ -lyase
Cys	L-Cysteine
CysNO	L-S-Nitrosocysteine (SNOC)
DAF-2 DA	DAF-2 diacetate, 4,5-diaminofluorescein diacetate
DAN	2,3-Diaminonaphthalene
deoxyHb	Deoxyhemoglobin (unliganded ferrous Hb)
DMSO	Dimethyl sulphoxide
DTNB	5,5'-Dithio-bis(2-nitrobenzoic acid), Ellman's reagent
DTPA	Diethylenetriaminepentaacetic acid
DTT	Dithiothreitol
EDRF	Endothelium derived relaxing factor ( $\bullet$ NO)
EDTA	Ethylenediamine tetraacetic acid
EPR	Electron paramagnetic resonance spectroscopy
ESI	Electrospray ionisation
EtOH	Ethanol
FAD	Flavin adenine dinucleotide
FMN	Flavin mononucleotide
FPLC	Fast protein liquid chromatography
Grx	Glutaredoxin
GSH	Glutathione, reduced
GSNO	S-Nitrosoglutathione
GSSG	Glutathione, oxidized
Hb	Hemoglobin
HbNO	Nitrosylhemoglobin
HbSNO	S-Nitrosohemoglobin

## Abbreviations

HO	Heme oxygenase
HPLC	High pressure liquid chromatography
HUVEC	Human vascular endothelial cells
IC <sub>50</sub>	Half-maximal inhibition concentration
IRP-1	Iron regulatory protein-1
LC/MS	Liquid chromatography/mass spectroscopy
LMW	Low-molecular-weight
L-NAME	<i>N</i> <sup>ω</sup> -Nitro-L-arginine methyl ester
Mb	Myoglobin
metHb	Methemoglobin (ferric Hb)
mtNOS	Mitochondrial NOS
NAT	2,3-Naphthotriazole
NOHA	<i>N</i> <sup>ω</sup> -Hydroxy-L-arginine
NOS	Nitric oxide synthase
NOS-1	Neuronal NOS (nNOS)
NOS-2	Inducible NOS (iNOS)
NOS-3	Endothelial NOS (eNOS)
NOX	NADPH oxidase
oxyHb	Oxyhemoglobin (oxygenated ferrous Hb)
PG	Prostaglandin
PGHS-2	Prostaglandin H synthase-2
PGI <sub>2</sub>	Prostacyclin
PN	Peroxynitrite
ppm	parts per million
PTP	Permeability transition pore
RLU	Relative light unit
RNS	Reactive nitrogen species
ROS	Reactive oxygen species
SD	Standard deviation
sGC	Soluble guanylate cyclase
SIN-1	3-Morpholino-sydnonimine
SMC	Smooth muscle cells
SNAP	<i>N</i> -(Acetyloxy)-3-nitrosothiovaline
SNP	Sodium nitroprusside
SOD	Superoxide dismutase
SOD1	Cu,Zn-SOD, cytosolic
SOD2	Mn-SOD, mitochondrial
SOD3	EC-SOD, extracellular Cu,Zn-SOD
TCA	Tricarboxylic acid
TLC	Thin-layer chromatography
Trx	Thioredoxin
Tx	Thromboxane
VEGF	Vascular endothelial growth factor
VSMC	Vascular smooth muscle cells
w/o	without
XO	Xanthine oxidase
YC-1	1-Benzyl-3-(5-hydroxymethyl-2-furyl)indazole

# Publications

Results from this work were published in the following articles:

A. Daiber, **D. Frein**, D. Namgaladze and V. Ullrich:  
Oxidation and nitrosation in the nitrogen monoxide/superoxide system.  
*J Biol Chem.* 2002;277(14):11882–11888.

V. Ullrich, D. Namgaladze and **D. Frein**:  
Superoxide as inhibitor of calcineurin and mediator of redox regulation.  
*Toxicol Lett.* 2003;139(2–3):107–110.

A. Daiber, M. Bachschmid, C. Kavaklí, **D. Frein**, M. Wendt, V. Ullrich and T. Münzel:  
A new pitfall in detecting biological end products of nitric oxide – nitration, nitros(yl)ation and nitrite/nitrate artefacts during freezing.  
*Nitric Oxide.* 2003;9(1):44–52.

A. Daiber, M. Bachschmid, **D. Frein** and V. Ullrich:  
Reply to "Trouble with the analysis of nitrite, nitrate, S-nitrosothiols, and 3-nitrotyrosine: freezing-induced artifacts".  
*Nitric Oxide.* 2004;11(3):214–215.

**D. Frein**, S. Schildknecht, M. Bachschmid and V. Ullrich:  
Redox regulation: A new challenge for pharmacology.  
*Biochem Pharmacol.* 2005;70(6):811–823.

If not otherwise indicated, all experiments presented within this work are performed by the author himself.

# Contents

<b>Acknowledgments</b>	<b>i</b>
<b>Abbreviations</b>	<b>ii</b>
<b>Publications</b>	<b>iv</b>
<b>1 Introduction</b>	<b>1</b>
<b>2 Aims of the Study</b>	<b>6</b>
<b>3 The Role of Small Signaling Molecules in the Vascular System</b>	<b>8</b>
3.1 Reactive Oxygen Species . . . . .	8
3.1.1 Superoxide . . . . .	9
3.1.2 Hydrogen Peroxide and the Hydroxyl Radical . . . . .	11
3.2 Nitric Oxide . . . . .	12
3.2.1 Nitric Oxide Synthases . . . . .	15
3.3 Peroxynitrite . . . . .	20
3.4 The Nitric Oxide/Superoxide System . . . . .	21
3.4.1 Reaction of Carbon Dioxide with Peroxynitrite . . . . .	25
3.5 Redox Regulation by the Nitric Oxide/Superoxide System . . . . .	27
3.5.1 Nitrosylation . . . . .	27
3.5.2 Nitrosation . . . . .	29
3.5.3 Oxidations by Peroxynitrite . . . . .	41
3.5.4 Oxidations by an Excess of Superoxide . . . . .	45
3.5.5 Oxidations by Hydrogen Peroxide . . . . .	46
3.6 Carbon Monoxide . . . . .	47
3.7 Hydrogen Sulfide . . . . .	52
<b>4 Materials and Methods</b>	<b>54</b>
4.1 Chemicals . . . . .	54
4.1.1 <i>S</i> -Nitrosoglutathione Synthesis . . . . .	55
4.1.2 <i>S</i> -Nitrosoalbumin Synthesis . . . . .	56
4.2 Methods . . . . .	57
4.2.1 CO Treatment of Rats . . . . .	57
4.2.2 NOS Spectra . . . . .	57
4.2.3 [ <sup>14</sup> C]Arginine NOS Assay . . . . .	58
4.2.4 Griess Assay . . . . .	58
4.2.5 Alcohol Dehydrogenase Activity Test . . . . .	59
4.2.6 Quantification of 4-Nitrosophenol . . . . .	60

## Contents

4.2.7	Oxyhemoglobin Assay . . . . .	60
4.2.8	Cytochrome c Assay . . . . .	60
4.2.9	<i>N</i> -Nitrosation of 2,3-Diaminonaphthalene . . . . .	61
4.2.10	GSH Oxidation . . . . .	62
4.2.11	<i>S</i> -Nitrosation of Albumin during Freezing . . . . .	62
4.2.12	<i>N</i> -Nitrosation of 2,3-Diaminonaphthalene during Freezing . . . . .	63
4.2.13	Kinetic Simulation . . . . .	63
4.2.14	Software . . . . .	64
4.2.15	Statistical Analysis . . . . .	64
<b>5</b>	<b>Results and Discussion</b>	<b>65</b>
5.1	Interaction between CO and NOS-1 . . . . .	65
5.2	Inactivation of Alcohol Dehydrogenase by Peroxynitrite . . . . .	81
5.2.1	<i>C</i> -Nitrosation of Phenol . . . . .	87
5.3	Mechanism of Nitrosation in the Nitric Oxide/Superoxide System . . . . .	90
5.3.1	<i>N</i> -Nitrosation of 2,3-Diaminonaphthalene . . . . .	90
5.3.2	Effect of Azide on 2,3-Diaminonaphthalene Nitrosation . . . . .	93
5.4	Effect of CO <sub>2</sub> on the Chemistry in the Nitric Oxide/Superoxide System . . . . .	96
5.5	Nitration and Nitrosation During Freezing of Samples . . . . .	100
5.5.1	<i>S</i> -Nitrosation of Albumin . . . . .	100
5.5.2	<i>N</i> -Nitrosation of 2,3-Diaminonaphthalene . . . . .	102
5.6	Kinetic Simulation of the Nitric Oxide/Superoxide System . . . . .	105
<b>6</b>	<b>Conclusions</b>	<b>119</b>
6.1	A Model for Redox Regulation by <i>S</i> -Nitrosation in the Cell . . . . .	121
<b>7</b>	<b>Summary</b>	<b>132</b>
<b>8</b>	<b>Zusammenfassung</b>	<b>134</b>
	<b>References</b>	<b>137</b>

# 1 Introduction

Redox chemistry is fundamental to life since energy in biological systems is stored and released by means of redox reactions. Only electron or hydrogen transfer are associated with changes in free energy sufficient to drive the vast demand for ATP production in higher organisms. Therefore it was no surprise to find regulation of oxygen supply and the control of mitochondrial and glycolytic pathways controlled by redox reactions. Current perspectives favor evidence for the existence of a redox-based network of regulatory mechanisms that are intimately linked to cellular function and, in diseased states, to malfunction of these mechanisms linked with the phenomenon of “oxidative stress”.

Enzymes catalyzing redox reactions, so-called oxidoreductases, are representing the first of the six main groups of enzymes. This enzymatic property is usually reflected by the presence of iron or other metal atoms at the enzyme’s active site and their dependence on cofactors like  $\text{NAD}^+$ ,  $\text{NADP}^+$ , FAD and FMN. Such cofactors are universal electron carriers and can be oxidized and reduced in a reversible manner. Therefore the balance between  $\text{NAD}^+/\text{NADH}$  and  $\text{NADP}^+/\text{NADPH}$  not only reflects the cellular redox state, it even defines the redox state of a biological system.

The cellular redox systems are considered to be tightly coupled and therefore every change in the cellular redox state is reflected in changes of several sets of metabolites. Especially glutathione (GSH) and the thioredoxin (Trx) and glutaredoxin (Grx) systems [2] are very sensitive to changes in cellular NADPH levels, as illustrated in



## 1 Introduction

reduced state; by acting as an electron donor, GSH reduces disulfide bonds of oxidized thiols back to cysteines. Therefore glutathione needs to be present almost exclusively in its reduced form; this is maintained by the NADPH-dependent enzyme glutathione reductase, which is constitutively active and inducible upon oxidative stress. Persistent oxidative stress in a cell leads to changes in the ratio of reduced to oxidized glutathione towards GSSG and this usually is a measure of cellular toxicity. If the cell's reductive power gets lost, which means oxidative stress and low levels of NADPH and GSH, oxidative damage and finally cell death should occur.

The term “oxidative stress” [3] defines a disturbed redox equilibrium with pathophysiological consequences. In this case, the main cellular redox systems undergo shifts to their oxidized state, cellular antioxidants like L-ascorbic acid, carotinoids, lipoic acid, uric acid, glutathione and  $\alpha$ -tocopherol become exhausted and protective enzymatic activities, e.g. catalase, superoxide dismutase, glutathione peroxidase will be inactive or overridden. The cell cannot withstand these oxidative conditions if they remain over long time periods. In that case of a breakdown of both reductive and repair mechanisms, the cell cannot reverse these oxidative reactions and therefore this represents a pathophysiological situation. As a consequence, toxic oxidizing and oxidized compounds like lipid hydroperoxides, oxidized proteins, damaged DNA, hydrogen peroxide and various oxygen radicals are accumulating in the cell. The emergence of these products of oxidative damage and their measurement leads to a phenomenological definition of oxidative stress.

Unlike oxidative stress, “redox regulation” or “redox signaling” describes a reversible phase of physiological regulatory reactions occurring over shorter time periods. In such circumstances, the oxidative reactions leading to posttranslational protein modification (*S*-glutathiolation, *S*-nitrosation, methionine sulfoxidation, zinc finger oxidations with disulfide formation) or to changes in the oxidation state of metals (prostaglandin endoperoxide synthase [4], calcineurin [5], guanylate cyclase [6]) are returned to the resting state by reductive pathways. The requirement for reduction and the implication

## 1 Introduction

that the oxidative event has regulatory consequences delineates redox regulation from “oxidative” stress, where the latter is not reversible for the cell and where the term “stress” indicates a deviation from the normal physiological state. Diabetes, atherosclerosis, hypertension, sepsis, ischemia-reperfusion and neurodegenerative diseases such as Alzheimer’s disease, amyotrophic lateral sclerosis (ALS) or Parkinson’s disease all have a strong component of oxidative stress. It remains unclear, however, whether the oxidative stress is causal in disease progression or the result of the cell death associated with cells dying by necrosis.

With the discovery of the radical nitric oxide ( $\bullet\text{NO}$ ) as an ubiquitous cellular messenger this picture changed and together with superoxide ( $\text{O}_2^{\bullet-}$ ) a more complex scenario became apparent. Now it is well accepted that both reductive and oxidative pathways are responsible for the sophisticated processes regulating cellular processes and even organ functions.

Redox reactions form a complex network of redox signaling, directly coupled and intrinsically tied to the regulation of cellular function such as oxygen supply and control of mitochondrial and glycolytic pathways. Under pathophysiological conditions, these regulatory mechanisms are then also involved in malfunction of cellular energy metabolism. This leads not only to cell damage, but in many cases this will affect the organism as a whole.

Within the scope of this work, several open questions in the chemistry of redox regulation will be addressed with regard to a physiological situation. Carbon monoxide (CO) and  $\bullet\text{NO}$  are both gaseous molecules, which are acting as messengers at low concentrations. Both have enzymatic sources in all higher organisms and, in the case of  $\bullet\text{NO}$ , the relevant signaling pathways are known and well-investigated. The opposite applies to CO, whereas besides its toxic effects at higher concentrations many regulatory effects are documented, but in most cases the underlying mechanisms are

## 1 Introduction

remaining unknown. A working hypothesis, where CO acts through activation of •NO biosynthesis, will be investigated to find an explanation for observed effects of CO.

The oxidation of zinc finger proteins in the •NO/O<sub>2</sub><sup>•-</sup> system as a relevant mechanism of inactivation was discovered to occur via peroxynitrite, as opposed to the mechanism discussed in literature. During these investigations, a reaction of •NO with superoxide was observed, which leads to a nitrosating intermediate. A reaction of •NO with peroxynitrous acid has been denied in previous publications but would allow to explain the mechanism of *S*-nitrosothiol formation in the organism. *S*-Nitrosation results in changes in activity of some key enzymes for cellular energy metabolism as well as for regulation of cellular redox systems, but the main mechanism for its *in vivo* formation was lacking until now. We postulate here that *S*-nitrosation may signal the transition to conditions of oxidative stress, and therefore, this signal is used to prepare the cell to such threatening conditions. In context of the newly discovered reaction between O<sub>2</sub><sup>•-</sup> and an excess of •NO, the chemistry in the •NO/O<sub>2</sub><sup>•-</sup> system will be put in a hypothetical model which explains the transition of cellular redox regulation towards oxidative stress. This model will be further discussed and linked with diseases where these otherwise meaningful regulatory mechanisms lead to cell damage.

## 2 Aims of the Study

Redox regulation of enzymes represents an emerging topic in current literature, but both the chemical mechanisms behind the oxidative modifications of amino acids and the consequences for metabolic pathways and physiological changes of the cell are far from being understood. The aim of this work is to provide both a more detailed and comprehensive idea about redox regulation by the combined action of nitric oxide ( $\bullet\text{NO}$ ) and superoxide ( $\text{O}_2^{\bullet-}$ ) and the investigation of the interplay between these systems with the newly discovered signaling by carbon monoxide (CO):

- Low doses of CO are reported to cause beneficial effects in the organism during conditions of imbalance in the cellular redox systems. The observed effects resemble those of  $\bullet\text{NO}$  and there are indications that nanomolar concentrations of CO are increasing levels of  $\bullet\text{NO}$ . But neither the receptor for CO nor the mechanism of the interaction with  $\bullet\text{NO}$  formation are known. One aim of this work is therefore the identification of the cellular target of CO, which should also allow to explain an increased  $\bullet\text{NO}$  synthesis triggered by CO.
- Within the scope of my diploma thesis it was discovered that a slight excess of  $\bullet\text{NO}$  prevents oxidations by peroxynitrite. The question remains, why  $\bullet\text{NO}$  is able to protect from peroxynitrite and what are the consequences for the cell.
- *S*-Nitrosation represents a posttranslational protein modification which regulates the activity of a set of cellular key enzymes. But the mechanism leading

## 2 Aims of the Study

to the observed *S*-nitrosations is only partly understood. This work should therefore provide further insights in the chemical mechanism of *S*-nitrosation at physiological conditions.

- And finally, it will be investigated if the reactions in the  $\bullet\text{NO}/\text{O}_2^{\bullet-}$  system are leading to meaningful mechanisms of redox regulation with distinct and subsequent steps in the sequence from  $\bullet\text{NO}$  signaling towards oxidative stress.

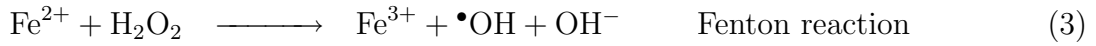
# 3 The Role of Small Signaling Molecules in the Vascular System

## 3.1 Reactive Oxygen Species

Until the discovery of nitric oxide ( $\bullet\text{NO}$ ) as an intra- and intercellular messenger, the biochemistry of oxidative stress and redox regulation was mainly focused on “reactive oxygen species” (ROS). Exogenic noxes, like irradiation, carbon tetrachloride intoxication, redox cycling by quinoid compounds, smoking damage, peroxide poisoning or excessive exposure to transition metals are leading to a burst of ROS, usually resulting in necrotic events. ROS production triggered by intracorporal events are less severe in nature—cell death during inflammation, ischemia-reperfusion or phagocytosis is mostly due to apoptosis.

Although oxygen itself is very reactive, it is not able to oxidize biomolecules because its diradicalic triplet state  ${}^3\text{O}_2$  ( $\bullet\text{O}-\text{O}\bullet$ ) contains two unpaired electrons with the same spin. Organic molecules are usually in a singlet state and the law of spin conservation does not allow one-step reactions between triplet oxygen and singlet molecules (spin-forbidden) and a spin conversion usually takes much longer ( $1-10^{-9}$  s) than there is time for an elementary reaction ( $10^{-13}$  s). However, with singlet oxygen ( ${}^1\text{O}_2$ ), superoxide ( $\text{O}_2^{\bullet-}$ ), hydrogen peroxide ( $\text{H}_2\text{O}_2$ ) and the hydroxyl radical ( $\bullet\text{OH}$ ) there are existing a variety of ROS which are in fact very reactive toward biological targets. The

ROS accompanying both necrosis and apoptosis were identified as hydrogen peroxide and hydroxyl radicals derived from superoxide anions under catalysis of ferrous ( $\text{Fe}^{\text{II}}$ ) iron (Haber-Weiss reaction):



### 3.1.1 Superoxide

The superoxide radical anion is formed as an unavoidable byproduct in the metabolism of all aerobes via one-electron reduction of molecular oxygen. It is estimated that 0.1–5 % of total oxygen consumption is reduced to  $\text{O}_2^{\bullet-}$ , mainly due to cellular respiration if electrons from the respiratory chain leak, especially as they pass through ubiquinone. During the innate immune response, NADPH oxidase is a second source in phagocytes, producing  $\text{O}_2^{\bullet-}$  by transferring electrons from NADPH to  $\text{O}_2$  via a flavoprotein and a cytochrome. Within this context disproportionation of  $\text{O}_2^{\bullet-}$  will lead to  $\text{H}_2\text{O}_2$ , serving as an oxidant for the oxidation of chloride by the enzymes chloroperoxidase and myeloperoxidase to yield the hypochlorite, which exhibits bactericidal properties. A third source for  $\text{O}_2^{\bullet-}$  is xanthine oxidase, the degradation product of xanthine dehydrogenase. By oxidation of SH-groups or proteolysis of xanthine dehydrogenase, xanthine oxidase will be formed, but the physiological role of this transformation remains unclear.

Radicals are usually highly reactive species, due to their unpaired electron spins, but in the case of  $\text{O}_2^{\bullet-}$ , the unpaired electrons are sufficiently stabilized by resonance. Therefore it reacts only with a limited number of cellular targets, like other radicals or transition metals with unpaired radicals. Furthermore, superoxide itself is not a strong oxidant but has rather reductive properties. In consequence, only reactions

### 3 The Role of Small Signaling Molecules in the Vascular System

involving the reduction of  $\text{Fe}^{3+}$  to  $\text{Fe}^{2+}$  seem to play a significant role at physiological conditions.

Despite of its low cytotoxicity and its fast disproportionation, the cell has developed highly efficient enzymes to scavenge  $\text{O}_2^{\bullet-}$ , superoxide dismutases (SOD). The rate of reaction of SOD is the fastest of any known enzyme and is close to the spontaneous diffusion rate [7]. Its high concentrations in nearly all cells exposed to oxygen (up to  $10\ \mu\text{M}$  SOD in brain and liver [8]) guarantees an effective dismutation of  $\text{O}_2^{\bullet-}$  to dioxygen and hydrogen peroxide, resulting in cellular  $\text{O}_2^{\bullet-}$  levels as low as  $10^{10}$ – $10^{11}$  M:



In humans, three different types of SOD are known. SOD1, the cytoplasmic variant, and the extracellular SOD3 (EC-SOD) both contain copper and zinc in its reactive centre and are therefore also known as Cu,Zn-SOD. In contrast, the mitochondrial isoform SOD2 has manganese in its reactive centre (Mn-SOD). But why needs the cell SODs? The resulting  $\text{H}_2\text{O}_2$  is a much stronger oxidants than  $\text{O}_2^{\bullet-}$  itself and the uncatalyzed disproportionation is sufficient to keep superoxide at low levels.

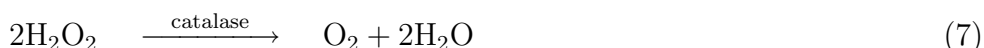
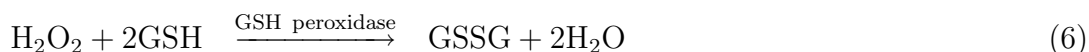
Considering the mitochondrial electron transport chain as a major source of  $\text{O}_2^{\bullet-}$ , SOD2 is indeed required to keep the mitochondrial levels of  $\text{O}_2^{\bullet-}$  low. The enzyme aconitase, one of the few biological targets of  $\text{O}_2^{\bullet-}$  and located in mitochondria, will profit from its protection. Therefore, SOD2 seems to exhibit a crucial role and SOD2<sup>-/-</sup> mice will die soon after birth with lung damage; the few surviving animals will have severe neurodegeneration [9, 10], whereas upregulation of SOD2 by the anti-aging hormone Klotho is a possible mechanism to suppresses aging [11]. SOD1 is believed to be only important at conditions of elevated oxidative stress and mice lacking SOD1 are usually healthy. It seems that they are able to adapt to the deficiency, but they show pronounced susceptibility to paraquat toxicity and the females a markedly reduced fertility [12]. Also in human, SOD1 is not an essential enzyme, but

point mutations in SOD1 have been linked to familial amyotrophic lateral sclerosis (FALS) in 20 % of the cases [13, 14].

To understand the biological role of SODs, a second aspect has to be considered. Since  $O_2^{\bullet-}$  reacts with  $\bullet NO$  in a very fast way, even low levels of  $O_2^{\bullet-}$  will prevent  $\bullet NO$ -dependent signaling pathways. And the product of this reaction, peroxynitrite, is a strong oxidant. In this view, SOD both enables nanomolar levels of  $\bullet NO$  to develop and prevents peroxynitrite formation and thus protects from oxidations by peroxynitrite.

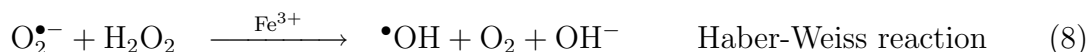
### 3.1.2 Hydrogen Peroxide and the Hydroxyl Radical

Hydrogen peroxide is the product of the dismutation of  $O_2^{\bullet-}$  and therefore, it can be produced in high amounts in the cell. Since it has strong oxidizing properties and can result in hydroxyl radical formation, the cell contains mechanisms to keep the cellular concentration at a low level. The main enzymes for  $H_2O_2$  degradation are the selenocysteine-containing enzyme glutathione peroxidase and catalase, an heme-containing enzyme:



If the cellular antioxidant systems fail to keep the levels of  $H_2O_2$  sufficient low, the formation of  $\bullet OH$  by the Fenton reaction can be a consequence. The Fenton reaction (Eq. 3) requires iron, but since  $O_2^{\bullet-}$  can reductively release iron from intracellular stores, excessive  $O_2^{\bullet-}$  production is a common trigger of oxidative stress. The highly reactive  $\bullet OH$  radical can attack all organic matter in a cell in radical chain reactions and therefore, a healthy cell has to prevent all conditions leading to  $\bullet OH$  formation.

Alternatively, hydroxyl radical formation from  $H_2O_2$  can occur via the Haber-Weiss reaction. Although the rate constant of its formation is negligible, the reaction can be accelerated by ferric iron ( $Fe^{III}$ ) (see Eqs. 1–4):



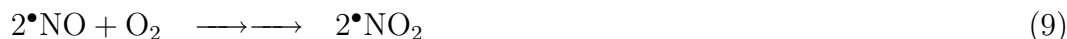
Reductants like ascorbate or  $\text{O}_2^{\bullet-}$  itself are then able to reduce ferric iron to the ferrous state, which would result in further acceleration due to cycling of iron.

## 3.2 Nitric Oxide

The discovery of  $\bullet\text{NO}$  as the “endothelium derived relaxing factor” proved to be a difficult task because its chemical properties were very distinct from other known hormones and hormone-like signaling molecules and it was also not known that higher organisms are able to synthesize  $\bullet\text{NO}$ . MURAD could show 1977 that nitrovasodilators are acting through  $\bullet\text{NO}$ , which then activates the soluble guanylate cyclase (sGC) [15]. Three years later FURCHGOTT observed that the dilatation of blood vessels in response to acetylcholine depends on intact endothelium and postulated the release of an unknown signaling molecule by endothelial cells, named “endothelium-derived relaxing factor” (EDRF) [16]. These two findings lead to the search for the EDRF, which in 1986 was independently by IGNARRO and FURCHGOTT identified to be  $\bullet\text{NO}$  [17, 18]. This discovery was in 1998 awarded with the Nobel price for medicine and led to the identification and purification of nitric oxide synthase as the  $\bullet\text{NO}$ -producing enzyme by BRED and SNYDER [19].

The free radical nitric oxide, or more correctly nitrogen monoxide, is a colorless, paramagnetic gas. Nitric oxide is often described as short lived and highly reactive, but in biological systems it represents a rather stable species and does only react with a limited number of compounds. Like  $\text{O}_2^{\bullet-}$ , the unpaired electrons are stabilized by resonance. At high concentrations in the presence of dioxygen, it usually decomposes very quickly to the highly reactive orange-brown gas nitrogen dioxide ( $\bullet\text{NO}_2$ ), which also reacts quickly with  $\bullet\text{NO}$  and in aqueous solutions finally decomposes to yield nitrite:

### 3 The Role of Small Signaling Molecules in the Vascular System



However, the special nature of this reaction prevents this oxidation at physiological levels of nitric oxide. Albeit this reaction is not entirely understood, it is described to be of pseudo third-order and of second order with regard to  $\bullet\text{NO}$  [8]:

$$\frac{d[\bullet\text{NO}]}{dt} = 4k_3[\text{O}_2][\bullet\text{NO}]^2 \quad k_3 = 2 \times 10^6 \text{ M}^{-2}\text{s}^{-1}$$

Therefore,  $\bullet\text{NO}$  can be rather stable at low concentrations; according to this equation the half-life of 1 mM  $\bullet\text{NO}$  is around 0.56 s at ambient oxygen concentrations, whereas at 0.1  $\mu\text{M}$  it should be more than 90 min, neglecting other reactions [8]. The mechanism of this reaction remains unclear; recent studies from the KOPPENOL group are suggesting an intermediate in this reaction (R. KISSNER, personal communication):



According to the kinetics it is a common simplification to neglect the autoxidation of  $\bullet\text{NO}$  in biological systems; only for the explanation of some secondary reactions like *S*-nitrosation one takes it into account. However, there is a second mechanism of autoxidation under discussion, which—if confirmed—will have an impact on the autoxidation of physiological concentrations of  $\bullet\text{NO}$  and therefore would explain some of the observed reactions. Theoretically,  $\bullet\text{NO}$  should be in equilibrium with its dimer,  $\text{N}_2\text{O}_2$ . Even if the concentrations of  $\bullet\text{NO}$  are low and these of  $\text{N}_2\text{O}_2$  are even lower, the following reaction with oxygen will become likely:



In contrast to the mechanism of autoxidation as written in textbooks, this mechanism would explain reactions observed in biological systems, which require the presence of

### 3 *The Role of Small Signaling Molecules in the Vascular System*

the nitrosonium ion ( $\text{NO}^+$ ), like nitrosations. Free nitrosonium itself is very unstable, it will react immediately with water to form nitrite. However, the nitrosonium ion moiety can be transferred between biological molecules, in particular by thiols.

As an auto- and paracrine messenger molecule, nitric oxide has interesting properties. The lack of a charge and the small size of the molecule allow free diffusion through membranes and the rapid diffusion through cells and tissues with only a small amount of  $\bullet\text{NO}$ -consuming reactions is one of its key properties. A higher solubility in regions of the cell which are less polar, e. g. membranes and non-charged part of the surface of proteins, allows higher local concentrations of  $\bullet\text{NO}$  in these regions and less interfering reactions [20]. Contrary to its stability in cells and tissues, it will be quickly eliminated in blood; after diffusion into red blood cells it will react with oxyhemoglobin to form nitrate.

In its main role as EDRF, nitric oxide activates the soluble guanylate cyclase through binding to ferrous heme. The activation of sGC results in the enzymatic conversion of GTP to cyclic guanosine monophosphate (cGMP) as second messenger with the consequence of relaxation of smooth muscle. In blood vessels, this leads to vasodilation and increased blood flow.

Additionally to its actions as EDRF,  $\bullet\text{NO}$  has further functions determined by its enzymatic source. In neuronal tissue in both the central and peripheral nervous system it exhibits a function as a neurotransmitter. Unlike most other neurotransmitters,  $\bullet\text{NO}$  can act on both presynaptic and postsynaptic and even on nearby neurons. It is conjectured that this process may be involved in memory through the maintenance of long-term potentiation. Finally, high amounts of  $\bullet\text{NO}$  produced by macrophages are playing an important role in the immune defense against pathogens.

$\bullet\text{NO}$  is a universal signaling molecule; this is reflected by the identification of NOS-like proteins not only in higher but also in primitive organisms. There is also evidence for  $\bullet\text{NO}$ -production in prokaryotes and plants, e. g. during pathogen defense, but this

could be due to mitochondrial-dependent nitrite-reducing activity. All mammals seem to produce and use •NO for similar reasons as humans do. Especially rodents are a common model to study the physiology of •NO, but it is a common mistake to ignore the differences in •NO-signaling, especially between rats and humans [21]. In rats, vessel regulation is based mainly on •NO, whereas in humans prostaglandins are acting as a second regulatory principle side by side with •NO. Therefore, it is not possible to transfer rat-based observations to the regulatory network in humans.

### 3.2.1 Nitric Oxide Synthases

The dimeric enzyme nitric oxide synthase (NOS) catalyzes the sequential five-electron oxidation of L-arginine to •NO and L-citrulline, using NADPH and O<sub>2</sub> as cosubstrates. Beside these substrates, the tightly-bound cofactors flavin adenine dinucleotide (FAD), flavin mononucleotide (FMN) and tetrahydrobiopterin (BH<sub>4</sub>) are essential to transfer the electrons from NADPH to the heme-bound oxygen and L-arginine at the active site of the enzyme.

Until now, three distinct isoforms of NOS have been identified, and despite over 50% homology between the human isoforms, they differ in gene regulation, localization, regulation and catalytic properties. Both the endothelial (eNOS, NOS-3) and the neuronal variant (nNOS, NOS-1), named after their main localization in endothelial cells or neurons, respectively, are constitutively expressed and regulated by Ca<sup>2+</sup> and the presence of all substrates and cofactors. The inducible NOS (iNOS, NOS-2), mostly found in macrophages, does not depend on Ca<sup>2+</sup> for its activation; a missing calmodulin (CaM) autoinhibitory loop in the FMN domain stabilizes CaM binding to such a degree that also in the absence of free cellular Ca<sup>2+</sup> CaM will remain bound to the hence active NOS-2. Therefore, NOS-2 exhibits a notably higher affinity for CaM and will be regulated mainly at the level of transcription, but to a smaller degree also on Ca<sup>2+</sup>. In the central nervous system, the recently discovered protein kalirin

### 3 The Role of Small Signaling Molecules in the Vascular System

serves as an inhibitory protein by prevention of NOS-2 dimerization; this may play a neuroprotective role during inflammation. The activity of both of the other two NOS relies on  $\text{Ca}^{2+}$ -mediated binding of CaM, but also other regulatory mechanisms exist.

NOS-1 and 3 are additionally regulated by phosphorylation. Fluid shear stress elicits phosphorylation of NOS-3 by protein kinase Akt, increasing electron flux through the reductase domain and  $\bullet\text{NO}$  production. In contrast, phosphorylation of NOS-1 by CaM-dependent kinases will lead to a decrease in enzyme activity. NOS-1 activity is also negatively affected by binding of protein inhibitor of NOS (PIN) to an *N*-terminal sequence. The chaperone heat-shock protein 90 (Hsp90) was identified as an activator of NOS-3; activation by the vascular endothelial growth factor (VEGF), histamine or shear stress increases the interaction between NOS-3 and Hsp90 and lead to activation of NOS-3. In addition to NOS-2, both NOS-1 and 3 expression can be induced, albeit by different stimuli, and all three can be constitutively expressed in some cells.

From a functional and structural view, NOS are composed by an *N*-terminal heme-containing oxygenase and a *C*-terminal reductase domain, linked with a CaM-binding sequence. NOS are considered to be P450 proteins, they have similar spectral characteristics in response to CO and especially the reductase domain is homologous to cytochrome P450 reductase. The separated domains are catalytically active and are often used for functional and crystallographic studies, mainly for reasons of easier purification and simpler handling compared with the full-length enzyme. The reductase domain consists of a NADPH reductase domain, followed by a FAD- and a FMN-binding domain; during catalysis, the electrons will be transferred from one domain to the adjacent in a linear way.

Contrary to the modular structure of the reductase domain, the core structure of the oxygenase domain is formed by one continuous fold, consisting mainly of  $\beta$ -sheets and arranged around the heme. Structural properties of this domain include  $\text{BH}_4$ - and L-Arg-binding sites, an extensive conserved dimer interface and a substrate channel.

### 3 The Role of Small Signaling Molecules in the Vascular System

The identical two  $\text{BH}_4$  binding sites of the dimer are each composed by residues from both polypeptides, indicating the importance of dimer formation. Dimerization is further stabilized by a shared Zn, ligated by two Cys residues each. There are multiple questions rising from the oxygenase structure; most notably about the role of  $\text{BH}_4$  in catalysis and the need for a dimeric NOS for catalysis.

Unlike other enzymes where  $\text{BH}_4$  is used as a source of reducing equivalents and is recycled by dihydrobiopterin reductase,  $\text{BH}_4$  will stay bound to NOS and obviously exhibits a different role in NOS. Besides of a postulated redox role in the reaction mechanism of NOS,  $\text{BH}_4$  is also suggested to promote coupling of NADPH oxidation to  $\bullet\text{NO}$  synthesis and inhibit  $\text{O}_2^{\bullet-}$  formation, to stabilize the dimer, to modify the heme to high-spin, to yield allosteric substrate binding effects or to protect against inactivation, whereas each of these functions is still under discussion [22, 23]. The most feasible interpretation of its role is, that  $\text{BH}_4$  activates heme-bound  $\text{O}_2$  by donating a single electron, which is then recaptured to enable  $\bullet\text{NO}$  release.

Only homodimeric NOS being able to transfer electrons from FMN to the oxygenase domain, a model of “domain swapping” was postulated by STUEHR *et al.*, where the electrons will be transferred from the reductase to the oxygenase domain of the adjacent subunit [24]. This model was supported by the observation that the electron transfer of the reductase domain only reduces heme iron of the adjacent subunit [25], but the solved crystal structures of different NOS oxygenase and reductase domains did not show the required proximity, putting the model into question. By further analysis of the crystal structures, the FMN domain was found to be very flexibly linked to NOS and could act as a one-electron shuttle between reductase and oxygenase domains by a swinging mechanism [26].

The mechanism of  $\bullet\text{NO}$  formation, which until now is not fully understand, consists of two main steps, both consuming NADPH and  $\text{O}_2$ . By hydroxylation of L-Arg,  $N^\omega$ -hydroxy-L-arginine (NOHA) will be formed as an intermediate, and in a second

step, this intermediate will be converted to the products  $\bullet\text{NO}$  and L-citrulline. This mechanism requires two times the activation of  $\text{O}_2$ . After binding of L-Arg into the substrate pocket, the ferric heme will be reduced to ferrous, consuming an electron from NADPH provided via the reductase domain. Dioxygen will then bind to the heme, forming a ferrous-oxy complex. Simultaneous addition of an electron and a proton will reduce the complex to a hydroperoxide. Further protonation leads to a ferryl iron ( $\text{Fe}^{\text{IV}}$ ) with a protein-bound cation radical, allowing rapid oxygenation of L-Arg to NOHA, whereas the resting ferric heme state will be recovered. The second step of  $\bullet\text{NO}$  synthesis then starts similar with subsequent  $\text{O}_2$  binding and the formation of a ferrous-oxy complex, which will then attack NOHA to yield L-citrulline and ferric-NO complex, and finally  $\bullet\text{NO}$  will be released.

Some details of this rather complex mechanism are still under discussion, although there are two critical steps during  $\bullet\text{NO}$  synthesis, which will contribute to the pathophysiology of already emerged situations of oxidative stress. The first critical step is the first formation of the ferrous oxy complex ( $\text{Fe}^{\text{II}}\text{-O}_2$ ), which is equivalent to a ferric superoxide complex ( $\text{Fe}^{\text{III}}\text{-O}_2^{\bullet-}$ ). In a process of uncoupling,  $\text{O}_2^{\bullet-}$  can be released, which brings the heme back to the initial ferric state. NOS uncoupling can occur under various suboptimal conditions, including disruption of the dimer formation, but mainly depends on  $\text{BH}_4$ . If  $\text{BH}_4$  is missing or not in the reduced state,  $\bullet\text{NO}$  formation is interrupted and will arrest at this stage, favoring  $\text{O}_2^{\bullet-}$  formation. Superoxide as an antagonist to  $\bullet\text{NO}$  will not only provide different effects, but additionally quench the remaining concurrent  $\bullet\text{NO}$  formation. In consequence, NOS will switch from a  $\bullet\text{NO}$  synthase to a peroxynitrite synthase up to a  $\text{O}_2^{\bullet-}$  synthase, which is of cause of high importance during an otherwise disturbed cellular redox equilibrium. This switch will be further assisted by the anticooperative binding of  $\text{BH}_4$ ; the first bound  $\text{BH}_4$  lowers the dimer's affinity for the second by at least an order of magnitude.

The rate-limiting step for the production of nitric oxide can be the availability of L-Arg in some cell types; this may particularly be important after the induction of NOS-2.

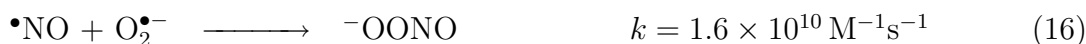
However, of higher importance is the release of the heme-bound  $\bullet\text{NO}$  since the  $\text{Fe}^{\text{III}}\text{-NO}$  can be reduced to the more stable ferrous nitrosyl complex, which was shown for both NOS-1 and 2. Due to its stability, this will lead to self-inactivation of these enzymes under certain conditions, rendering the release of  $\bullet\text{NO}$  as the rate-limiting step. In particular for NOS-1 it was reported that up to 95% of the enzyme can be in the  $\text{Fe}^{\text{II}}\text{-NO}$  form during steady state [27] and the addition of  $\bullet\text{NO}$  scavengers is not able to release this NOS-1-autoinhibition [27, 28]. Autoinhibition in NOS-2 appears to be weaker, partly due to a fast reaction of the  $\text{Fe}^{\text{II}}\text{-NO}$  complex with  $\text{O}_2$  generating nitrate and ferric iron, whereas in NOS-1 a conserved tryptophan residue is responsible for the stabilization of the ferrous nitrosyl complex [29]. By competing with  $\text{O}_2$ ,  $\bullet\text{NO}$  rises the  $K_m$  for oxygen of NOS-1, making  $\bullet\text{NO}$  synthesis oxygen-dependent throughout the physiological range and suggesting that this may represent a signal transduction mechanism in which signal intensity is directly related to  $\text{O}_2$  concentration, resembling an  $\text{O}_2$  sensor.

Based on their different functions in the organism, the NOS isoforms exhibit big differences in their activity, if activated. The endothelial isoform is only able to provide basal levels of  $\bullet\text{NO}$  in the low nanomolar range, sufficient for regulation of vascular tone and inhibition of platelet aggregation, leukocyte adhesion and smooth muscle cell proliferation. NOS-1 is not only localized to neurons, but also plays an important role in skeletal muscle [30], myocytes [31] and in mitochondria. It has to be mentioned that in mitochondria, in addition to the possibility of a reductive  $\bullet\text{NO}$  formation, there is striking evidence for the existence of a mitochondrial NOS (mtNOS), in most cases characterized as a splice variant of NOS-1 [32–35]. NOS-1 exhibits an about 10 times higher activity than NOS-3; if one accounts its high rate of autoinhibition, it has to be considered that a mechanism able to release this inhibition should result in high rates of  $\bullet\text{NO}$  formation. Even if such a release of NOS-1 autoinhibition has not been discovered until now, it is not implausible to assume such a mechanism. This would allow increased  $\bullet\text{NO}$  production, without the need for *de novo* protein

synthesis. This mechanism represents the basis for our later discussed hypothesis of the interplay between CO and  $\bullet$ NO signaling. Transcription of NOS-2, which lacks the autoinhibitory loop and is therefore roughly 20 times more active than NOS-3, will lead to massive  $\bullet$ NO synthesis, consistent with its role in immune defense in macrophages.

### 3.3 Peroxynitrite

Peroxynitrite,  ${}^{-}\text{OONO}$ , the “ugly side of nitric oxide” [8] is known since 1901 and is now accounted to be responsible for most of the toxic effects derived from  $\bullet$ NO and represents the most important intermediate in the biochemistry of  $\bullet$ NO and  $\text{O}_2^{\bullet-}$ . However, the focus on peroxynitrite research in biological systems started 1985 with the discovery of its production by the spontaneous reaction between  $\bullet$ NO and  $\text{O}_2^{\bullet-}$  in aqueous solutions [36]. The formation from this two free radicals is one of the fastest known bimolecular reactions and is mainly diffusion-controlled:



This high rate constant, which KISSNER and KOPPENOL determined by flash photolysis [37], is four times higher than the values obtained by pulse radiolysis [38–41] and therefore provoked enduring discussions in literature [42, 43].

Contrary to  $\bullet$ NO and  $\text{O}_2^{\bullet-}$ , peroxynitrite seems to be such a powerful oxidant that it has been reported to react with a broad variety of cellular targets, yielding in DNA strand breaks and 8-oxoguanine formation, protein sulfoxidations, nitrations and hydroxylations, peroxidations of lipids and low-density lipoproteins, oxidation of monohydroascorbate and NAD(P)H at sufficient concentrations. However, the majority of these reactivities seems not to be based on  ${}^{-}\text{OONO}$ , but on its acid. With a  $\text{p}K_{\text{a}}$  of approximately 6.6 [43], peroxynitrite will be protonated to its conjugated acid HOONO (peroxynitrous acid) at physiological conditions. The acid itself is very unstable and therefore the half-life of peroxynitrite at pH 7 is around one

second. Peroxynitrite and its more reactive acid are usually collectively referred as “peroxynitrite” and, if not otherwise indicated, also in this work. Depending on the pathway of peroxynitrite decomposition, nitrate and nitrite will be the stable end products.

Peroxynitrous acid is reported to exist in two conformers, the *trans*- and the *cis*-isomer, whereas the latter is approx. 14.2 kJ/mol lower in energy and therefore seems to be the dominating species in solutions [44, 45]. However, in biological systems  $^-OONO$  and  $HOONO$  are formed in a continuous process and the *trans*-form could be of increased importance if it will be formed initially, because interconversion from *trans*- to *cis*-form has to overcome a relatively large barrier of approx. 33.5 kJ/mol. Results from REITER *et al.*, however, suggest that at a neutral pH, the *cis*- and not the *trans*-conformer of peroxynitrite is formed during *in situ* generation by  $\bullet NO$  and  $O_2^{\bullet -}$  [46]. But other experiments revealed that *trans*- and *cis*-peroxynitrous acid exist in comparable concentration within 0.5 s after  $HOONO$  formation [45] or at least that both conformers exhibit comparable stability and are in rapid equilibrium [47, 48].

## 3.4 The Nitric Oxide/Superoxide System

The knowledge of the discussed reactions of nitric oxide, superoxide and its resulting product peroxynitrite is not sufficient to explain the biological outcome of the presence of these two radicals. At physiological conditions, the concentrations of  $\bullet NO$  and  $O_2^{\bullet -}$  stay in regions controlled by the cellular antioxidant systems and only a few specific reactions—either with radicals itself or with transition metals containing unpaired radicals—can occur. Even at such low levels of  $\bullet NO$  and  $O_2^{\bullet -}$ , the reactivities with these targets are high, whereas reactions with spin-paired compounds occur only rarely. However, the outcome of these reactions is determined mostly by the balance between these radicals and to a lesser extent by their actual concentrations. Depending on the

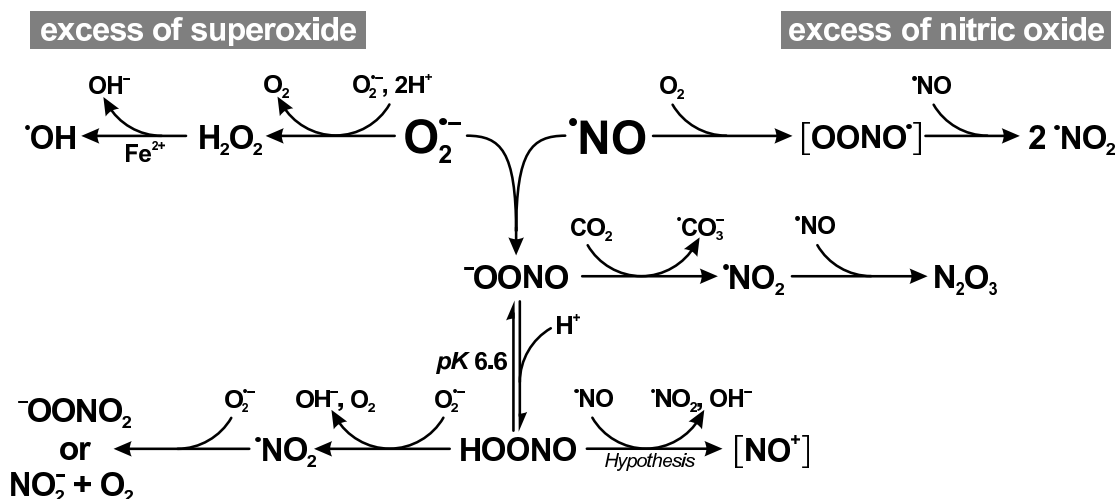


Figure 3.1: **Reactions between superoxide and nitric oxide.** The main product of the reaction between equal amounts of nitric oxide ( $\text{NO}^\bullet$ ) and superoxide ( $\text{O}_2^{\bullet-}$ ) is the peroxynitrite anion ( $\text{OONO}^-$ ), which exists at neutral pH in equilibrium with its acid. Peroxynitrous acid ( $\text{HOONO}$ ) has strong oxidizing properties and seems to react with  $\text{NO}^\bullet$  to yield a nitrosating intermediate; the hypothetical mechanism of this reaction was investigated within this work and will be discussed later. Carbon dioxide, which is present in concentrations up to 1 mM in biological systems, shifts the product pattern towards nitrogen dioxide radicals ( $\text{NO}_2^\bullet$ ) and a slight excess of  $\text{NO}^\bullet$  should lead to the formation of  $\text{N}_2\text{O}_3$ . Autoxidation of  $\text{NO}^\bullet$  requires relatively high concentrations of  $\text{NO}^\bullet$ . Superoxide seems to react with  $\text{HOONO}$ , giving  $\text{NO}_2^\bullet$  [49], and further reaction with  $\text{O}_2^{\bullet-}$  could lead to peroxynitrate ( $\text{OONO}_2^-$ ). If  $\text{O}_2^{\bullet-}$  outweighs  $\text{NO}^\bullet$  this can cause significant formation of hydrogen peroxide ( $\text{H}_2\text{O}_2$ ), enabling Fenton chemistry and formation of  $\text{OH}^\bullet$ -radicals, and thus will initiate toxicity with all signs of oxidative stress.

ratio of  $\text{NO}^\bullet$  and  $\text{O}_2^{\bullet-}$ , different cascades of secondary reactions will occur, leading to different cellular responses.

The spectrum of redox conditions in the  $\text{NO}^\bullet/\text{O}_2^{\bullet-}$  system ranges from states with only  $\text{NO}^\bullet$ , 2–3fold excess of  $\text{NO}^\bullet$  over  $\text{O}_2^{\bullet-}$ , equal levels of both radicals, and an excess of  $\text{O}_2^{\bullet-}$ . Considering this dependency on the balance between  $\text{NO}^\bullet$  and  $\text{O}_2^{\bullet-}$  and the usually low levels of  $\text{NO}^\bullet$  and  $\text{O}_2^{\bullet-}$ , one arrives at the rather simple but fascinating scenario, in which the chemistry described in Fig. 3.1 can be correlated with cellular redox biochemistry and physiological regulation. A chemical basis and a

physiological concept for the redox regulation in this system will be provided in the following sections.

The  $\bullet\text{NO}/\text{O}_2^{\bullet-}$  system can be assessed by an experimental approach. Simultaneous generation of  $\bullet\text{NO}$  and  $\text{O}_2^{\bullet-}$  through producing systems (e. g. spermine NONOate and xanthine oxidase/hypoxanthine or SIN-1) instead of bolus addition of the radicals or peroxyxynitrite yields in different results. One reason is that at higher concentrations the reactions will become mainly unspecific, but the main reason is that most of the observed reactions rely on complicated reaction chains. These chains will only take place if all intermediates are present in the system at sufficient concentrations. Therefore, the usage of  $\bullet\text{NO}/\text{O}_2^{\bullet-}$  or peroxyxynitrite producing systems instead will result in a different reaction pattern with higher biological significance.

The key to the chemistry in the  $\bullet\text{NO}/\text{O}_2^{\bullet-}$  system lies in the reactions of peroxyxynitrous acid with  $\bullet\text{NO}$  and  $\text{O}_2^{\bullet-}$ , respectively. If there is some excess of one of the radicals, secondary reactions will occur instead of oxidations by peroxyxynitrite, leading to different mechanisms of redox regulation. CROW and BECKMAN were the first who obtained results pointing in this direction; they observed that addition of peroxyxynitrite to a solution of  $\bullet\text{NO}$  in phosphate buffer at physiological pH results in rapid loss of the chemiluminescent signal from  $\bullet\text{NO}$  [50]. Their data already indicates that the yields of both nitrating and nitrosating species are increased (4-nitrosophenol formation), peaking at a  $^-\text{OONO}/\bullet\text{NO}$  ratio of 2:1. Since the observed nitrosation was pH dependent, HOONO was proposed to react with  $\bullet\text{NO}$ .

Our first observations on the strong dependency of the ratio of  $\bullet\text{NO}$  and  $\text{O}_2^{\bullet-}$  production on the reactions feasible were made during analysis of the inhibition of alcohol dehydrogenase (ADH) [51]. Our insights of oxidation and nitrosation in this system will be discussed later in Section 5.2. Further experiments on nitrosation in this system by ESPEY *et al.* revealed maximal nitrosation with a flux of  $\bullet\text{NO}$  and a  $\bullet\text{NO}:\text{O}_2^{\bullet-}$  ratio between 2:1 and 3:1 for the nitrosation of the fluorescent probe

2,3-diaminonaphthalene (DAN) [52]. Interestingly, addition of SOD to the  $\bullet\text{NO}/\text{O}_2^{\bullet-}$  system results in enhancement of nitrosation and, at the same time, broadening of the bell-shaped curve of nitrosative conditions. In physiological context this means that in the presence of SOD, in addition to its beneficial effects, nitrosation will become much more likely.

Complementary to the investigation of nitrosation in this system, oxidations were also studied. MILES *et al.* [53] observed that only equimolar fluxes of  $\bullet\text{NO}$  and  $\text{O}_2^{\bullet-}$  yield in oxidations like those known for chemically synthesized peroxyxynitrite, as demonstrated for the oxidation of dihydrorhodamine (DHR) to rhodamine. However, excess production of either radical virtually eliminated the observed oxidations. Subsequent studies by JOURD'HEUIL *et al.* [49] revealed a  $\bullet\text{NO}/\text{O}_2^{\bullet-}$  ratio of 2:1 for maximal oxidation of DHR and NADH, but a direct reaction of  $\bullet\text{NO}$  (and  $\text{O}_2^{\bullet-}$ ) with peroxyxynitrite was seen as unlikely or at least negligible. Instead, a reaction pathway involving self-decomposition of HOONO to  $\bullet\text{OH}$  and  $\bullet\text{NO}_2$  and subsequent reactions with  $\bullet\text{NO}$  or  $\text{O}_2^{\bullet-}$  were proposed. This view gained further backing by independent studies by GOLDSTEIN and CZAPSKI, who proposed a different, radical pathway for NADH oxidation by simultaneous generation of  $\bullet\text{NO}$  and  $\text{O}_2^{\bullet-}$ , starting from the self-decomposition of HOONO. They argued that a small excess of  $\bullet\text{NO}$  over  $\text{O}_2^{\bullet-}$  yields in maximal oxidation because peroxyxynitrite formation in this system competes with the reaction of  $\bullet\text{NO}$  with the later formed  $\bullet\text{NO}_2$  [54].

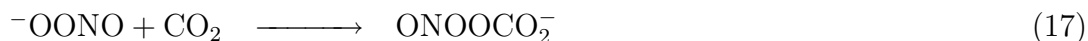
3-Nitrotyrosine as a common biomarker of peroxyxynitrite was subject to similar studies of the  $\bullet\text{NO}/\text{O}_2^{\bullet-}$  system. PFEIFFER and MAYER analyzed tyrosine nitration during simultaneous generation of  $\bullet\text{NO}$  and  $\text{O}_2^{\bullet-}$  [55]. Due to inappropriate experiments, further studies by other groups were performed [46, 55–58], but the gained results were of limited use for understanding the system as a whole. Recently a model for tyrosine nitration in the  $\bullet\text{NO}/\text{O}_2^{\bullet-}$  system was calculated by QUIJANO *et al.* using computer assisted simulations [59] and they could approve the current view on the mechanism of tyrosine nitration, given that  $\text{CO}_2$  is present. Under these conditions,

a bell-shaped profile of tyrosine nitration is observed where nitration is maximal at equimolar fluxes of  $\bullet\text{NO}$  and  $\text{O}_2^{\bullet-}$  and decreases fast under an excessive flux of either one of the radicals, in agreement with previous reports. This underlines the need to study the actions of  $\bullet\text{NO}$ ,  $\text{O}_2^{\bullet-}$  and peroxynitrite by generating the intermediates *in situ* in a continuous manner, but at the same time shows the lack of explanation of the reactions in the absence of  $\text{CO}_2$ .

In the meantime it is well accepted to favor fluxes by  $\bullet\text{NO}$ - and  $\text{O}_2^{\bullet-}$ -generating systems instead of bolus addition of the radicals or peroxynitrite during investigations concerning these intermediates and their impact in biological systems. The mechanisms of the reactions in the  $\bullet\text{NO}/\text{O}_2^{\bullet-}$  system remain in large parts unsolved, but their understanding is necessary for evaluation of the biological impact of the actions of the two radicals. Especially the analysis of the reactions of  $\text{HOONO}$  with  $\bullet\text{NO}$  and  $\text{O}_2^{\bullet-}$  were neglected. One reason for this nuisance is the discovery of a reaction between  $\text{CO}_2$  and  $^-\text{OONO}$ , which permits an explanation for significant parts of the observed reactions and will be discussed in the following section.

### 3.4.1 Reaction of Carbon Dioxide with Peroxynitrite

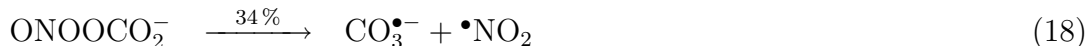
It is known since 1969 that bicarbonate buffers react with peroxynitrite [60], but LYMAR and HURST were the first who observed that this occurs due to a direct reaction of carbon dioxide with peroxynitrite [61]:



The bicarbonate anion is one of the most abundant constituents of the extracellular milieu (25 mM in plasma) and its equilibrium with carbon dioxide maintains the level of  $\text{CO}_2$  around 1.3 mM *in vivo*. With a rate constant  $k = 3 \times 10^4 \text{ M}^{-1}\text{s}^{-1}$  [61], this reaction is therefore fast enough to be one of the predominant pathways of  $^-\text{OONO}$  disappearance in physiological fluids.

### 3 The Role of Small Signaling Molecules in the Vascular System

The product,  $\text{ONOOCO}_2^-$ , decomposes fast with a kinetic rate constant of  $k = 1.9 \times 10^9 \text{ M}^{-1}\text{s}^{-1}$  [62] via two pathways, whereas one third yields in both  $\text{CO}_3^{\bullet-}$  and  $\bullet\text{NO}_2$  radical formation [59, 63]:



Nitrogen dioxide itself has oxidizing properties, and because it will react with an excess of  $\bullet\text{NO}$  to yield dinitrogen trioxide ( $\text{N}_2\text{O}_3$ ), this pathway is able to explain the observed oxidations and nitrosations in physiological systems.

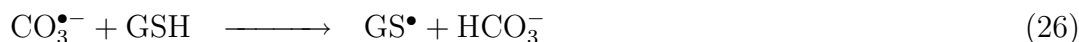
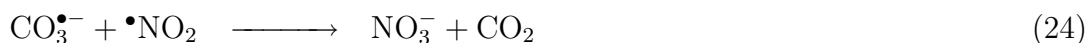
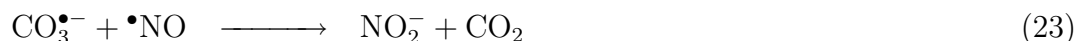


Indeed, addition of  $\text{CO}_2$  [52] or bicarbonate buffer increases nitrosations and oxidations in the  $\bullet\text{NO}/\text{O}_2^{\bullet-}$  system by 50 %, without changing the stoichiometry between  $\bullet\text{NO}$  and  $\text{O}_2^{\bullet-}$  (this work, Section 5.4). Beyond the  $\bullet\text{NO}/\text{O}_2^{\bullet-}$  system,  $\text{CO}_2$  also increases tyrosine nitration after bolus addition of peroxynitrite [63–65]. This is in line with a free radical mechanism of tyrosine nitration via  $\bullet\text{NO}_2$  [56, 66].

Another consequence of the presence of  $\bullet\text{NO}_2$  can be the formation of peroxynitrate ( $\text{O}_2\text{NOO}^-$ ) and  $\text{N}_2\text{O}_4$ , as was demonstrated by GOLDSTEIN and CZAPSKI [67]. Besides the lack of knowledge about the reactivities toward biomolecules, the biological significance of these intermediates has still to be shown.



The  $\text{CO}_3^{\bullet-}$  radical itself is able to react with other radicals in the  $\bullet\text{NO}/\text{O}_2^{\bullet-}$  system to yield  $\text{CO}_2$  or bicarbonate and hence not only increases peroxynitrite decomposition, but will also have an impact on  $\bullet\text{NO}$  and  $\text{O}_2^{\bullet-}$  itself. It will also react with the large amounts of cellular thiols like glutathione to yield the corresponding radicals, which can be the intermediate step for oxidations, nitrosations and nitrations.



The discovery of the reactivity of  $\text{CO}_2$  as an omnipresent molecule in biological system helped to gain deeper understanding of the  $\bullet\text{NO}/\text{O}_2^{\bullet-}$  system and its mechanisms of action [62]. This provides a mechanism for the observed oxidations and nitrosations, but on the other hand demonstrates again that the present knowledge of nitrosations, especially in the absence of bicarbonate, lacks important details.

## 3.5 Redox Regulation by the Nitric Oxide/Superoxide System

In context of this work, not only the complex chemistry of the  $\bullet\text{NO}/\text{O}_2^{\bullet-}$  system is of interest, but rather its direct link to physiological regulatory processes. The high sensitivity to slight changes in the balance between  $\bullet\text{NO}$  and  $\text{O}_2^{\bullet-}$ , the different patterns of reactions depending on this balance and the high specificity of the intermediates to only a selected amount of cellular targets guide to a complex network of cellular redox regulation. The reactivities of the intermediates in the  $\bullet\text{NO}/\text{O}_2^{\bullet-}$  system towards biological targets will be explained in this section, where the main focus will be on mechanisms of redox regulation.

### 3.5.1 Nitrosylation

Nitrosylation and nitrosation are frequently used synonymous in literature, mainly to avoid further differentiation about the exact mechanism; the term “*S*-nitrosylation” is usually preferred to express the analogy to the similar regulative mechanism of phos-

phorylation. However, since these terms are defined from a mechanistic perspective, nitrosations and nitrosylations are occurring at different functional groups and cellular conditions. The term “nitrosyl” is usually used if an NO-group is associated to a metal and hence, the term “nitrosylation” should be used to express the addition of  $\bullet\text{NO}$  to metals. In contrast, “nitrosation” is defined as a reaction involving the nitrosonium cation ( $\text{NO}^+$ ) or a related species, whereas the prefix “nitroso-” is not mechanistically defined and only stands for the functional group. Therefore, “nitrosylation” should only be used to express the formation of a metal-NO complex and “nitrosation” to describe an  $-\text{NO}$  function connected to another functional group, e.g. *S*- or *N*-nitrosation.

In consequence, nitrosations are only possible during oxidative conditions involving increased superoxide production or autoxidation of  $\bullet\text{NO}$ . Nitrosylation does not require oxidative conditions and is therefore happening during resting and reducing conditions. Resting cells are characterized by low levels of  $\text{O}_2^{\bullet-}$  arising from unavoidable spontaneous autoxidations as all potential sources are effectively down-regulated and superoxide dismutases maintain such levels in the range of  $10^{-11}$  to  $10^{-10}$  M. A release of  $\bullet\text{NO}$  in the nanomolar range after activation of NOS-3 therefore will not be interfered by basal levels of  $\text{O}_2^{\bullet-}$  and sGC can be stimulated by nitrosylation at its ferrous heme-containing subunit. The formation of an  $\text{Fe}^{\text{II}}-\text{NO}$  complex is the main regulative event during  $\bullet\text{NO}$  signaling in the resting cell. In cells this condition signals relaxation because cGMP via its corresponding G-kinases lowers  $\text{Ca}^{2+}$  levels again, and by feedback inhibition, can switch of  $\text{Ca}^{2+}/\text{CaM}$ -dependent nitric oxide synthases. The  $\text{Ca}^{2+}$ -independent NOS-2 does not seem to play a major role in the resting cell, whereas in contrast, much of the chemistry in diseased states relies on the participation of this isoenzyme [68].

There are increasing evidences that cytochrome *c* oxidase will be nitrosylated, if the levels of  $\bullet\text{NO}$  are rising due to activation of NOS-1 or 3 [69]. In competition with oxygen, its heme iron:copper binuclear center can become nitrosylated with an affinity

of  $K_D = 0.2 \text{ M } \bullet\text{NO}$  for the oxygen-binding ferrous heme site [70]. This competition decreases mitochondrial respiration and in consequence oxygen consumption and cellular ATP levels will be lowered, although the biological relevance of this interaction still has to be demonstrated.

### 3.5.2 Nitrosation

*S*-Nitrosation of protein cysteine residues, the reversible formation of *S*-nitrosothiols ( $-\text{S}-\text{NO}$ ), is a posttranslational modification that fully meets the requirements of a redox-regulated process. In addition to nitrosation of thiols, *N*-nitrosation can also occur *in vivo* but until now there are no indications that this is connected with regulatory processes. Nitrosation is dependent on elevated levels of cellular  $\text{O}_2^{\bullet-}$  at simultaneous production of  $\bullet\text{NO}$ , but at least a twofold excess of  $\bullet\text{NO}$  is necessary. This is reflected on the current view on the mechanism of *S*-nitrosation as well as on the collected experimental data.

Until now, a high number of enzymes are reported to become *S*-nitrosated at specific cysteines under certain conditions *in vivo* and, considering the important role of thiol groups in enzyme catalysis and in the building of protein tertiary structure, an *S*-nitrosation modification could easily influence enzyme activities. The process of transnitrosation in the presence of GSH enables the reversal of these reactions which then meet the requirements for redox regulation.

#### 3.5.2.1 Mechanism of Nitrosation

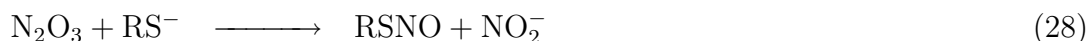
As a common misunderstanding, nitrosation is believed to occur via the direct reaction of thiols with  $\bullet\text{NO}$ . It was shown 1995 by KHARITONOV *et al.* that this cannot be the case and *S*-nitrosation by  $\bullet\text{NO}$  requires at least the presence of oxygen [71]. A direct

### 3 The Role of Small Signaling Molecules in the Vascular System

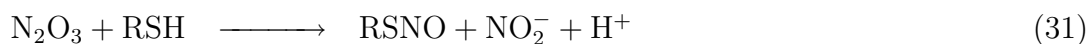
reaction of thiol groups with  $\bullet\text{NO}$  is as well unlikely due to stoichiometric reasons, but rather requires  $\text{NO}^+$  or the presence of a one-electron acceptor together with  $\bullet\text{NO}$ :



Since  $\text{NO}^+$  is unlikely to exist at pH 7, it has been proposed that  $\text{N}_2\text{O}_3$  could be the nitrosating intermediate [71]:



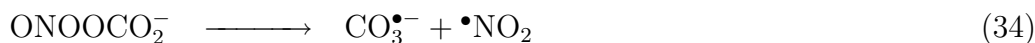
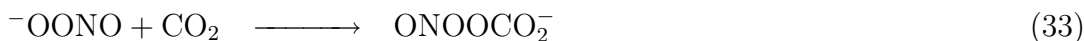
And since  $\text{N}_2\text{O}_3$  is the product of the reaction of  $\bullet\text{NO}$  with the  $\bullet\text{NO}_2$  radical, it is likely to be formed in biological systems during the autoxidation of  $\bullet\text{NO}$ . Also the proposed alternative pathway of  $\bullet\text{NO}$ -autoxidation could lead to nitrosation via  $\text{NO}^+$  (Eqs. 14 and 15):



Considering the special kinetic of this reaction and, since  $\bullet\text{NO}$  concentrations in the resting cell will stay in the nanomolar range and oxygen concentrations in tissue are also not very high, this mechanism is unlikely to present the major pathway of the observed *S*-nitrosations *in vivo*.

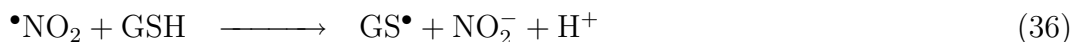
These shortcomings do not mean that nitrosation via autoxidation of  $\bullet\text{NO}$  cannot occur in the cell; in fact, NEDOSPASOV *et al.* calculated that this autoxidation will be likely inside protein-hydrophobic cores. Dioxygen,  $\bullet\text{NO}$ ,  $\bullet\text{NO}_2$  and  $\text{N}_2\text{O}_3$  are uncharged and it is known that  $\text{O}_2$  and  $\bullet\text{NO}$  will be enriched at hydrophobic regions. Therefore  $\text{N}_2\text{O}_3$  can be formed directly at the target protein which in consequence will be *S*-nitrosated in an autocatalytic way [20].

In consideration of the  $\bullet\text{NO}/\text{O}_2^{\bullet-}$  system, the discussed reactivity of peroxynitrite with  $\text{CO}_2$  could partly explain the observed *S*-nitrosations:



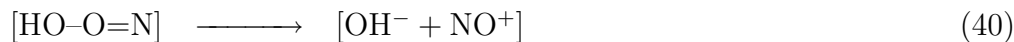
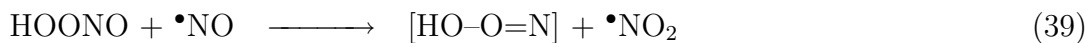
However, as already discussed, a subsidiary mechanism is necessary to explain experimental data, because nitrosation under these conditions occurs also in the absence of  $\text{CO}_2$ /bicarbonate. And all of the discussed mechanisms utilize the electrophile  $\text{N}_2\text{O}_3$  as the main nitrosating intermediate, which does not necessarily has to be the case. Even if  $\text{N}_2\text{O}_3$  plays an important role in homogeneous aqueous buffer solutions under physiological, aerobic model conditions, it won't play the same role in heterogeneous systems, including all living systems [72]. In fact, scavenging  $\text{N}_2\text{O}_3$  with azide [73] at aerobic conditions can only partly prevent nitrosation by  $\bullet\text{NO}$  alone or in the  $\bullet\text{NO}/\text{O}_2^{\bullet-}$  system, as will be presented in Section 5.2.1 [51, 52].

A free radical pathway of nitrosation via thiyl radicals ( $\text{RS}\bullet$ ) also seems feasible, as proposed independently by SCHRAMMEL *et al.* [74] and JOURD'HEUIL *et al.* [75]. Due to its high availability, glutathione represents the most likely target for *S*-nitrosation in this case. The *S*-nitrosation of protein targets will therefore occur via transnitrosation, in which a thiolate anion nucleophilically attacks the nitrogen atom of a *S*-nitrosothiol, resulting in the transfer of the nitroso group to the thiol:



This pathway could compete with the reaction of  $\text{GS}\bullet$  with  $\text{O}_2$ , yielding in the thiylperoxyl radical  $\text{GSOO}\bullet$ . However, since this reaction is in rapid equilibrium with its back reaction and steady-state levels of thiyl radicals should be low, and furthermore, reactions of the product are relatively slow, this should exhibit only little effect at quenching thiyl radicals at physiological conditions [76]. Contrary to

literature, a mechanism based on the reaction of HOONO with  $\bullet\text{NO}$  is proposed in this work.



As discussed earlier, this reaction is in principle known in literature, although its mechanism, products and kinetic properties still remain to be determined. This would indeed explain the large amounts of *S*-nitrosation even in the absence of  $\text{CO}_2$  or in the presence of azide. The reaction and its relevance will be discussed in detail in Section 5.3.

The nature of the specific thiol residue is of particular importance for its ability to become *S*-nitrosated. Thiols with a lower  $\text{p}K_{\text{a}}$  value tend to become easier nitrosated compared to those who cannot be deprotonated at physiological conditions. Especially Cys-149 of glyceraldehyde-3-phosphate dehydrogenase (GAPDH) exhibits one of the lowest known  $\text{p}K_{\text{a}}$  value for a cellular thiol and will easily become *S*-nitrosated [77]. All analyzed *S*-nitrosations occur at L-cysteines, which represent the exclusive source of thiols at protein level. If nitrosation, as is out of question, represents a regulative mechanism, it has to be limited to specific cysteines. Therefore, the specificity of nitrosation of protein-bound cysteines can only be controlled by the electrostatic properties of the surrounding amino acids, besides steric obstacles. By analyzing enzymes which are known to be regulated by *S*-nitrosation, STAMLER *et al.* proposed a consensus motif for *S*-nitrosation [78] whereas the cysteine in question will be surrounded by charged amino acids, with a basic and an acidic amino acid at the adjacent positions. Transnitrosation between low-molecular-weight *S*-nitrosothiols and protein thiols could then occur via acid-base catalysis. It is well-established that deprotonation of thiols is suppressed and enhanced, respectively, by neighboring acidic and basic groups [79]. By querying databases, the general motif (Arg|His|Lys)Cys(Asp|Glu) was found to be particularly significant [78].

As the thiol  $pK_a$  is crucial for transnitrosation and the  $pK_a$  of a thiol may be altered by amino acids that are close in space, it is likely that thiol environment rather than a consensus sequence is an important factor for *S*-nitrosothiol formation [80]. Further decrease of thiol  $pK_a$  can be realized in some cases by the coordination of  $Zn^{2+}$  by Cys in metalloproteins and in other proteins by the interaction of surrounding aromatic side chains. It is worth noting that literature frequently does not differentiate between the state of the thiol group and therefore most described reaction constants are defined at a given pH value.

As already mentioned, *S*-nitrosations of enzymes do not necessarily have to occur due to direct nitrosation, as a matter of fact in many cases the *S*-nitrosocysteine will be yielded by transnitrosation from *S*-nitrosoglutathione (GSNO). This implicates that glutathione-binding motifs surrounding a cysteine can lead to transnitrosation, as was reported in several cases [79]. In aldose reductase, the redox-reactive Cys-298 features a surrounding glutathione-binding site, but exhibits a notable more complex behavior; glutathione-binding possibly results in denitrosation if already nitrosated, which will be discussed later [81–83].

#### 3.5.2.2 Redox Regulation by S-Nitrosation

Based on the proposed mechanisms as well as on experimental data, it can be assumed that *S*-nitrosations in the organism are requiring production of  $\bullet NO$  at elevated levels of  $O_2^{\bullet -}$ . In context of this work only *S*-nitrosation will be discussed—however, both *N*- and *O*-nitrosation have been shown to be potentially important biological modifications [84, 85]. In general, thiols and thiolate anions are much stronger nucleophiles than their corresponding alcohols and amines and therefore represent kinetically superior targets for electrophilic nitrosating agents.

In chemical systems, *S*-nitrosothiols were known to be very unstable and to decompose to yield  $\bullet NO$  and thiyl radicals. However, this reaction was greatly overestimated

due to the unrecognized fact that trace levels of metal ions, especially iron and copper, are effective catalysts of their decomposition, and in addition, *S*-nitrosothiols are susceptible to photolytic decomposition. In the organism these decomposition pathways are negligible and *S*-nitrosothiols have to be considered as intrinsically stable entities, except in the case of LMW *S*-nitrosothiols. These short-lived species tend to transfer the nitroso-group to other thiols.

Nitrosation occurs in the organisms mainly at the level of cells, dependent on the sub-cellular location of the relevant radical sources. Especially in blood direct nitrosation seems improbable—the omnipresent hemoglobin, more precisely oxyhemoglobin, will scavenge free  $\bullet\text{NO}$  prior to further reactions, and the nitrosating intermediates itself are too unstable to affect targets beyond the location of their formation. Prior to the discovery of the *S*-nitrosation of oxyHb, studies of  $\bullet\text{NO}$  and Hb have focused almost entirely on the fast reactions of oxyHb and deoxyHb with  $\bullet\text{NO}$  to yield the ferric methemoglobin (metHb) and ferrous nitrosyl hemoglobin (HbNO), respectively. These reactions account to the low concentrations of  $\bullet\text{NO}$  in blood, which usually remain in the low nanomolar range. However, *S*-nitrosothiols are transported in blood as *S*-nitroso albumin (and *S*-nitrosohemoglobin), as is known since more than a decade. This circulating pool of *S*-nitrosothiols is coupled with the cellular *S*-nitrosoglutathione and finally, via transnitrosation, stands in balance with the nitrosation of cellular proteins. In this respect, nitrosation has to be considered as a phenomenon affecting not only the location of its formation. Contrary to the widespread assumption, *S*-nitrosothiols do not provide a source for free  $\bullet\text{NO}$  in the organism, just as  $\bullet\text{NO}$  itself is not a nitrosating intermediate. Therefore, these high amounts of *S*-nitrosothiols in the cardiovascular system may not represent a storage pool for  $\bullet\text{NO}$ , but rather for nitrosation, and therefore only transnitrosation may be feasible.

Serum albumin exhibits exactly one accessible cysteine, Cys-34, and its remarkably low  $\text{p}K_{\text{a}}$  permits easy nitrosation. STAMLER *et al.* found that human plasma contains

### 3 The Role of Small Signaling Molecules in the Vascular System

approximately 7  $\mu\text{M}$  *S*-nitrosothiols, of which 79% is accounted for by *S*-nitroso serum albumin. At the same time the level of  $\bullet\text{NO}$  in plasma stayed in the low nanomolar range, excluding plasma and blood as source of nitrosating intermediates [86]. Albumin itself can easily and effectively be nitrosated via transnitrosation by low-molecular-weight (LMW) *S*-nitrosothiols like GSNO and *L-S*-nitrosocysteine (CysNO) whereas a direct nitrosation is remarkably less favorable [87]. And by isotope labelling, it was also demonstrated, that  $\text{GS}^{15}\text{NO}$  indeed transfers the NO-group to yield  $\text{S}^{15}\text{NO}$ -albumin *in vivo* [87].

Besides serum albumin, hemoglobin (Hb) is the other target of nitrosation in blood which gained increased interest. STAMLER *et al.* discovered that Cys-93 of the  $\beta$ -globin chain will be *S*-nitrosated in a reversible way, dependent on the oxygen tension [88]. Only oxyhemoglobin (oxyHb) can be nitrosated, and deoxygenation (deoxyHb) will cause a conformational change which will yield in the reversal of the nitrosation. A proximate histidine residue will permit a base-catalyzed nitrosation in the relaxed (R) conformation of the protein, which has higher affinity for  $\text{O}_2$ , and due to conformation-dependent positioning, denitrosation will be promoted by the proximity of the aspartate in the tense state (“T conformation”) [78]. This allosteric mechanism was proposed to deliver  $\bullet\text{NO}$  to the cardiovascular system [88, 89], but the mechanism of heme nitrosation as well as the formation of free  $\bullet\text{NO}$  from HbSNO is questionable [90] and need further analysis.

Current knowledge therefore favors *S*-nitrosoalbumin as the stable storage and transport medium of *S*-nitrosothiols in the circulation, whereas LMW *S*-nitrosothiols are rather unstable under these conditions, but occupy this role in cellular context. It was many times observed that administration of *S*-nitrosothiols results in vasodilation and inhibition of platelet aggregation [91], both not necessarily in a cGMP mediated pathway. The missing link in this picture of a comprehensive model for redox regulation by *S*-nitrosation, the transfer of *S*-nitrosation equivalents between cells and plasma, is assumed to occur via CysNO. Based on the observation that the presence of Cys (or

cystine) is required for the cellular uptake of *S*-nitrosothiols, that L-isomers of LMW *S*-nitrosothiols are more effective in their bioactivity than their D-counterpart, and that inhibition of L-type amino acid transporters prevents intracellular *S*-nitrosothiol formation, ZHANG and HOGG hypothesized that the plasmatic *S*-nitrosothiols, after transnitrosation to CysNO, will be transported to the cytosol by amino acid transporters [92] and CysNO can then transfer the nitroso group to GSH, yielding the more stable GSNO.

In the cell, GSNO will act via transnitrosation and will be in equilibrium with protein *S*-nitrosothiols, but it still has to be shown if this is the primary pathway of protein *S*-nitrosation. The second order rate constants of *S*-nitrosothiol-thiol exchanges between Cys, GSH and their *S*-nitrosated variants were determined by MEYER *et al.* to be in the range of  $k_2 = 80\text{--}100 \text{ M}^{-1}\text{s}^{-1}$  [93]. Given the low concentrations of reduced Cys and GSH in plasma, these transnitroations should be very slow in plasma, but would explain the rapid conversion of imported *S*-nitrosothiols to GSNO. At first glance this observation collide with the assumption that the cellular import of *S*-nitrosothiols has to occur via CysNO. However, the cell's surface  $\chi_c^-$  transporter is able to reduce cystine [92], which is present in the range of 30–65  $\mu\text{M}$  in human plasma, to Cys enabling transnitrosation close to the cell surface.

The glutathione-dependent formaldehyde dehydrogenase, an alcohol dehydrogenase III, seems to be the crucial enzyme in GSNO metabolism. JENSEN *et al.* were the first who discovered the NADH-dependent GSNO degrading activity of the isolated enzyme—in fact it showed much greater activity toward GSNO than any other substrate [94]. Later it was shown that this enzyme affects intracellular GSNO levels *in vivo*, protects against nitrosative stress and is evolutionarily conserved from bacteria to humans [95] and was therefore named “GSNO reductase” (GSNOR). The products of the irreversible GSNO reduction were determined to be glutathione sulfinamide and GSSG [96]. Taken together, the cytosolic and nuclear localized GSNOR [97] seems to represent the main denitrosating activity. But also Cu,Zn-SOD exhibits

an important function in catalyzing the decomposition of *S*-nitrosothiols through its copper center [98]. This mechanism requires the presence of GSH, presumably for the reduction of  $\text{Cu}^{2+}$  to  $\text{Cu}^+$  prior to the denitrosation step, yielding in  $\bullet\text{NO}$  and the corresponding disulfide [99, 100]. Familial ALS (FALS)-related mutations in SOD1 result in an increase of its denitrosation activity, which seems to lead to depletion of intracellular *S*-nitrosothiols and therefore could contribute to ALS pathogenesis [101]. Besides GSNOR and Cu,Zn-SOD, a variety of enzymes are also reported to catalyze decomposition of *S*-nitrosothiols *in vitro*, e. g. glutathione peroxidase [102, 103], the thioredoxin system [104], cell-surface protein disulfide isomerase [105],  $\gamma$ -glutamyl transpeptidase [106] and xanthine oxidase [107]. The importance of these proteins in this context and the detailed mechanism of denitrosation still has to be analyzed. And in addition, ascorbate [100, 108, 109],  $\text{O}_2^{\bullet-}$  [107] and GSH itself [110] are able to reduce *S*-nitrosothiols.

Persistent *S*-nitrosations in the cell will lead to so-called “nitrosative stress”, where intracellular thiols are significantly decreased. When production of a metabolite exceeds either the physiological requirements or the compensatory capacity of the system resulting in accumulation of an end product, a situation of chemically induced “stress” appears. Based on this definition, nitrosative stress has to occur in the context of the here discussed picture of redox regulation. However, biological stress, e. g. oxidative stress, implies that these accumulating products will harm the cell, whereas nitrosative stress can be seen as an embracing reaction of the cell to avoid or to be at least prepared to oxidative stress [111]. Therefore, a fine balance between oxidative and nitrosative stress must exist in the cell in order to maintain a normal physiological and alert state [112].

In many cases *S*-nitrosations, especially under conditions of nitrosative stress, are linked with sulfenic acid and disulfide formation [113] as signs of oxidative stress. Disulfide formation, or *S*-thiolation, occurs when a thiolate anion nucleophilically attacks the sulfur atom of an *S*-nitrosothiol, resulting in the formation of nitroxyl

anion ( $\text{NO}^-$ ) and a disulfide. This disulfide can appear as intra-, inter-protein or mixed disulfide formation. The formation of mixed disulfides occurs mainly as a so-called *S*-glutathiolation (or *S*-glutathionylation), and under normal conditions will be quickly reduced by the Trx and Grx systems (Fig. 1.1). Glutathiolation via this mechanism or via transfer from GSSG and subsequent reduction after the cell's reductive systems have recovered represents an alternative route for denitrosation.

But during oxidative stress, where NADPH levels will remarkably decrease, these post-translational disulfide modifications will accumulate and affect enzyme activities. *S*-Glutathiolation associated with modified enzyme activity or protein structure was reported in many cases for proteins, which were later also discovered to be regulated by *S*-nitrosation, e. g. creatine kinase [114], GAPDH [77], caspase-3 [115] and aldose reductase [116]. These examples of *S*-glutathiolation and their link to cellular redox cofactor metabolism are of high importance in the later discussed model of redox regulation by *S*-nitrosation. Other examples of similar regulated proteins are rather linked with  $\text{H}_2\text{O}_2$  formation [113] and will be addressed at the according section.

A series of proteins have been found in an *S*-nitrosated state and even a “nitrosylome” has been postulated [117]; considering the differences between nitrosylation and nitrosation, a more appropriate term would have been “nitrososome”. But one has to be cautious regarding the inflation of proteins reported to be *S*-nitrosated under certain conditions. Especially the proteomic approach of the biotin-switch method for detection of *S*-nitrosated proteins [118] leads to the detection of a variety of targets [117, 119–121], but is in the meantime known to also produce false-positives. This method is based on the ascorbate-mediated reduction of *S*-nitrosothiols, but recently it was shown that ascorbate will also reduce some weak disulfides [122]. Furthermore, the conditions where *S*-nitrosation was measured were often problematic by itself. In many cases, cells or purified proteins were treated with inadequate and too strong nitrosating or oxidizing substances, resulting in unspecific reactions which do not necessarily reflect biological meaningful mechanisms. A selection of proteins reported

### 3 The Role of Small Signaling Molecules in the Vascular System

to be *S*-nitrosated is compiled in the following table, and if known, the effect of *S*-nitrosation on enzymatic activity is indicated:

Protein	Activity	References
<i>Blood</i>		
Hemoglobin		[88]
Albumin		[86]
<i>Reductive systems and energy metabolism</i>		
GAPDH	–	[117, 121, 123, 124]
NADPH-dependent isocitrate dehydrogenase	–	[125]
Thioredoxin	+	[2, 126–128]
Peroxiredoxin 1		[117, 121]
GSH		
<i>Transcription factors</i>		
NF $\kappa$ B	–	[129–131]
Activator protein-1 (AP-1)	–	[132]
Hypoxia-inducible factor-1 $\alpha$ (HIF-1 $\alpha$ )	+	[133]
p53	+	[79]
<i>Apoptosis-related proteins</i>		
Procaspase-3	–	[115, 128, 134, 135]
Procaspase-9	–	[136–138]
Apoptosis signal-regulating kinase 1 (ASK1)	–	[139]
Jun <i>N</i> -terminal kinase (JNK)	–	[79]
<i>Small GTPases</i>		
Ras	+	[128]
Ran		[140]
Dexas1	+	[79, 141]
<i>Arginine metabolism and NOS-related proteins</i>		
Argininosuccinate synthase	–	[142]
Dimethylarginine dimethylaminohydrolases	–	[79, 143]
Ornithine carboxylase	–	[79]
Methionine adenosyltransferase	–	[79]
<i>S</i> -Adenosylmethionine decarboxylase	–	[79]
Hsp90	–	[120, 144]
<i>N</i> -Methyl-D-aspartate (NMDA) receptor	–	[145, 146]
<i>Matrix metalloproteases</i>		
MMP-9	+	[147]
TNF $\alpha$ -converting enzyme	+	[79]
<i>Structural proteins</i>		
$\beta/\gamma$ -Actin	–	[117, 121, 148]
T-plastin		[117]
Tropomyosin 4		[117]
<i>Insulin metabolism, diabetes and diabetic complications</i>		
Aldose reductase (ALR2)	+	[83]
Akt/PKB	–	[149, 150]

### 3 The Role of Small Signaling Molecules in the Vascular System

Insulin receptor/Insulin receptor substrate 1	–	[150]
Glucokinase	–	[151]
<i>Phosphatases</i>		
Protein tyrosine phosphatase 1B	–	[79]
<i>Membrane receptors, ion channels and related proteins</i>		
Ryanodine receptor	+	[152]
Epidermal growth factor receptor tyrosine kinase	–	[79]
G-protein coupled receptors		[79]
Annexin A2	–	[117, 153]
<i>Ubiquitination</i>		
Parkin	+/-	[154–156]
Ubiquitin-conjugating enzyme (UbcH7)	–	[121]

---

An interesting example of *S*-nitrosation has been reported for caspases. In addition to their existence as pro-enzymes, *S*-nitrosation of their essential thiol groups appears to provide a further mechanism of inactivation. Reduction can lead to caspase activation and thus, to apoptosis [134, 136]. Similarly, the NF $\kappa$ B pathway was found to be blocked by S-NO formation at the p50 subunit, ready to be converted back under the reducing conditions prevailing in the nucleus [129].

Not only signaling pathways are regulated by *S*-nitrosation, also the cellular redox status itself is regulated by Trx and its associated reducing system (Trx, Trx reductase, NADPH). The Trx system together with Grx and GSH represent the reductive system of the cell [2]; their reductive power is driven by NADPH. Trx reduces oxidized cysteine groups on proteins, scavenges ROS together with Trx peroxidase and acts as a transcriptional activator via NF $\kappa$ B. *S*-Nitrosation of Trx at Cys-69 is necessary for its redox regulatory function [126], whereas the inactivating oxidation of Cys-32 and 35 causes apoptosis via apoptosis signal-regulating kinase 1 [127]. Additionally, Trx gets inactivated by *S*-glutathiolation of Cys-73. Therefore, the Trx system is a key regulator of the cellular redox state, regulated by the cellular redox state itself. The impact on the systems regulated by *S*-nitrosation and the interplay of these systems will be discussed later in this work.

### 3.5.3 Oxidations by Peroxynitrite

The balance between  $\bullet\text{NO}$  and  $\text{O}_2^{\bullet-}$  formation is the crucial variable in the  $\bullet\text{NO}/\text{O}_2^{\bullet-}$  system. Peroxynitrite will be formed whenever both of the radicals are present, but only when the rates of  $\text{O}_2^{\bullet-}$  formation in an activated cell approaches that of  $\bullet\text{NO}$ , the subsequently formed peroxynitrite will lead to thiol oxidation, methionine sulfoxidation and tyrosine nitration. A slight excess of either one of the radicals will result in a distinct reaction pattern.

#### 3.5.3.1 Thiol Oxidation

Although peroxynitrite is a potent oxidant, its actual levels will usually stay in the nanomolar range. Under these conditions, oxidations by peroxynitrite often occur in a metal catalyzed manner, as in the case for tyrosine nitration and oxidation of zinc-containing proteins. Peroxynitrite will react with protein thiols to sulfenic acids which then readily form mixed disulfides with GSH. In the case of zinc fingers,  $\text{Zn}^{2+}$  will be released after disulfide formation between adjacent Cys residues [51, 157, 158]. Since zinc fingers are abundant in transcription factors and required for DNA binding, their oxidation will prevent transcription. Under these oxidative conditions also DNA strand breaks will prevail, therefore this seems to be a meaningful regulation to prevent reading of the unrepaired DNA. The identification of peroxynitrite as the zinc finger-oxidizing intermediate was achieved in context of this work [51] and will be discussed at the accordant position.

Matrix metalloproteinases (MMP) are a family of zinc-containing endopeptidases, responsible for the degradation of extracellular matrix. They are synthesized as pro-enzymes and are known to be activated by oxidant species including peroxynitrite. Breakage of the bond between Cys and  $\text{Zn}^{2+}$  at the catalytic centre is necessary for its activation; this can be achieved by proteolytic cleavage, conformational changes or oxidants like peroxynitrite [159–161]. Both MMP-2 [159] and MMP-8 [160] are

reported to be activated by peroxynitrite. This oxidative activation during conditions of oxidative stress can lead to degradation of the extracellular matrix, linked with tissue injury [159, 161, 162]. But apart from roles of MMPs in these long-term remodeling processes, there is increasing evidence that some MMPs like MMP-2 can also rapidly regulate diverse cellular functions, e. g. platelet activation, vascular tone and attenuation of inflammatory signals. These are regulatory mechanisms fitting in the depicted network of complex redox regulative events, especially considering the conditions where oxidations by peroxynitrite occur—if the systems are shifting slowly from nitrosative conditions to oxidative stress. Besides zinc-thiolate targets, increased levels of  $^-OONO$  can also lead to damage of iron prosthetic groups in enzymes, e. g. the iron-sulphur clusters in aconitase [163–165], accompanied with enzyme inactivation.

#### **3.5.3.2 Methionine Sulfoxidation**

Methionine (Met) is one of the most readily oxidized amino acid constituents of proteins [166]. Many oxidants in biological systems will attack Met, besides  $H_2O_2$  and hydroxyl radicals also peroxynitrite. The product of these oxidations is methionine sulfoxide [167], which can be reduced back by methionine sulfoxide reductase. Sulfoxidations are in many cases connected with changes in enzyme activity. Therefore, methionine sulfoxidations are presenting a mechanism of redox regulation. A prominent example of this regulatory mechanism presents the redox regulation of proteolysis at the level of antiproteases. Some protease inhibitors are reported to be blocked by Met sulfoxidation during physiological processes [168], giving way for protease activation. This seems feasible during immune response and, more generally, at all kinds of inflammation processes.

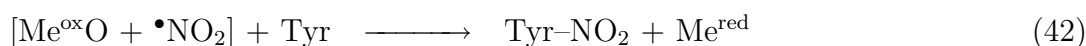
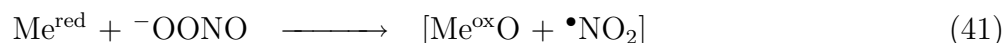
### 3.5.3.3 Nitration

Seminal work by BECKMAN *et al.* [169] and ISCHIROPOULOS *et al.* [170] demonstrated the capacity of peroxynitrite to cause protein tyrosine nitration *in vitro* and postulated that this nitration could occur likewise *in vivo*. The formation of 3-nitrotyrosine at protein level *in vivo* as a result of the combined action of  $\bullet\text{NO}$  and  $\text{O}_2^{\bullet-}$  is now well accepted, whereas the chemical mechanism of protein nitration as well as the relevance in redox regulation caused enduring debates. In context of redox regulation, the specificity of Tyr-nitration as well as a regulatory function of this covalent posttranslational protein modification are essential requirements. Eventually, the reversal of nitration stays an unsolved problem, if seen as a regulatory mechanism.

Regarding the mechanism of protein nitration, two distinct pathways leading to 3-nitrotyrosine (3-NT) have to be differentiated. Peroxynitrite itself is unable to yield Tyr-nitration, despite the fact that 3-NT formation is seen as a biomarker for peroxynitrite or at least  $\bullet\text{NO}$  formation *in vivo*. GOLDSTEIN *et al.* postulated a free radical pathway of nitration in response to the observation that the Tyr-nitration during simultaneous production of  $\bullet\text{NO}$  and  $\text{O}_2^{\bullet-}$  at physiological conditions causes a reaction profile very distinct from that of a bolus addition of peroxynitrite and the different effects of  $\text{CO}_2$  on the 3-NT yield [56]. Based on these observations and on pulse radiolysis studies, a mechanism requiring a tyrosyl radical was developed. The formation of a tyrosyl radical can be the consequence of the oxidative actions of  $\text{CO}_3^{\bullet-}$  or oxo-metal complexes and, to a lesser extent,  $\bullet\text{OH}$ . The Tyr radical itself can react with  $\bullet\text{NO}_2$  to yield 3-NT as well as with  $\bullet\text{NO}$ , yielding 3-nitrosotyrosine and followed by a sequential two-electron oxidation to 3-NT.

It is now clear that Tyr-nitration does not occur with any Tyr residue at physiological  $^-\text{OONO}$  levels but requires catalysis by metal centers [171, 172]. According to this mechanism, peroxynitrite would first form a complex with the transition metal, allowing nitration of a proximal Tyr residue [1, 66, 172]:

### 3 The Role of Small Signaling Molecules in the Vascular System



So far Mn-SOD [173–175] and prostacyclin (PGI<sub>2</sub>) synthase [176] are the only known enzymes which will be nitrated even at very low levels of peroxynitrite, allowing nitration not only at conditions of severe oxidative stress. This autocatalytic mechanism of Tyr-nitration at the metal center of an enzyme would allow to explain these sensitive nitrations. ZOU *et al.* demonstrated that 50 nM peroxynitrite are sufficient to nitrate PGI<sub>2</sub> synthase *in vitro* [176], and later MALINSKI *et al.* reported 150 nM <sup>-</sup>OONO as sufficient to inhibit PGI<sub>2</sub> formation in intact cells [177]. This nitration was shown to occur solely at Tyr-430 of the bovine enzyme [178] and inhibits enzymatic activity irreversibly. The relevance of a selective nitration and inhibition of PGI<sub>2</sub> synthase was demonstrated by BACHSCHMID *et al.* in an *ex vivo* model of endothelial cell activation, leading to vasospasm [179]. Since PGHS is still active under such conditions, PGH<sub>2</sub> will accumulate and bind to the TxA<sub>2</sub>/PGH<sub>2</sub>-receptor on the surface of VSMC, the antagonistic signal to PGI<sub>2</sub>, to evoke vessel constriction. Considering that under these conditions <sup>•</sup>NO will be blocked by O<sub>2</sub><sup>•-</sup>, the two main pathways of vasorelaxation are effectively blocked, leading to endothelial cell activation and dysfunction.

A chemical reversibility of Tyr-nitration has not yet been found in the case of PGI<sub>2</sub> synthase, and hence, this does not exactly meet the requirements of a mechanism of redox regulation but rather has to be considered as a consequence of oxidative stress. In a biological sense, however, 3-NT formation is a reversible process—PGI<sub>2</sub> synthase exhibits a half-life of approximately 30 h (GRAF, ULLRICH; unpublished results) and nitrated proteins are subject of increased degradation by proteasomal pathways and will be replaced through protein synthesis. The relevant sources of O<sub>2</sub><sup>•-</sup> required for nitration of PGI<sub>2</sub> synthase as well as the pathophysiological consequences of its inhibition are also supporting a view of this nitration as a mechanism of oxidative stress.

Under conditions of severe oxidative stress, not only PGI<sub>2</sub> synthase and Mn-SOD will be nitrated, but additionally, a higher number of enzymes was found in a nitrated state. In an cell culture-model, stimulation by cytokines results in Tyr-nitration of aldolase A, GAPDH and actin [175], whereas the latter was also found nitrated *in vivo* in a model of sickle cell disease [180]. Likewise, a model of hypoxia/reoxygenation revealed a dynamic pattern of protein nitration in mitochondria [175].

#### 3.5.4 Oxidations by an Excess of Superoxide

If all potential sources for O<sub>2</sub><sup>•-</sup> are activated, the resulting O<sub>2</sub><sup>•-</sup> levels may far exceed that of •NO. Especially mitochondria will contribute to O<sub>2</sub><sup>•-</sup> production in a controlled process involving Ca<sup>2+</sup>, ROS and structural changes triggered by the opening of the permeability transition pore (PTP). Reduction of O<sub>2</sub> to O<sub>2</sub><sup>•-</sup> may occur by autooxidation of redox components in complex I or III. The combined activity of Mn-SOD and GSH peroxidase should prevent mitochondrial O<sub>2</sub><sup>•-</sup> to leave the mitochondrial space, but GSH depletion and oxidative inactivation eventually would cause an increase also of cytosolic levels. These mitochondria-derived O<sub>2</sub><sup>•-</sup> production will by far exceed those levels originating from NADPH oxidase and thus may have severe consequences for the redox state of cytosolic components. In consequence, mitochondrial and subsequently cytosolic GSH is oxidized, followed by oxidation of vitamins C and E. Although these are conditions of severe oxidative stress, the cell's rescue mechanisms can be able to reverse the oxidative stress as well as the activation of O<sub>2</sub><sup>•-</sup> sources.

Persistent O<sub>2</sub><sup>•-</sup> production will result in oxidation of tetrahydrobiopterin to BH<sub>2</sub>—•NO synthesis will cease and NOS will switch to NADPH-dependent O<sub>2</sub><sup>•-</sup> production. Besides further increased O<sub>2</sub><sup>•-</sup> production, this abolishes the O<sub>2</sub><sup>•-</sup>-quenching actions of •NO, leading to even higher O<sub>2</sub><sup>•-</sup> levels allowing Fenton chemistry, yielding in •OH-radical formation. Lipid peroxidations will finally lead to cell death.

Apart from this pathway to severe oxidative stress,  $O_2^{\bullet-}$  can act on some enzymes as a regulator of enzyme activity. Calcineurin (CaN), a  $Ca^{2+}$ /calcineurin-dependent protein serine/threonine phosphatase, exhibits a binuclear  $Fe^{II}-Zn^{II}$  center at its active site, which will be oxidized by  $O_2^{\bullet-}$  to  $Fe^{III}-Zn^{II}$ , resulting in inhibition of the phosphatase function of the enzyme [5]. This oxidation will occur at low levels of  $O_2^{\bullet-}$  and can be reversed *in vitro* by mild reducing agents like ascorbate. Although much more potent oxidants are formed in the  $\bullet NO/O_2^{\bullet-}$  system, only  $O_2^{\bullet-}$  itself is able to attack the  $Fe^{II}-Zn^{II}$  center at physiological conditions. This, together with the role of CaN as a key regulator of various signaling processes, demonstrates the role of  $O_2^{\bullet-}$  as a direct messenger [181].

The already mentioned aconitase and its reactive  $[Fe_4S_4]^{2+}$  cluster will be oxidized by  $O_2^{\bullet-}$ , but also by peroxynitrite, resulting in inhibition of both the mitochondrial and the cytosolic isoform [163, 164]. Oxidation of the iron-sulphur cluster occurs at the non-cysteine coordinated iron centre and results in loss of this iron. Considering the essential role of mitochondrial aconitase in the tricarboxylic acid (TCA) cycle, its inactivation will lead to depletion of ATP and NADPH. The cytosolic isoform, also known as iron regulatory protein-1 (IRP-1), plays a central role in the regulation of iron metabolism—the loss of iron will lead to binding to the iron response element, contained within the mRNA of iron-related proteins. Therefore, production of iron storage molecules will be inhibited. This shows that aconitase is not only a crucial sensor for iron, but at the same time also for oxidative stress.

#### 3.5.5 Oxidations by Hydrogen Peroxide

Hydrogen peroxide, if its formation cannot be prevented, will lead at high levels to oxidative modifications of cellular thiol groups. This disulfide formation can occur as intra- and inter-protein disulfides, or in the case of *S*-glutathiolation, between

glutathione and the protein [113]. Some interesting regulatory mechanisms are derived from thiol oxidations by  $H_2O_2$ .

The GTPase Ras will be activated by *S*-glutathiolation at Cys-118 after stimulation by  $H_2O_2$  in a similar way than its activation by *S*-nitrosation [128]. This was shown to be important in angiotensin II (Ang II) signaling in vascular smooth muscle cells (VSMC), where Ang II in an NADPH oxidase-dependent mechanism leads to a burst of  $H_2O_2$  and contributes to vascular hypertrophy. This induces Ras activity by *S*-glutathiolation and subsequent p38 and Akt phosphorylation, which contributes to the induction of protein synthesis [182].

The formation of intra-protein disulfides in response to cellular  $H_2O_2$  formation was observed at protein phosphatase Cdc25C, a critical component of cell cycle progression and checkpoint control. Oxidation by  $H_2O_2$  was demonstrated to cause an intra-protein disulfide formation between Cys-330 and Cys-377 [183], leading to increased degradation of the enzyme. These results suggest that oxidative stress may induce cell cycle arrest in part through the degradation of Cdc25C.

In addition, inter-protein disulfide formation triggered by  $H_2O_2$ -mediated thiol oxidation can occur, as is the case in receptor protein-tyrosine phosphatases  $\alpha$  (RPTP $\alpha$ ). Disulfide formation at the catalytic Cys results in dimerization and inhibition, whereas catalytic activity will be restored after decay of the oxidative stress and subsequent refolding of the protein to its active conformation [184].

## 3.6 Carbon Monoxide

In the past, carbon monoxide (CO) was mainly known to be a toxic molecule due to its high affinity to hemoglobin, connected with numerous death cases by CO-poisoning. But there is an increasing number of investigations indicating that small doses of carbon monoxide are beneficial under conditions of a disturbed oxygen supply in the

living organism. In addition, endogenously produced CO will provide physiologically relevant concentrations of 3–30  $\mu\text{M}$  [185]. Within this context CO seems to have similar effects as the vasodilator  $\bullet\text{NO}$ , but the main question, why CO acts similar to  $\bullet\text{NO}$ , remains unsolved and there is still no satisfying explanation for this phenomenon.

The importance of CO as a not only toxic molecule was revised since the enzyme heme oxygenase was discovered as a CO-synthase. Heme oxygenase (HO) catalyzes the degradation of heme to biliverdin IX $\alpha$ , iron and CO. One should also mention that biliverdin IX $\alpha$  is acting as a potent antioxidant, but that does not explain the observed beneficial effects. First CO was seen as an unwanted byproduct of heme degradation, but it was shown that there are conditions where the cell invests high amounts of energy for heme synthesis just as a substrate for HO. In the meantime three isoforms of heme oxygenase are known, two constitutive (HO-2, HO-3) and an inducible (HO-1). The inducible isoform will be expressed at conditions of cellular stress, whereas HO-2 may exist in most tissues in the absence of stress; the significance and role of HO-3 remains unclear. Heme oxygenases perform a substantial role in the turnover of hemoglobin during the metabolism of senescent erythrocytes, especially in spleen, liver and kidney, and regulates the intracellular concentration of heme. Similar to NOS-1 and NOS-1-derived  $\bullet\text{NO}$ , HO-2 and CO are acting as coneurotransmitters in the peripheral autonomic nervous system, whereas in many cases both enzymes are reported to be colocalized [186–191]. In endothelial cells, the inducible isoform localizes to caveolae and its activity is attenuated via direct interaction with caveolin-1 [192], which both also applies to constitutive NOS.

The beneficial effects of CO are mainly due to its  $\bullet\text{NO}$ -like properties like smooth muscle relaxation and inhibition of platelet aggregation [193, 194] and its prevention of apoptosis during critical conditions. In this respect CO is reported to protect in animal models against organ graft rejection [195, 196], arteriosclerotic lesions associated with chronic graft rejection and balloon injury [195], septic shock and cytokine-induced apoptosis [197–201] and ischemia/reperfusion damage [196, 202–205]. If HO expression

is suppressed under such conditions, the symptoms will get worse, and the exogenous administration of CO is reported to be beneficial. MOTTERLINI *et al.* developed metal carbonyls as a new class of CO-releasing drugs which were demonstrated to protect against hypertension, ischemia, platelet aggregation and organ rejection, besides vasorelaxation [206, 207].

A fast growing number of articles is dealing with CO as a signaling molecule, but the main problem remains unsolved: If CO is a messenger, it needs some kind of receptor, a protein with a high affinity towards CO. Carbon monoxide has a similar molecular weight and solubility to •NO, but contrary to •NO it is a very inert substance. Interactions with amino acids are not possible, only ferrous iron is a feasible cellular target. The highest known affinity of a biomolecule towards CO has Hb, which cannot be responsible for the observed effects at low doses of CO. The concentrations where CO acts as a messenger seems to be in the range of 0.1–1  $\mu\text{M}$ , at these low concentrations toxic effects of HbCO formation can be ruled out. As early as 1959 it was shown that there could be a target for CO with higher affinity than Hb. In humans, HALPERIN *et al.* could demonstrate that the visual sensitivity was decreased *in vivo* by treatment with CO, but did not recover immediately after HbCO vanished in blood [208]. Unfortunately, this target has not been identified up until now.

First indications showed that sGC will be activated by CO [193, 209], which would explain the similar effects of CO and •NO. But in the mean time it is well accepted that relevant concentration of CO are not sufficient to excite sGC activation. A solution to this dilemma could be the sensibilization of sGC towards CO by a substance with an effect comparable to 1-benzyl-3-(5-hydroxymethyl-2-furyl)indazole (YC-1). The substance YC-1 is able to sensitize sGC towards CO in such a way that CO will be able to activate sGC like •NO would do [210]. In this context it interesting to speculate whether there may be an endogenous physiological counterpart of YC-1.

Besides sGC, a couple of other cellular targets are discussed to be the receptor for CO. p38 mitogen-activated protein kinase and p51 are reported to be a target for CO, but they do not contain a heme residue, therefore it is difficult to see a mechanism of interaction with CO. One possibility discussed in literature would be that the free iron derived from HO could bind to proteins, enabling CO interaction [211].

Big-conductance  $\text{Ca}^{2+}$ -activated  $\text{K}^+$  ( $\text{BK}_{\text{Ca}}$ ) channels are also discussed to be a target of CO signaling and in the meantime there exists increasing evidence that they represent one of the major targets during CO signaling. They are activated by intracellular  $\text{Ca}^{2+}$  and also by membrane potential depolarization and are abundant in vascular smooth muscle cells. Physiological activation of vascular  $\text{BK}_{\text{Ca}}$  channels may be an important mechanism to counteract vessel depolarization and constriction. Because of their large conductance, the activity of relatively few channels can exert a large effect. It was demonstrated by WANG *et al.* that CO is able to excite vasorelaxation through interaction with  $\text{BK}_{\text{Ca}}$  channels and that this interaction does not depend on  $\bullet\text{NO}$  or cGMP [212]. Nitric oxide is also known to activate  $\text{BK}_{\text{Ca}}$  channels, but subsequent publications revealed that this activation occurs at a different subunit of the channel as is discussed for CO interaction [213]. The role of CO in  $\text{BK}_{\text{Ca}}$  channel activation is emphasized by the finding that HO-2 is part of the  $\text{BK}_{\text{Ca}}$  channel complex where it seems to exert the function of an oxygen sensor [214]. Heme oxygenase-2 enhances  $\text{BK}_{\text{Ca}}$  channel activity during normoxia, whereas knockdown of HO-2 expression reduces channel activity, which can be restored by CO itself. This provides further evidence that CO is an endogenous regulator of  $\text{BK}_{\text{Ca}}$  channel activity, but without giving further hints about the nature of the required CO sensor. The exact mechanism of CO interaction remains therefore unsolved and because  $\text{BK}_{\text{Ca}}$  channels do not provide heme, no way of direct interaction with CO seemed feasible until now. However, recent results from JAGGAR *et al.* revealed that heme, which can bind to  $\text{BK}_{\text{Ca}}$  channels, seems to be the required sensor for CO [215]. Binding of heme or hemin to a conserved heme-binding domain of the channel's  $\alpha$  subunit triggers its inhibition;

CO can modify the binding of reduced heme and therefore releases BK<sub>Ca</sub> channel inhibition. In addition, due to the colocalization of HO with BK<sub>Ca</sub> channels, HO activation may also reduce membrane associated heme, which would in consequence elevate BK<sub>Ca</sub> channel activity.

CO and •NO signaling are known to intersect each other, resulting in similar effects, and indeed, in most cases the response to CO can be abolished by inhibition of sGC. The action of •NO could also be taken into account for the CO-derived vasorelaxation, inhibition of platelet aggregation as well as antiapoptotic effects. This indicates that CO may act through •NO. ISCHIROPOULOS, THOM *et al.* provided further results pointing in this direction; they observed a remarkably increase in 3-NT formation in the brain after CO treatment of rats [216, 217], as well as lipid peroxidations in the brain [218]. Furthermore, electron paramagnetic resonance spectroscopy (EPR) revealed a ninefold increased •NO signal immediately after CO treatment, which vanished after 20 min. In an *ex vivo* model, THORUP *et al.* were able to show CO-mediated •NO release in isolated renal resistance arteries within seconds after treatment, peaking at 100 nM CO [219]. All of these effects could be abolished by the treatment with the NOS inhibitor *N*<sup>ω</sup>-nitro-L-arginine methyl ester (L-NAME) [216, 217, 219]. Although this, taken together, gives a strong hint that •NO production will be immediately increased by a CO signal and therefore most of the actions of CO are due to increased levels of •NO.

In the lack of a convincing mechanism for an increased •NO production through CO, a release of •NO from a large intra- or extracellular “pool” was proposed. This pool was thought to consist of metal-bound •NO, which will be released after displacement by CO. Although no adequate store for •NO was found until now and despite the fact that this hypothesis is not able to explain most of the above discussed details, it became widely accepted in literature. These findings lead us to a hypothesis, which would allow to explain a direct activation of NOS through the action of CO. Based on the finding that during metabolic turnover NOS-1 will be present mainly in its

inactive  $\text{Fe}^{\text{II}}\text{-NO}$  form due to autoinhibition (see page 18), we hypothesize that CO is able to release this autoinhibition. This would allow markedly increased rates of  $\bullet\text{NO}$  formation, and because NOS-1 is in the meantime known to be present in a variety of different tissues, would allow to explain most of the signaling events derived from low doses of CO.

CO could react with the heme of NOS at two steps during  $\bullet\text{NO}$  synthesis; either with the  $[\text{FeO}]^{2+}$  or with the  $\text{Fe}^{\text{II}}\text{-NO}$  complex. The first possibility would result in NOS inhibition, which is not the case at the relevant concentrations of CO. The second possibility would result in an increased release of  $\bullet\text{NO}$  from this complex and therefore an increased  $k_{\text{off}}$  kinetic for  $\bullet\text{NO}$ . The same mechanism would lead, in the absence of the cofactor  $\text{BH}_4$ , to an increased formation of  $\text{O}_2^{\bullet-}$ . This hypothesis was tested within this work in cooperation with DR. HARRY ISCHIROPOULOS<sup>1</sup> and DR. DENNIS STUEHR<sup>2</sup>. Although a large part of this work dealt with the proof of this hypothesis, we were unable to provide further evidences in context of this thesis.

### 3.7 Hydrogen Sulfide

Hydrogen sulphide ( $\text{H}_2\text{S}$ ), known for its cytotoxic properties, has recently been proposed as a novel neuromodulator [220]. Its  $\text{p}K_{\text{a}}$  of 6.9 is significant lower than those of thiols and is additionally a much stronger reductant. Besides  $\bullet\text{NO}$  and CO it represents the third gas which will be endogenously produced and has a number of biological functions. It is produced from cysteine by various enzymes. Cystathionine  $\beta$ -synthase (CBS), located at chromosome 21, seems to be the only source of  $\text{H}_2\text{S}$  in the brain, whereas the liver synthesizes  $\text{H}_2\text{S}$  via cystathionine  $\gamma$ -lyase (CSE) and in the heart, the 3-mercaptopyruvate pathway is used [221]. The usually homotetrameric CBS contains one heme cofactor per monomer and binding of CO or  $\bullet\text{NO}$  to it

---

<sup>1</sup>The Children's Hospital of Philadelphia, Philadelphia, USA.

<sup>2</sup>Cleveland Clinic Foundation, Cleveland, Ohio, USA.

results in enzyme inhibition [222, 223]. Carbon monoxide binding to CBS is strongly anticooperative and the two dissociation constants of human CBS, 1.5 and 68  $\mu\text{M}$  [222, 224], are suggesting that CO binding should occur as a physiological process, which would provide a mechanism of interaction between CO and H<sub>2</sub>S signaling.

Hydrogen sulphide is known to act as a vasodilator and is also active in the brain, where it increases the response of the *N*-methyl-D-aspartate (NMDA) receptor. It should be also mentioned that the NMDA receptor-associated ion channel can be inhibited by *S*-nitrosation of a cysteine on its NR2A subunit [145, 146]. In the brain it is found in relatively high concentrations, the endogenous levels of range between 50 and 160  $\mu\text{M}$  [225]. In context of the brain and its very low extracellular GSH levels, H<sub>2</sub>S could possibly take over its role as a reductant. Although a neuromodulatory role of H<sub>2</sub>S has been demonstrated, little is known of its other biological functions. H<sub>2</sub>S seems to act as an inhibitor of HOCl-mediated processes *in vivo* [225]. Administration of exogenous H<sub>2</sub>S can also be beneficial; it effectively protects myocytes and contractile activity, at least by its direct scavenging of oxygen-free radicals and reducing the accumulation of lipid peroxidations [226].

Two diseases are linked with changes in H<sub>2</sub>S metabolism; the H<sub>2</sub>S synthesis in the brains of Alzheimer's disease patients is markedly decreased in trisomy 21, its synthesis is increased due to the overexpression of CBS. Although the role of H<sub>2</sub>S in regulatory processes is accepted, detailed knowledge of its endogenous actions is still lacking.

## 4 Materials and Methods

### 4.1 Chemicals

L-NIO, 1400 W, *N*<sup>ω</sup>-propyl-L-arginine, DMNQ and L-NMMA were purchased from Alexis Biochemicals (Grünberg, Germany); L-[U-<sup>14</sup>C] arginine monohydrochloride from Amersham Bioscience (Munich, Germany); NADP<sup>+</sup> and NADPH from Biomol (Hamburg, Germany); SIN-1 and xanthine oxidase (from butter milk) from Calbiochem (Darmstadt, Germany); SNAP, DAF-2 DA, spermine NONOate, diethylamine NONOate, DETA NONOate and L-NAME from Cayman Chemicals (Ann Arbor, USA); sodium nitroprusside, myoglobin (from horse heart), neocuproine and DTPA from Fluka and Sigma-Aldrich (Seelze, Germany); MitoTracker Green FM, MitoTracker Red CM-H2XROS and dihydrorhodamine 123 from Molecular Probes (Karlsruhe, Germany); Cu,Zn-SOD (from bovine erythrocytes), alcohol dehydrogenase, catalase (from beef liver), NAD<sup>+</sup> (grade II), nitrate reductase (from *Aspergillus* species) from Roche Molecular Biochemicals (Manheim, Germany); glutathione reductase, 2,3-diaminonaphthalene, NADP<sup>+</sup>, NADPH, oxidized and reduced glutathione, albumin (from bovine serum), hemoglobin (bovine), DTT, DTNB, Cu,Zn-SOD (from bovine erythrocytes), hypoxanthine, ascorbic acid, catalase (from bovine liver), xanthine oxidase (grade III from buttermilk) from Sigma (Munich, Germany).

The cell culture reagents Earles salt solution (with 2.2 g/l NaHCO<sub>3</sub>), penicillin, streptomycin, FCS, hEGF, hydrocortisone, trypsin, collagenase type I and glutamine

were purchased from Biochrom (Berlin, Germany). MCDB-131 medium (without glutamine) was purchased from Gibco Invitrogen (Karlsruhe, Germany) and gelatine type A 300 Bloom (from porcine skin) from Sigma (Munich, Germany).

NOS-1 and the oxygenase domains of all three NOS isoforms were a kind gift of DR. DENNIS STUEHR (Cleveland Clinic Foundation, Cleveland, Ohio, USA).

Peroxynitrite was synthesized from  $\bullet\text{NO}$  and potassium superoxide according to KISSNER *et al.* [41] and residual  $\text{H}_2\text{O}_2$  was removed with  $\text{MnO}_2$ .

All chemicals were purchased at analytical grade, in most cases from Sigma (Munich, Germany). Twice distilled water was used for all experiments.

### 4.1.1 S-Nitrosoglutathione Synthesis

S-Nitrosoglutathione (MW = 336.32 g/mol) was synthesized according to HART [227]. In short, 765 mg of GSH were solved in 4 ml water. While everything was stirred and kept on ice, 1.25 ml 2 M HCl were added to the suspension. After subsequent addition of 173 mg sodium nitrite, the orange solution was kept on ice for 40 minutes, followed by addition of 4 ml acetone to precipitate the product. After 10 minutes everything was filtered and the filter with the precipitate was washed 5 times with each 1 ml water, 3 times with each 5 ml acetone and finally 3 times with each 5 ml diethylether. The washed precipitate was dried in vacuum and purity was determined as 78 % by measuring  $E_{545}$  ( $\varepsilon_{545} = 15.9 \text{ M}^{-1}\text{cm}^{-1}$  [227]) of the solved product. The S-nitrosoglutathione was stored in the dark at 4 °C; at these conditions it was stable over months, after 26 months the purity had declined down to 44 %.

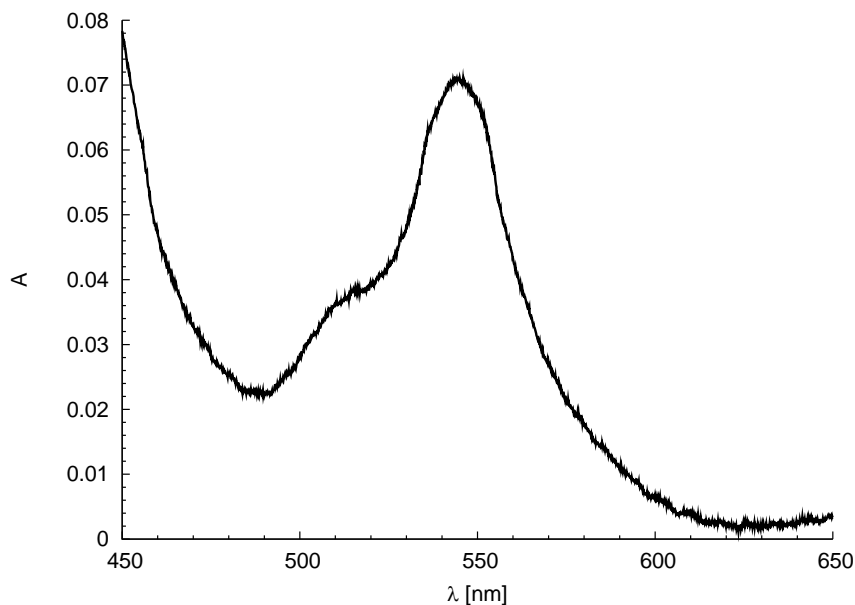


Figure 4.1: **Spectrum of *S*-nitrosoglutathione.** Typical spectrum of a solution of *S*-nitrosoglutathione (4.5 mM) in 0.1 M phosphate buffer, pH 7.4 ( $\epsilon_{545} = 15.9 \text{ M}^{-1}\text{cm}^{-1}$ , MW = 336.32 g/mol)

#### 4.1.2 *S*-Nitrosoalbumin Synthesis

The synthesis of *S*-nitrosoalbumin was done as described by STAMLER and FEELISCH [228]. BSA was solved in water to a final concentration of 900 g/ml and dialysed over night to remove traces of metals. For all further steps the solution was kept cold and protected from light. Diethylenetriaminepentaacetic acid (DTPA) and sodium nitrite were dissolved in the BSA solution to final concentrations of 1 mM and 50 mM, respectively. The synthesis was started by adding an equal volume of 1 M HCl. After 7 minutes an equal volume of 100 mM potassium phosphate buffer at pH 7.4 was added and after another 23 minutes the solution was slowly titrated with 10 M NaOH to a final pH of 6.5. Salts were removed by dialysis over night and the remaining solution was lyophilized to gain *S*-nitrosoalbumin. The purity was 43% at minimum, as determined by the oxyhemoglobin assay after addition of 100  $\mu\text{M}$   $\text{CuCl}_2$ . The dry powder was stored at 4 °C in the dark.

## 4.2 Methods

### 4.2.1 CO Treatment of Rats

Wistar male rats (Charles River Laboratories, Wilmington, USA) were treated according to the method developed by THOM [216, 218]. In a chamber the animals were exposed for 40 min to a continuous flow of 8 l/min air mixed with CO to yield 1000 ppm. The CO concentration was then increased to 3000 ppm for another 20 min. Animals were removed from the chamber back to room air after 20 min or earlier if they lost consciousness. After the indicated time, rats were killed and its brains removed for immunohistochemical identification of 3-nitrotyrosine and PGI<sub>2</sub> synthase with the corresponding antibodies, as previously described [216]. Colocalization was quantified by analysis of the slides and counting of vessels positive for one or both of the stainings.

### 4.2.2 NOS Spectra

Spectra of full-length NOS as well as from the oxygenase domains of the different isoforms were recorded with an Aminco DW-2a UV/vis spectrophotometer in 100 mM potassium phosphate buffer at pH 7.4. Heme reduction was obtained by the addition of either small amounts of solid sodium dithionite or immediate titration with a freshly prepared solution. Solutions of CO were produced by bubbling of water for at least 10 min at 20 °C with CO gas, giving 1.08 mM. Prior to production of •NO solutions, water was usually boiled and gassed with Ar. After solving •NO, a saturated solution of 1.95 mM was obtained. Gas solutions were stored during the experiment in sealed vials and transferred with a syringe into the cuvette. The herein reproduced spectra are representative for at least three independent experiments. Hemoglobin and myoglobin spectra were recorded using the same method and conditions as those of NOS.

### 4.2.3 [<sup>14</sup>C]Arginine NOS Assay

The method used for determining NOS activity is based on the one described by KUMAR *et al.* [229]. Samples of each 20  $\mu$ l were consisting of 0.8 % glycerol, 6  $\mu$ M FAD and FMN each, 100  $\mu$ M BH<sub>4</sub>, 1 mM Ca<sup>2+</sup>, 2.5  $\mu$ g/ml calmodulin, 3 mM DTT, 5  $\mu$ M L-arginine, 5  $\mu$ M L-[<sup>14</sup>C]arginine and 10.9  $\mu$ M recombinant NOS-1 in 32 mM HEPES, pH 7.4. If CO had to be added to the samples, the vials were in addition filled with a gaseous mixture of CO and air of the corresponding partial pressure. After samples reached 37 °C, enzymatic turnover was started by the addition of 250  $\mu$ M NADPH. After 20 min at 37 °C, reaction was stopped by adding 2.5 volumes of cold methanol and the samples were kept on ice until analysis.

If necessary, samples were centrifuged at 15000 *g* for 10 minutes at 4 °C. 20  $\mu$ l of each sample was spotted on silica gel 60 plates (Merck, Darmstadt, Germany) and dried before transfer to the chromatography chamber. The mobile solvent consists of ammonium hydroxide:chloroform:methanol:water (4:1:9:2). After the thin-layer chromatography, the plates were dried in an oven and after 1–3 days of exposure to Molecular Dynamics storage phosphor screens, read out with a Molecular Dynamics PhosphorImager and analyzed. Spots of L-arginine ( $R_f = 0.39$ ) and L-citrulline ( $R_f = 0.88$ ) were identified according to their  $R_f$ -values and integrated with Molecular Dynamics ImageQuant 3.30.

### 4.2.4 Griess Assay

Nitrite was determined by the Griess assay [230] based on the formation of a diazonium intermediate from the reaction of nitrite and sulfanilamide and subsequent azo coupling with naphthylethylenediamine to yield an azo compound with maximal absorption at 540 nm. 30  $\mu$ l of 12.5  $\mu$ M sulfanilamide and 30  $\mu$ l of 6 M HCl were mixed with 300  $\mu$ l of sample at room temperature and incubated for 5 min. Absorbance

was measured before and after addition of 25  $\mu\text{l}$  of *N*-(1-naphthyl)ethylenediamide (12.5 mM) at 560 nm using a microplate reader. Nitrite concentrations were calculated from a simultaneously produced  $\text{NaNO}_2$  standard curve in the range of 0.5–50  $\mu\text{M}$ . Nitrate in these samples was quantified after conversion to nitrite by nitrate reductase prior to the Griess reaction.

### 4.2.5 Alcohol Dehydrogenase Activity Test

The activity of alcohol dehydrogenase (ADH) was measured with an Aminco DW-2a UV/vis spectrophotometer in the dual wavelength mode. A 33 nM solution of ADH in 0.1 M potassium phosphate buffer, pH 7.4, was placed in a cuvette equipped with a magnetic stirrer, and after addition of  $\text{NAD}^+$  (300  $\mu\text{M}$ ), the temperature was adjusted to 37 °C. The reduction of  $\text{NAD}^+$  to NADH was started by addition of ethanol (172 mM) from a syringe through a septum to the stirred solution. The formation of NADH was followed at 340 *versus* 400 nm, and the specific activity of ADH was calculated for the first 30 s of measurements in the linear region of the curves by using an extinction coefficient for NADH of  $\epsilon_{340} = 6220 \text{ M}^{-1}\text{cm}^{-1}$  [157]. The specific activity for freshly prepared ADH was  $65 \pm 3 \mu\text{mol min}^{-1}\text{cm}^{-1}$  (units/mg). For all experiments, the same stock solutions of ADH (3.3  $\mu\text{M}$  in water) and  $\text{NAD}^+$  (3 mM in buffer) were used, aliquots of which were frozen at  $-70$  °C.

For the determination of ADH inhibition under various conditions, the solution without  $\text{NAD}^+$  was incubated for 2 h at 37 °C with 0.5 U/ml xanthine oxidase, 1 mM hypoxanthine and varying concentrations of spermine NONOate. The decay rate for spermine NONOate was determined using the oxyhemoglobin assay; 5  $\mu\text{M}$  will produce  $2.4 \pm 0.1 \text{ nM/s}$  under the given conditions. For 0.5 U/ml xanthine oxidase and 1 mM hypoxanthine,  $3.0 \pm 0.2 \text{ nM/s}$   $\text{O}_2^{\bullet-}$  will be produced, as determined with the cytochrome *c* assay.

### 4.2.6 Quantification of 4-Nitrosophenol

The formation of 4-nitrosophenolate ( $pK \approx 6$ ) during the reaction of phenol (5 mM) with SIN-1 (200  $\mu$ M) and/or spermine NONOate (100  $\mu$ M) in 0.1 M potassium phosphate buffer, pH 7.4 at 37 °C, was monitored spectrophotometrically at 400 *versus* 500 nm over a time period of 2 h [231]. Its yield in these samples was determined with an HPLC method described previously [232].

### 4.2.7 Oxyhemoglobin Assay

The oxyhemoglobin assay for quantification of  $\bullet$ NO, as described by K<sub>E</sub>L<sub>M</sub> *et al.* [233], is based on the oxidation of oxyHb to metHb. This conversion was monitored at the Soret band at 401 nm *versus* an isosbestic point at 411.5 nm with an Aminco DW-2a UV/vis spectrophotometer in the dual wavelength mode. Usually the assay was performed in 100 mM potassium phosphate buffer, pH 7.4, with a sufficient excess of oxyHb from a frozen stock solution.  $\bullet$ NO-concentrations were calculated using a molar extinction coefficient of  $\varepsilon_{401-411.5} = 49500 \text{ M}^{-1}\text{cm}^{-1}$  [233].

### 4.2.8 Cytochrome c Assay

Similar to the oxyhemoglobin assay, the generation of superoxide can be followed via the reduction of cytochrome *c* to its ferrous form [233]. The same setup as in the oxyHb assay was used. Reduction of ferricytochrome *c* was monitored at 550 nm *versus* 525 nm as the isosbestic point.  $\text{O}_2^{\bullet-}$  concentrations were calculated using a molar extinction coefficient of  $\varepsilon_{550-525} = 19500 \text{ M}^{-1}\text{cm}^{-1}$  [233].

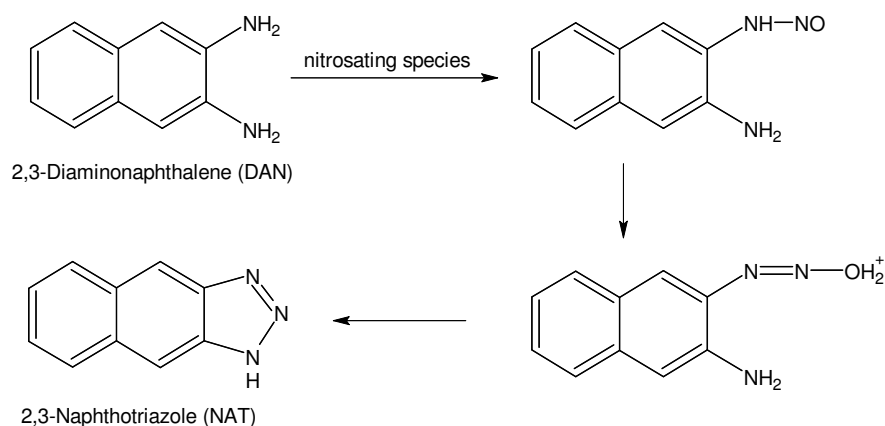


Figure 4.2: Reaction of 2,3-Diaminonaphthalene with a nitrosating species.

#### 4.2.9 N-Nitrosation of 2,3-Diaminonaphthalene

2,3-Diaminonaphthalene (DAN) represents a convenient probe for nitrosations. After an intermediate step, its *N*-nitrosation results in ring closure and the final product is the fluorescent substance 2,3-naphthotriazole (NAT) (Fig. 4.2). Depending on the experiment, samples of 1 ml, containing 5  $\mu\text{M}$  spermine NONOate, 0–3.2 mU/ml xanthine oxidase, 1 mM hypoxanthine, 10  $\mu\text{M}$  DAN (from a stock solution in dimethyl sulphoxide, DMSO) in 100 mM potassium phosphate buffer, pH 7.4, were prepared and incubated for 20 min at 37 °C. In case of the experiments with bicarbonate, 25 mM bicarbonate was present in buffer. 5  $\mu\text{M}$  spermine NONOate will produce 3.87 nM/s  $\bullet\text{NO}$ , whereas 1 mU/ml xanthine oxidase will produce 2.43 nM/s  $\text{O}_2^{\bullet-}$  under these experimental conditions. After incubation, samples usually had to be diluted in the according buffer to yield 2 ml and transferred in a Perkin Elmer LS 50B fluorimeter with a thermostated cuvette holder. NAT fluorescence was determined by measuring the fluorescence at  $\lambda_{\text{em}} = 420 \text{ nm}$  using an excitation wavelength of  $\lambda_{\text{ex}} = 375 \text{ nm}$  [234]; both slits were set to 10 nm. If necessary, samples were diluted prior to fluorescence determination. Base fluorescence of DAN from untreated samples was subtracted during data analysis.

During the bicarbonate concentration series, the desired bicarbonate concentrations were obtained by mixing of 100 mM bicarbonate in 200 mM potassium phosphate

buffer, pH 7.4, with 200 mM potassium phosphate buffer, pH 7.4 and subsequent control of the final pH value. Samples were prepared containing 0–100 mM bicarbonate, 5  $\mu$ M spermine NONOate, 0.53 mU/ml XO, 10  $\mu$ M DAN, 200 mM potassium phosphate at pH 7.4. Further treatment of samples was performed as described above.

For determination of the effect of azide, the above method was modified since azide will inhibit xanthine oxidase. Samples therefore contained 3.75  $\mu$ M spermine NONOate (2.90 nM/s  $\bullet$ NO), 7  $\mu$ M SIN-1 (ca. 0.97 nM/s  $\bullet$ NO and  $O_2^{\bullet-}$ ), 1 mM sodium azide and, if demanded, 25 mM bicarbonate in 100 mM potassium phosphate buffer, pH 7.4.

### 4.2.10 GSH Oxidation

GSH (5  $\mu$ M) was incubated with spermine NONOate (5  $\mu$ M), hypoxanthine (1 mM) and xanthine oxidase (0–3.2 mU/ml) in 100 mM potassium phosphate buffer, pH 7.4 in the absence or presence of 25 mM potassium hydrogencarbonate. 5  $\mu$ M Spermine NONOate yields 3.87 nM/s  $\bullet$ NO, whereas 1 mU/ml xanthine oxidase corresponds 2.44 nM/ml  $O_2^{\bullet-}$  under these conditions, as determined by the oxyHb or cytochrome *c* assay, respectively (see 4.2.7 and 4.2.8). After 20 min at 37 °C, 10  $\mu$ M 5,5'-dithio-bis(2-nitrobenzoic acid) (DTNB, Ellman's reagent) was added, and after subsequent incubation (5 min at room temperature),  $E_{409.5}$  was determined with an Aminco DW-2a UV/vis spectrophotometer ( $\epsilon_{409.5} = 14150 \text{ M}^{-1}\text{cm}^{-1}$ ).

### 4.2.11 S-Nitrosation of Albumin during Freezing

#### 4.2.11.1 Determination of Nitrosation with 2,3-Diaminonaphthalene

Metal-free solutions containing 25  $\mu$ M BSA with or without 10 mM sodium or potassium nitrite in sodium or potassium phosphate buffer were frozen at  $-20$  °C. After thawing of the samples, *S*-nitrosation was determined after repeated 10 kDa exclusion

centrifugation (Microcon, Millipore, Bedford, USA), addition of DAN (30  $\mu\text{M}$  from a stock solution in DMSO) and subsequent addition of  $\text{CuCl}_2$  (100  $\mu\text{M}$ ) by measuring the resulting fluorescence of NAT with a Perkin Elmer LS 50B fluorimeter ( $\lambda_{\text{ex}} = 375 \text{ nm}$ ,  $\lambda_{\text{em}} = 420 \text{ nm}$ , both slits at 10 nm). By comparison with a GSNO standard, the yield of nitrosation was calculated to be one *S*-nitrosocysteine per molecule albumin ( $23.98 \pm 5.93 \mu\text{M}$ ), which means complete nitrosation under these conditions. To prove that the  $\bullet\text{NO}$ -signal after  $\text{CuCl}_2$ -addition is due to *S*-nitrosation, the same experiments were performed after blocking the thiol groups of albumin by iodoacetamide (10 mg/ml) or DTNB (1 mM).

### 4.2.11.2 Determination of Nitrosation with the oxyHb Assay

Samples containing 40 mg/ml BSA (600  $\mu\text{M}$ ) in sodium phosphate buffer (100 mM, pH 7.4) and 1 mM  $\text{NaNO}_2$  were stored overnight at  $+4^\circ\text{C}$  or  $-20^\circ\text{C}$ . *S*-Nitrosation of albumin was determined via the oxyHb assay (see 4.2.7) by addition of  $\text{CuCl}_2$  (1 mM) and measurement of the resulting  $\bullet\text{NO}$ -release after 10 min of incubation.

### 4.2.12 N-Nitrosation of 2,3-Diaminonaphthalene during Freezing

Samples containing 10  $\mu\text{M}$  sodium or potassium nitrite and 30  $\mu\text{M}$  DAN in sodium or potassium phosphate buffer (100 mM, pH 7.4) were stored for 2.5 h at  $+4^\circ\text{C}$  or  $-20^\circ\text{C}$ . As a control the experiment was also performed in the absence of nitrite. After thawing, NAT fluorescence was measured with a Perkin Elmer LS 50B fluorimeter ( $\lambda_{\text{ex}} = 375 \text{ nm}$ ,  $\lambda_{\text{em}} = 430 \text{ nm}$ ).

### 4.2.13 Kinetic Simulation

Kinetic simulation of the  $\bullet\text{NO}/\text{O}_2^{\bullet-}$  system was performed using COPASI 4.0 (build 18) [235]. The model includes the reactions listed in 5.6, which represents current

knowledge concerning the reactions between the intermediates in the system and pathways leading to nitrosation. Initial conditions of 25 mM hydrogen carbonate, 1.3 mM carbon dioxide, 225  $\mu$ M oxygen at pH 7.4 and 5  $\mu$ M or 5 mM GSH were used. The computer-assisted kinetic simulation was performed with the deterministic LSODA method calculating the conditions 1200 s after production of  $\bullet$ NO (10 nM/s) and  $O_2^{\bullet-}$  (0–100 nM/s) started.

### 4.2.14 Software

The following software was used for data processing and representation: Kinetic simulations were calculated with COPASI 4.0 (build 18)<sup>1</sup>. Quantification of <sup>14</sup>C labeled TLC plates was accomplished by scanning of the plates and integration with Molecular Dynamics ImageQuant 3.30. All data was plotted and analyzed with gnuplot 4.2.0<sup>2</sup>. Typesetting of this work was done using the L<sup>A</sup>T<sub>E</sub>X typesetting system.

### 4.2.15 Statistical Analysis

Unless otherwise indicated, each result presented in this work is the outcome of at least three independent experiments. All data points are presented as mean values and errors were calculated as standard deviation (SD). If necessary, significance was calculated using Student's *t*-test. A probability value of less than 0.05 was considered to represent a statistically significant difference.

---

<sup>1</sup><http://www.copasi.org>

<sup>2</sup><http://www.gnuplot.info>

# 5 Results and Discussion

## 5.1 Interaction between CO and NOS-1

Both carbon monoxide (CO) and nitric oxide ( $\bullet$ NO) are produced in higher organisms by constitutive and inducible enzymes and share many properties as signaling molecules. Both reveal similar physical properties like their appearance as gasses at normal temperature and pressure, their molecule size, solubility and both are uncharged. But due to their contrary chemical properties, they reveal a contrary stability and reactivity in the organism. Despite these chemical differences, both CO and  $\bullet$ NO are signaling molecules with similar and overlapping functions, both targeting at iron-containing receptors. In the case of CO, the relevant receptor still has to be found, but only ferrous heme iron should provide the required affinity towards CO. In contrast to the well-known toxic effects of CO, its signaling functions will take place at concentrations of 0.1 up to 1  $\mu$ M and therefore requires a receptor with sufficient affinity. The reversible binding to Hb with an affinity 200 times higher than O<sub>2</sub> is not able to disrupt oxygen distribution in the organism at these low concentrations to a significant degree. First indications revealed sGC (soluble guanylate cyclase) as the corresponding receptor [193, 209], but further studies showed that it lacks the required sensitivity towards CO.

Early reports showed that CO triggers smooth muscle relaxation [194] including vasodilation [236–239] and to exhibit platelet aggregation [193], whereas its vascular

effects are not caused by hypoxia [240]. After it became accepted that CO inhibits a role as a signaling molecule, further investigations revealed that low doses of CO possess beneficial properties during severe conditions like septic shock, xenotransplantation, lung injury and during ischemia/reperfusion [195–205], whereas inhibition or cellular depletion of heme oxygenase (HO) will lead to worsening of these conditions [186, 192, 197, 200, 241–243]. These beneficial effects could be also attributed to the action of •NO; this big overlap of CO and •NO functions together with the parallels between HO and nitric oxide synthases (NOS), led to the hypothesis that CO could act through •NO and its known signaling pathways. But despite numerous subsequent investigations, the mechanism of the action of low doses of CO remain largely elusive.

The first indication of the formation of RNS during CO poisoning was provided by THOM in 1990; treatment with CO in the range<sup>1</sup> of 1000–3000 ppm was discovered to lead to lipid peroxidation in rat brain which was not caused by hypoxia [218]. Subsequent results from THOM and ISCHIROPOULOS could demonstrate a striking increase of •NO levels and perivascular Tyr nitration in brain after CO treatment of rats, whereas pretreatment with the NOS inhibitor *N*<sup>ω</sup>-nitro-L-arginine methyl ester (L-NAME) abolished •NO production, 3-nitrotyrosine (3-NT) formation and lipid peroxidation [216]. In cell culture experiments with bovine pulmonary artery endothelial cells, 50 nM CO were sufficient to increase nitrite, nitrate, RNS and 3-NT formation; pretreatment of L-NAME abolished parts of these effects [244].

These findings led us to a cooperation with THOM and ISCHIROPOULOS<sup>2</sup> to study the effect of low doses of CO and to address the target of the reported Tyr nitration. During these studies especially PGI<sub>2</sub> synthase appeared to be a target of nitration under these conditions (Fig. 5.1). Our subsequent experiments mainly focused on the mechanism of the increase in •NO by CO, lead by a hypothesis which would nicely explain such an outcome.

---

<sup>1</sup>100 nM CO  $\approx$  100 ppm; at 20 °C and 101.3 kPa, 2.3 ml CO can be solved in 100 ml H<sub>2</sub>O, giving a 0.956 mM solution.

<sup>2</sup>The Children’s Hospital of Philadelphia, Philadelphia, USA.

Subsequent publications revealed that treatment of rats for 1 h with 50 ppm CO leads to 3-NT formation also in the aorta, which could be repressed by pretreatment with L-NAME [217]. Finally, THORUP *et al.* demonstrated that 100 nM CO leads to an immediate increase of •NO production from isolated renal resistance arteries, which was at least partly due to increased NOS activity as NOS inhibition or Arg depletion attenuates the effect of CO [219]. However, contrary to CO-induced traces of •NO production, the simultaneous vasorelaxation seems to depend only partly on •NO signaling, since only simultaneous inhibition of both cGMP signaling and BK<sub>Ca</sub> channels could prevent relaxation [212].

These results indicate an increased •NO production by administration of low doses of CO and led us to the assumption that this effect could be due to a direct activation of NOS, more precisely its neuronal isoform (NOS-1). NOS-1 is located not only to neurons, but also reported to be expressed in a variety of other cell types. It possesses a 10 times higher activity compared to NOS-3, but as STUEHR *et al.* discovered, up to 95 % of the enzyme can be present as its inactive Fe<sup>II</sup>-NO complex [27]. The formation of the ferrous nitrosyl complex takes place during the last step of •NO synthesis; instead of •NO release, the ferric nitrosyl complex can be reduced to the more stable ferrous complex. Further stabilization of the complex is provided by a Trp residue specific to NOS-1 [29]. The evolution of this Trp residue, which renders •NO release as the rate-limiting step during its synthesis, indicates that NOS-1 autoinhibition could represent a regulatory mechanism and that there could be conditions in the cell leading to a release of this inhibition. Nitric oxide scavengers are neither able to enter the enzyme's active site nor to lead to increased substrate turnover, therefore only a direct displacement of the complex would represent a possible mechanism to release NOS-1 autoinhibition. We hypothesize that CO, which is only able to bind to ferrous heme, could accelerate the release of •NO and by subsequent binding of O<sub>2</sub> enzymatic turnover and •NO production could be in consequence increased.

To address this hypothesis, •NO production and NOS activity of recombinant NOS-1<sup>3</sup> as well as preparations from rat brain, cell cultures of endothelial cells (EC) and isolated mitochondria were investigated at different conditions. Formation of the different heme complexes was determined by UV/vis spectrometry, substrate turnover by NOS via NADPH consumption and L-citrulline formation, •NO formation during *in vitro* experiments with a •NO electrode system from Innovative Instruments, Inc., the oxyhemoglobin assay and nitrite and nitrate formation with the Griess assay. During cell culture experiments, the fluorescent probes MitoTracker Red CM-H<sub>2</sub>XROS and DAF-2 DA (4,5-diaminofluorescein diacetate) were employed to monitor •NO and RNS formation inside cells.

In collaboration with HARRY ISCHIROPOULOS, rats were exposed to 1000 up to 3000 ppm CO for 1 h according to their previously described method [216]. During this treatment, the animals were kept in a continuous flow of 1000 ppm CO for 40 min and then CO concentration was increased up to 3000 ppm for another 20 min. In this model, some animals lose consciousness and were removed to breath room air. The remaining animals were rendered unconscious with another bolus of CO and then removed from the chamber. After 7 or 21 days, the rats were killed and its brain removed for immunohistochemical analysis. Figure 5.1 shows a representative resulting immunofluorescence staining of brain slices. The red staining corresponds to 3-nitrotyrosine (3-NT) formation, indicating increased •NO-formation *in vivo*, the green co-staining against PGI<sub>2</sub> synthase shows its localization predominantly at the vessel walls. The overlay of both stainings reveals a high level of colocalization of PGI<sub>2</sub> synthase and 3-NT—in total more than 75 % of the vessels counted from different slides are positive for both. Even 21 days after CO treatment nitration was still present.

---

<sup>3</sup>Purified recombinant NOS-1 and oxygenase domains of the three NOS isoforms were provided as a kind gift by DR. DENNIS STUEHR, Cleveland Clinic Foundation, Cleveland, Ohio, USA.

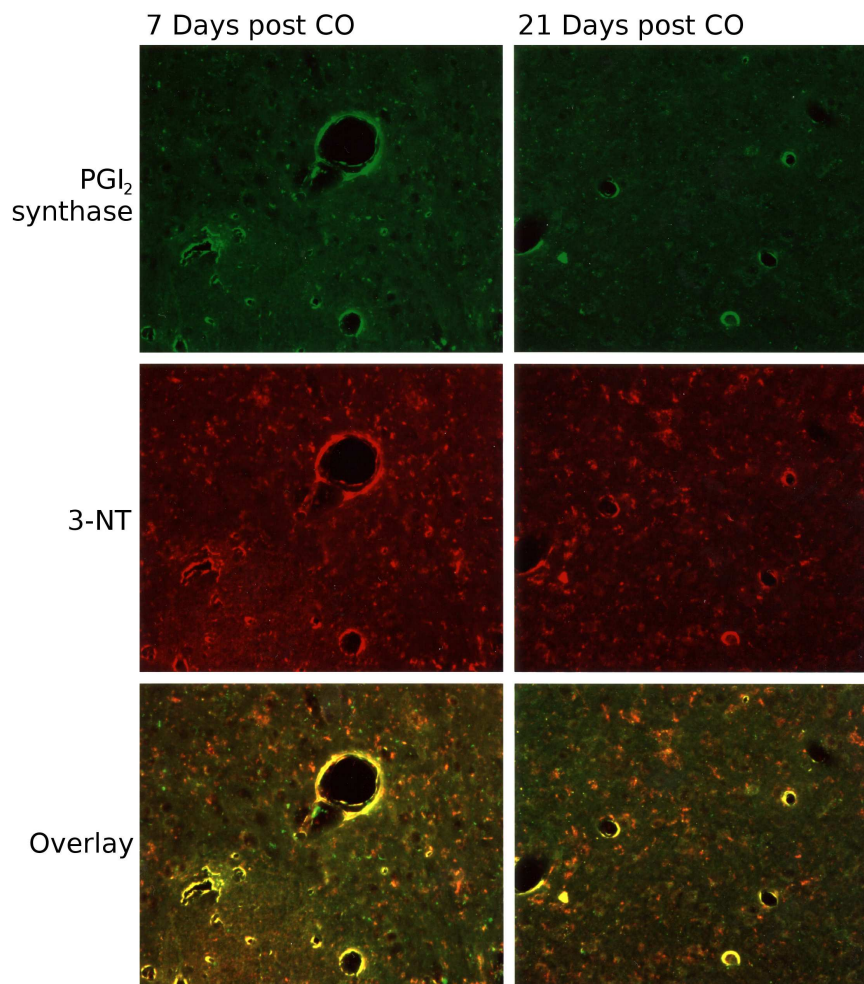


Figure 5.1: **Protein nitration in rat brain after CO-exposure.** Rats were exposed to 1000–3000 nM CO for 1 h and killed 7 or 21 days later. Slices from brain were stained with antibodies against prostacyclin (PGI<sub>2</sub>) synthase (green fluorescence) and 3-nitrotyrosine (3-NT; red fluorescence). Only the vessels show immunofluorescence of PGI<sub>2</sub> synthase; in total the overlay indicates colocalization of 3-NT and PGI<sub>2</sub> synthase in over 75% of the vessels. Even after 21 days the nitration was still detectable. These experiments were done in collaboration with HARRY ISCHIROPOULOS; representative photographs were shown.

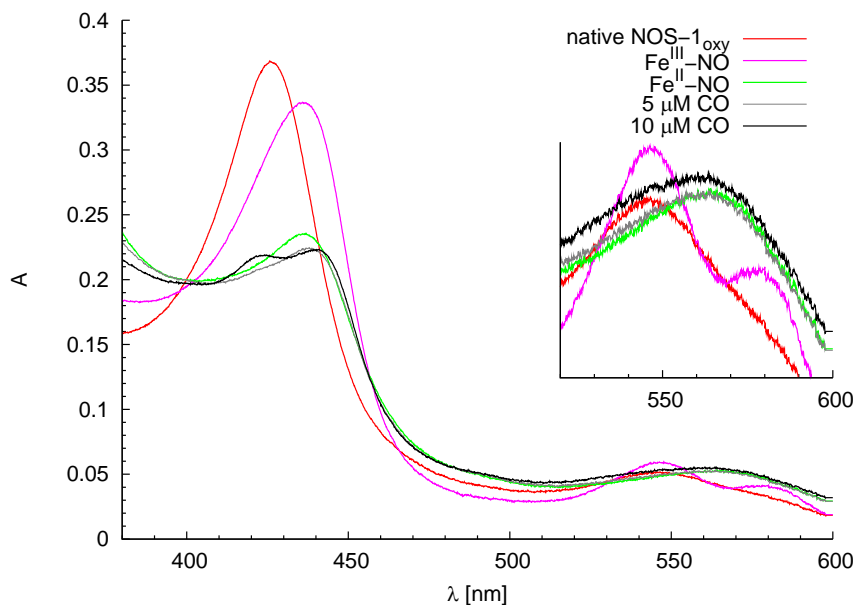


Figure 5.2: **Replacement of nitric oxide by carbon monoxide from the  $\text{Fe}^{\text{II}}\text{-NO}$  complex of the purified oxygenase domain of NOS-1.** After the reduction of the  $\text{Fe}^{\text{III}}\text{-NO}$  complex of NOS-1<sub>oxy</sub> (436 nm) by addition of dithionite, the  $\text{Fe}^{\text{II}}\text{-NO}$  complex (436 nm) was titrated with CO. Concentrations in the low micromolar range were sufficient to yield the  $\text{Fe}^{\text{II}}\text{-CO}$  complex (444 nm) and at 10  $\mu\text{M}$  CO also the P420-form appeared (422 nm).

The formation of CO- and NO-complexes of NOS was determined via photospectrometric analysis. The oxygenase domain of NOS-1 (NOS-1<sub>oxy</sub>) was titrated with an anaerobic solution of  $\bullet\text{NO}$  until complete formation of the ferric NO-complex with a Soret band at 436 nm. Reduction with dithionite led to the ferrous complex (also 436 nm, but lower  $\varepsilon$ ) and simultaneously to removal of  $\bullet\text{NO}$  from the solution. Subsequent titration with a CO solution results in formation of the ferrous CO complex at 444 nm, as is presented in Fig. 5.2.

NOS-1 activity at various concentrations of CO was determined with the L-[ $^{14}\text{C}$ ]Arg assay (Fig. 5.3), based on the method described by KUMAR *et al.* [229]. After addition of NADPH to the preheated samples, the reaction was stopped after 20 min at 37 °C by addition of cold methanol. The turnover of L-[ $^{14}\text{C}$ ]Arg to L-[ $^{14}\text{C}$ ]citrulline was quantified by separation of citrulline and Arg by TLC and analysis of the plates with a phosphorimager.

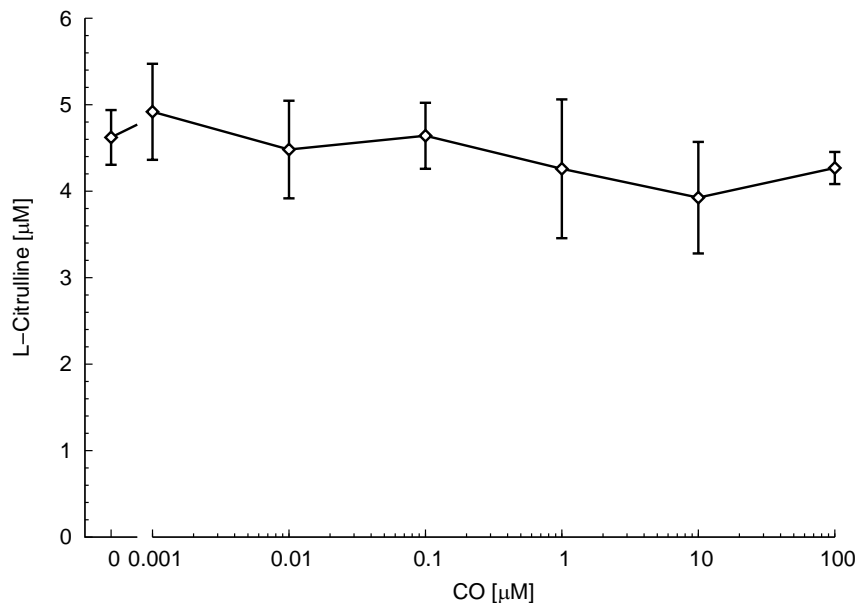


Figure 5.3: **Effect of carbon monoxide on citrulline formation by NOS-1.** To samples containing 0.8 % glycerol, 6  $\mu\text{M}$  FAD and FMN each, 100  $\mu\text{M}$   $\text{BH}_4$ , 1 mM  $\text{Ca}^{2+}$ , 2.5  $\mu\text{g/ml}$  calmodulin, 3 mM DTT, 5  $\mu\text{M}$  L-Arg, 5  $\mu\text{M}$  L- $^{14}\text{C}$ Arg and 11  $\mu\text{M}$  NOS-1 in 32 mM HEPES, pH 7.4, CO was added to yield the indicated concentration and after addition of 250  $\mu\text{M}$  NADPH, incubated for 20 min at 37 °C. Turnover of L- $^{14}\text{C}$ arginine to citrulline was determined after separation by TLC and subsequent analysis with a phosphorimager. Data are mean values  $\pm$  SD;  $n = 3$ .

Besides Arg turnover, also nitrite and nitrate formation by NOS-1 were determined in the presence of CO (Fig. 5.4). Nitrite and nitrate as stable end products of  $\bullet\text{NO}$  decomposition were quantified with the Griess assay, which is based on the formation of a diazonium species from sulfanilamide and nitrite and a subsequent azo coupling to yield an azo compound with maximal absorption at 540 nm. Detection of nitrate required its reduction to nitrite by nitrate reductase previous to the Griess assay (results not shown).

The effect of increased levels of  $\bullet\text{NO}$  on NOS-1 activity was determined in order to check if NOS-1 autoinhibition can be increased (Fig. 5.5). The  $\bullet\text{NO}$  donor diethylamine NONOate, which will decompose under these conditions with  $t_{1/2} = 2$  min, was added during the L- $^{14}\text{C}$ Arg NOS-1 activity assay and after addition of NADPH and 20 min of enzymatic turnover, NOS activity was determined with the  $^{14}\text{C}$ Arg NOS assay. In

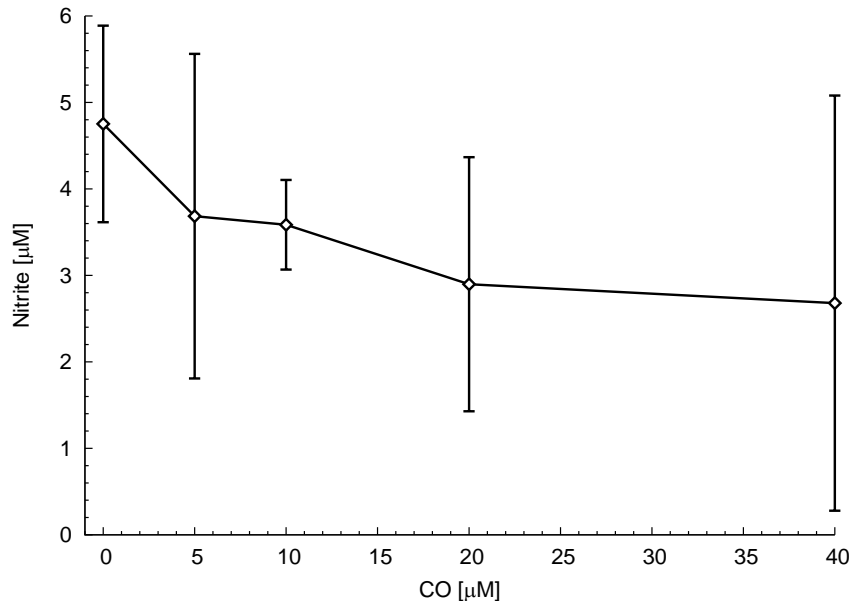


Figure 5.4: **Effect of carbon monoxide on nitrite production by NOS-1.** Nitrite formation during NOS-1 activity (210 nM NOS-1) was determined with the Griess assay after 5 min of catalytic activity at 37 °C in the presence of varying concentrations of CO. Data are mean values  $\pm$  SD;  $n = 4$ .

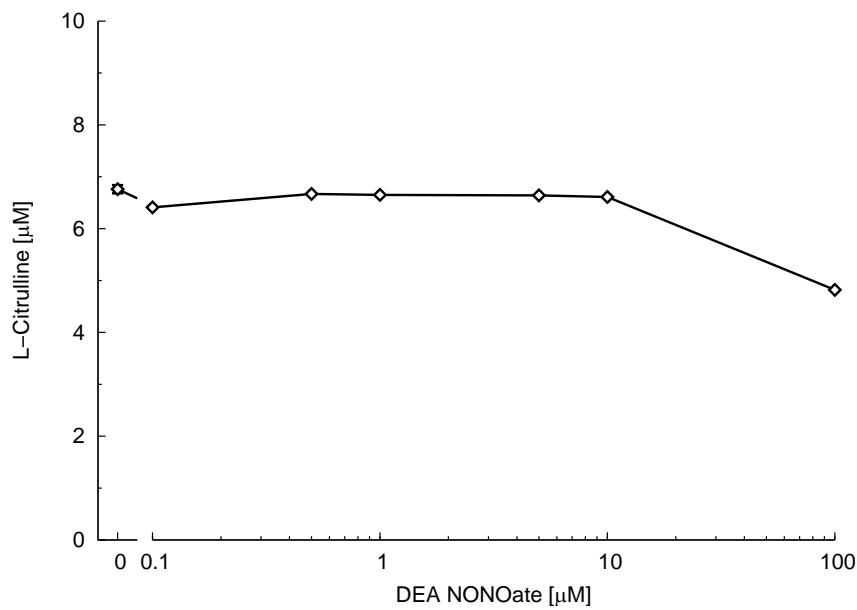


Figure 5.5: **Effect of nitric oxide on NOS-1 activity.** NOS-1 autoinhibition by supplemental  $\bullet\text{NO}$  formation from diethylamine NONOate was determined with the [ $^{14}\text{C}$ ]Arg NOS assay and 20 min incubation at 37 °C.

addition, the same experiment was performed in the presence of up to 1 mM spermine NONOate ( $t_{1/2} = 39$  min) and also NADPH consumption at the same conditions was monitored in the presence of diethylamine NONOate or spermine NONOate via determination of  $E_{340}$  (results not shown). On the whole, the two NONOates were not able to influence activity of NOS-1 at relevant concentrations.

In Figs. 5.6 and 5.7, typical spectra of NOS-1 and its complexes with CO and  $\bullet$ NO are shown. Experiments were performed with 3.2  $\mu$ M recombinant NOS-1 in 100 mM potassium phosphate buffer, pH 7.4 at room temperature. The Soret bands were determined to be at 439 nm, 432 nm and 444 nm for the ferric and ferrous NO-complex and the ferrous CO-complex of NOS-1, respectively. The transfer of the ferrous NO- to the CO-complex was analyzed in Fig. 5.8. After titration with  $\bullet$ NO, the ferric NO-complex was reduced to the ferrous by addition of sodium dithionite. Stepwise additions of CO (5–100  $\mu$ M) were then performed in order to investigate the postulated shift to the ferrous NOS-1-CO complex.

Prostacyclin synthase is known to become nitrated at very low levels of peroxynitrite [176]. It seems that only Mn-SOD and PGI<sub>2</sub> synthase can be nitrated at physiological levels of peroxynitrite without the involvement of conditions of severe oxidative stress (cf. 3.5.3.3). Therefore, it was of interest if the reported protein nitrations in response to a treatment with CO occur at the level of PGI<sub>2</sub> synthase. The results in Fig. 5.1 indicates that treatment with CO has to result in an increase in peroxynitrite formation which manifests itself in an increased 3-NT formation compared to untreated animals (not shown; see [216]). The same pattern of protein nitration was already shown to be present immediately after CO treatment [216], but this increase in 3-NT was still visible three weeks after the treatment (Fig. 5.1). Degradation of PGI<sub>2</sub> synthase usually occurs within 30 h (GRAF, ULLRICH; unpublished data); the observed long-term effect could be explained by an inflammatory component triggered within this model by CO or hypoxia. This delayed nitration should not interfere with the investigated immediate effects of CO and therefore, no further experiments concerning this aspect

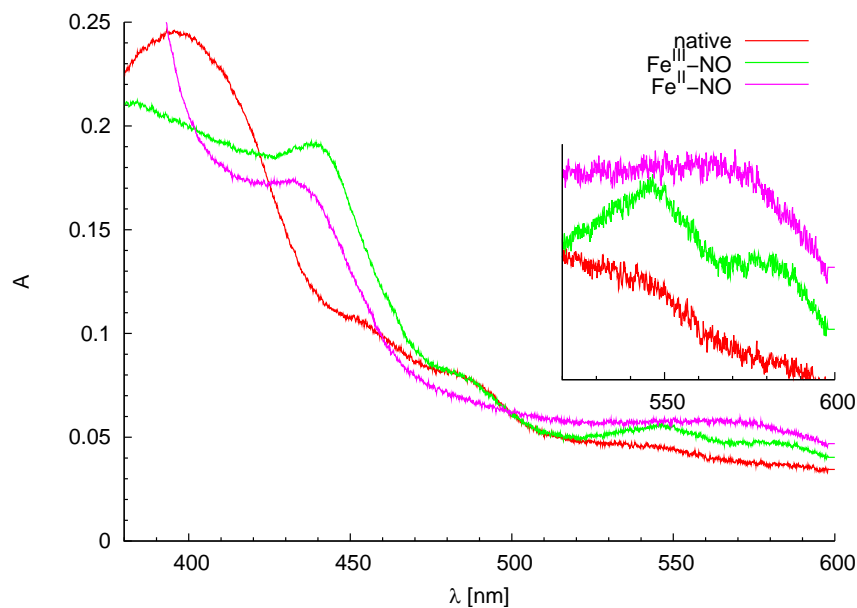


Figure 5.6: **Ferric and dithionite-reduced ferrous NO-complexes of NOS-1.** NOS-1 ( $3.2\ \mu\text{M}$ ) was titrated with  $\bullet\text{NO}$  from a fresh stock solution in oxygen-free water till formation of the ferric  $\text{Fe}^{\text{III}}\text{-NO}$  complex (Soret band at  $439\ \text{nm}$ ,  $\alpha$ - and  $\beta$ -band at  $546$  and  $582\ \text{nm}$ ). After reduction by addition of solid sodium dithionite the ferrous NO-complex became apparent ( $432\ \text{nm}$ ).

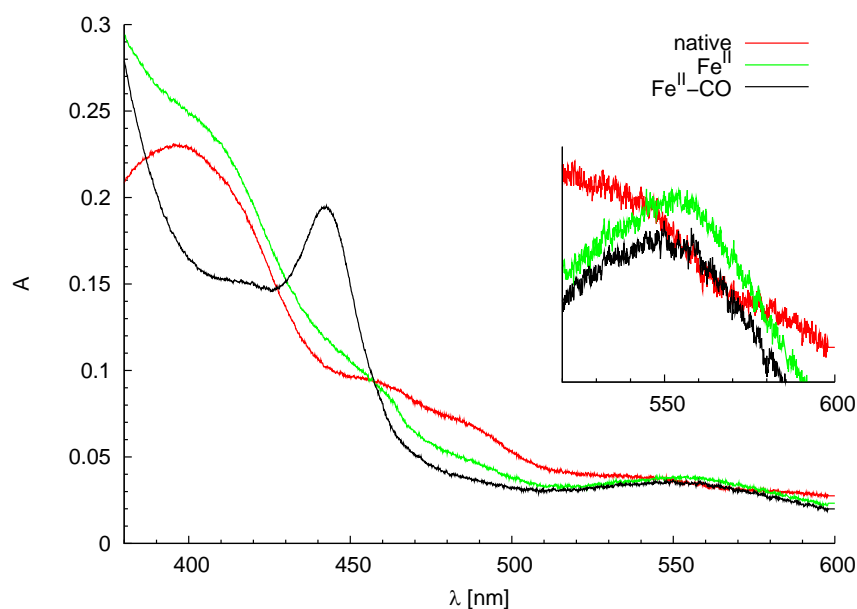


Figure 5.7: **Ferrous CO-complex of NOS-1.** NOS-1 ( $3.2\ \mu\text{M}$ ) was reduced by the addition of solid sodium dithionite and afterward titrated with CO solution. The Soret band of the resulting  $\text{Fe}^{\text{II}}\text{-CO}$  complex had its maximum at  $444\ \text{nm}$ .

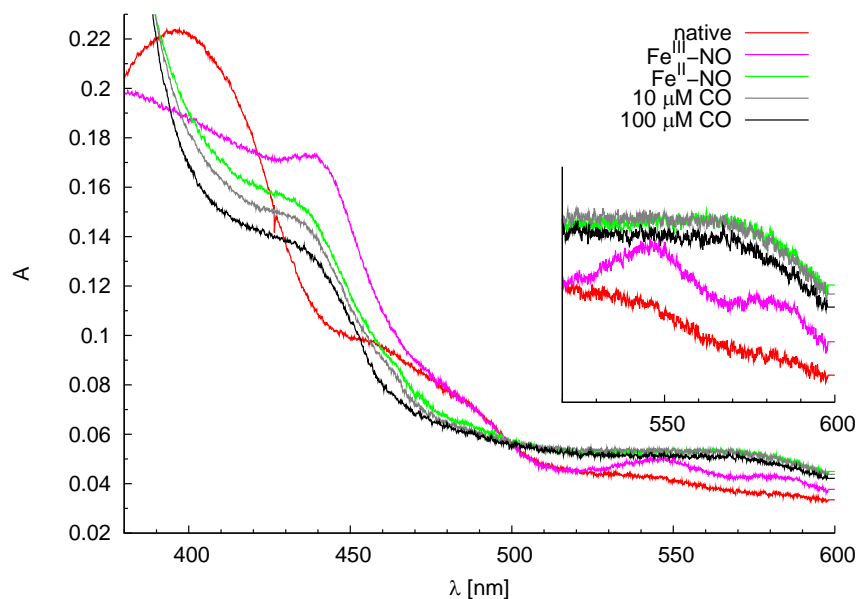


Figure 5.8: **Replacement of nitric oxide in the  $\text{Fe}^{\text{II}}\text{-NO}$  complex of NOS-1 by carbon monoxide.** NOS-1 ( $3.2\ \mu\text{M}$ ) was titrated with a solution of  $\bullet\text{NO}$  to the  $\text{Fe}^{\text{III}}\text{-NO}$  complex. After addition of sodium dithionite the  $\text{Fe}^{\text{II}}\text{-NO}$  is formed. Gradual additions of CO does not lead to a spectral shift towards 444 nm. Typical spectra out of four independent experiments; only selected titration steps are shown.

were performed. In accordance with 3-NT,  $\text{PGI}_2$  synthase staining is found mainly around vessels. In fact, the overlay of both stainings shows a high level of colocalization between nitrotyrosine and  $\text{PGI}_2$  synthase and more than 75 % of the counted vessels are positive for both antibodies. This high level of colocalization indicates that  $\text{PGI}_2$  synthase could be a possible target of nitration in this model, at least this proves that nitration under these conditions is a specific process which predominantly occurs at vessels. This increase in 3-NT should therefore not be interpreted as a consequence of severe oxidative stress, which should had lead to a less specific pattern of 3-NT formation. The model of CO treatment of the animals includes relatively high concentrations of CO, levels which would by itself argue against a physiological process of CO signaling under these conditions. However, THOM and ISCHIROPOULOS could demonstrate later that treatment of rats with less than 100 ppm CO over 1 h are

sufficient to lead to 3-NT formation in aorta at the same order of magnitude as in the above experiment [217].

These preliminary experiments, done in collaboration with HARRY ISCHIROPOULOS<sup>4</sup>, were our first indication that there is a link between small doses of CO and •NO-release and led us to the development of the above explained hypothesis and further studies in order to verify the hypothesis. The possible nitration of PGI<sub>2</sub> synthase after CO treatment together with ISCHIROPOULOS' observation that these effects could be blocked by inhibiting •NO synthases, lead us to suppose that CO causes an increased release of •NO. This is also in accordance with results from THORUP *et al.* [219], who measured CO-dependent •NO release in perfused renal resistance arteries with a •NO-electrode system. They found •NO release to be highest at 100 nM CO and the non-selective NOS-inhibitor L-NAME could abolish •NO release.

The central prerequisite for our hypothesis is the requirement that CO is able to displace •NO from the ferrous NO-complex of NOS-1. The formation of the NO-complexes of NOS and its interaction with CO was first studied with the oxygenase domains of all three NOS isoforms, which were provided by DENNIS STUEHR. As is shown in Fig. 5.2, it was discovered that 5  $\mu$ M CO were able to replace •NO from the Fe<sup>II</sup>-NO complex of NOS-1<sub>oxy</sub>. This was only observed with NOS-1<sub>oxy</sub> and not with both of the other isoenzymes (results not shown). However, the formation of a P420 spectrum at 10  $\mu$ M CO indicates some undesired changes at the heme center during the experiments. In summary, the spectral data collected with the oxygenase domains of the different NOS isoforms allowed us to conclude that the basic assumptions of our hypothesis are valid.

After these successful experiments, our hypothesis was tested against NOS-1 itself, which was also provided by DENNIS STUEHR as a purified recombinant enzyme with full catalytic activity. The L-[<sup>14</sup>C]Arg assay represents a reliable and sensitive test

---

<sup>4</sup>The Children's Hospital of Philadelphia, Philadelphia, USA.

for the determination of NOS activity. In the case of NOS, NADPH consumption itself is not a meaningful indicator of  $\bullet\text{NO}$  production, especially considering the phenomenon of NOS uncoupling. The conditions of the NOS activity assay resemble those commonly used in literature and includes the presence of the cofactors  $\text{BH}_4$ , FAD and FMN, calmodulin and  $\text{Ca}^{2+}$ , normal atmospheric  $\text{O}_2$  partial pressure and an excess of both L-Arg and NADPH. Reaction time was limited to 20 min and performed in sufficient small vials to prevent loss of CO by diffusion. This activity assay, however, includes 100  $\mu\text{M}$   $\text{BH}_4$ , which was shown to provoke substantial  $\text{O}_2^{\bullet-}$  formation by itself. This caused concern that this  $\text{O}_2^{\bullet-}$  could have scavenged  $\bullet\text{NO}$  within the performed experiments and therefore could have prevented NOS-1 autoinhibition. With a short series of experiments it was therefore tested if lower concentrations of  $\text{BH}_4$  are leading to a different outcome, but CO-dependent L-citrulline formation remained unchanged; these high concentrations of  $\text{BH}_4$  did not seem to cause a negative effect in this context.

The result of testing the NOS-1 activity in the presence of CO is shown in Fig. 5.3. All of those experiments revealed that concentrations below 100  $\mu\text{M}$  CO had no effect on L-citrulline formation, which implies that  $\bullet\text{NO}$  formation also is not affected by these concentrations of CO. Likewise, CO had no effect on NADPH consumption, as was determined by monitoring  $\text{E}_{340}$  (data not shown). Other experiments showed that nitrite formation, as a stable end product of  $\bullet\text{NO}$  decomposition, was also not affected by the presence of CO (Fig. 5.4).

According to STUEHR, during catalytic activity NOS-1 will be present within seconds mainly as its  $\text{Fe}^{\text{II}}\text{-NO}$  complex, which is also the central assumption of the investigated hypothesis. Contrary to the other NOS isoforms, both formation of the ferrous heme-NO complex and catalytic inhibition of NOS-1 are described to be insensitive to supplementation as well as to scavenging of  $\bullet\text{NO}$  [27, 28]. This difference between the isoforms could be explained with the action of a conserved tryptophan residue which seems to stabilize the  $\text{Fe}^{\text{II}}\text{-NO}$  complex [29]. But as was observed in other publications and confirmed by STUEHR (personal communication), this property of NOS-1 mostly

depend on the quality of the enzyme preparation, and especially in context of our hypothesis, activity of the NOS-1 preparation should be dependent on the levels of free •NO in the solution. Therefore, it had to be ensured that the enzyme exhibits the required behavior under the given conditions and is present mostly in its rate-limiting ferrous nitrosyl complex. This was verified by measurement of enzyme activity in the presence of increased concentrations of •NO provided by diethylamine NONOate and spermine NONOate (Fig. 5.5). The supplement of the •NO donors diethylamine and spermine NONOate was not able to elicit further feedback inhibition. Further experiments also revealed that a decreased level of •NO in solution by the addition of oxyhemoglobin also did not alter NOS-1 activity. This rises the question if the available NOS-1 preparation was in principle suitable to investigate our hypothesis.

In consequence on the negative results of the experiments involving the purified recombinant NOS-1, different *in vitro* models were tested for an effect of CO on •NO formation. The dialyzed 15000 g supernatant from rat brain homogenates, which contains large amounts of NOS-1, were tested with the L-[<sup>14</sup>C]Arg assay as well as with a •NO electrode system from Innovative Instruments, Inc. These electrochemical sensors allow direct and sensitive measurement of •NO formation below 1 nM [245, 246] but both methods were also not able to support an increased •NO production in response to CO in our samples (results not shown). In an attempt to broaden the focus, isolated mitochondria from bovine heart muscle and rat liver were included in the investigation. This represents a topic of increased interest since it is assumed that mitochondria contain a specific mitochondrial NOS, which seems to be a splice variant of NOS-1 [32–35]. Mitochondria exhibit transport mechanisms for L-Arg [247], therefore the L-[<sup>14</sup>C]Arg assay was the preferred method for these studies. But mitochondrial conversion of L-Arg to L-citrulline was not affected by CO at concentrations relevant for the proposed mechanism (results not shown). Investigations in cell culture systems includes the human microvascular endothelial cell line HMEC-1 [248] and primary cell culture of human vascular and bovine aortic endothelial cells, which were monitored

by the fluorescent probes MitoTracker Red CM-H<sub>2</sub>XRos, dihydrorhodamine 123 and DAF-2DA; all of them are membrane permeant and non-fluorescent until oxidized by ROS or peroxynitrite or in the case of DAF-2DA, by the nitrosonium cation. These dyes should allow measurement of •NO formation indirectly in the living cell by different mechanisms, but especially DAF-2DA as an analytical reagent for nitrosations relies also on basal O<sub>2</sub><sup>•-</sup> formation [52]. Measurement of total fluorescence or image analysis did not indicate an increase in fluorescence within a time scale of 30 min after addition of CO (results not shown).

All experiments involving determination of NOS activity and •NO production at the level of purified enzyme, brain homogenate and endothelial cells were not able to prove an increase in either NOS activity nor •NO-formation by low doses of CO within 30 min. The sum of negative results lead us to a re-examination of the positive spectrophotometric results gained with NOS-1<sub>oxy</sub>. In a second series of experiments the relevant experiments were replicated with the recombinant full-length NOS-1. The spectra of the CO- and NO-complexes is shown in Figs. 5.6 and 5.7 and a difference of 12 nm between the maxima of both ferrous spectra should allow distinction of both complexes. However, in Fig. 5.8 such a shift could not be observed. The Fe<sup>II</sup>-NO complex is only visible as a shoulder due to the interfering with the dithionite spectrum; however these levels of dithionite were necessary to prevent oxidation during the experiments. The results were in addition verified with lower concentrations of dithionite which also did not lead to formation of the CO-complex. Sometimes formation of the P420 form was observed, but in none of the experiments a significant formation of the CO-complex at 444 nm became apparent.

In context of the spectra from recombinant full-length NOS-1, the results with NOS-1<sub>oxy</sub> could be interpreted that the Fe<sup>II</sup>-NO complex was not completely developed. This explains the observed partial formation of the ferrous CO-complex in Fig. 5.2; during the subsequent experiments with full-length NOS-1, the complete transition to the NO-complex was always verified by addition of small amounts of •NO to the dithionite-

reduced solution. These results demonstrated that our initial hypothesis at least could not be proved with the present NOS-1 preparation. Another possible mechanism would be that CO blocks the heme in myoglobin or hemoglobin and therefore prevents binding of •NO. This should result in an increase in free •NO and could provide an explanation for some of the observed effects. In the meantime binding of heme to BK<sub>Ca</sub> channels has been discovered [215] and it has to be shown if this complex represents the searched CO sensor.

## 5.2 Inactivation of Alcohol Dehydrogenase by Peroxynitrite

The homodimeric enzyme alcohol dehydrogenase (ADH) is reported to get inactivated by a variety of RNS, including  $\bullet\text{NO}$ , peroxynitrite and *S*-nitrosothiols [157, 249, 250]. In addition, different mechanisms of inactivation are under discussion, whereas it is clear that the inactivation occurs due to an attack on the zinc center located at its active site. ADH contains two zinc thiolate centers per monomer; the  $\text{ZnCys}_2\text{His}$  center is located at the active site and essential for catalytic activity, whereas the  $\text{ZnCys}_4$  center seems to be involved in enzyme stability. The fourth coordinate position of the  $\text{ZnCys}_2\text{His}$  center serves as a substrate binding site for the hydroxyl group of ethanol; enzymatic activity is absolutely dependent on maintaining the integrity of zinc coordination at the  $\text{ZnCys}_2\text{His}$  center.

The dependency of catalytic activity on an intact Zn center together with a reliable enzyme assay and commercial availability of the enzyme provides a good model for investigation of  $\text{ZnCys}$  centers. Considering the importance of zinc finger proteins and the lack of an *ex vivo* model to investigate their regulation, this model could provide new insights in their function. A zinc finger is a protein domain that is able to bind to DNA and a common motif, especially in transcription factors. Zinc fingers consist of two antiparallel  $\beta$ -strands and an  $\alpha$ -helix, held together by a Zn ion. Most of the analyzed zinc fingers possess a  $\text{ZnCys}_2\text{His}_2$  motif with structural similarity to the  $\text{ZnCys}_2\text{His}$  center of ADH [157].

An inhibition of ADH by *in situ* generation of  $^-\text{OONO}$  by SIN-1 was first observed by DIMMELER and BRÜNE [249], but the lack of knowledge concerning SIN-1 decomposition led to the conclusion that  $\bullet\text{NO}$  was the inhibiting intermediate. Under aerobic conditions, SIN-1 decays to  $\bullet\text{NO}$  and  $\text{O}_2^{\bullet-}$  in equimolar concentrations, resulting in  $^-\text{OONO}$  formation. A direct inhibition of ADH by peroxynitrite was later studied in

detail by CROW *et al.* [157]. They observed ADH inhibition and a loss of 0.85 Zn/ADH subunit after a bolus addition or *in situ* generation of  $^-OONO$ . However, subsequent studies by GERGEL' and CEDERBAUM were discussing an additional inhibition of ADH by  $\bullet NO$ , studied by bolus addition of  $\bullet NO$  as well as with SNAP (*N*-(acetyloxy)-3-nitrosothiovaline) and  $\bullet NO$ -generating NONOates [250]. Additionally, they observed *S*-nitrosation of ADH under these conditions and concluded that ADH can be inhibited by  $\bullet NO$  and  $\bullet NO$ -releasing substances, presumably via *S*-nitrosation of the cysteines of the zinc thiolate center at the enzyme's active site.

During the work on the author's diploma thesis [251] the mechanism by which ADH will get inactivated by RNS was investigated by following NADH formation after incubation of the enzyme at different rates of  $\bullet NO$  and  $O_2^{\bullet -}$  formation. Xanthine oxidase and spermine NONOate allow the simultaneous production of  $O_2^{\bullet -}$  and  $\bullet NO$  at similar rates and are therefore favored to mimic the conditions in the  $\bullet NO/O_2^{\bullet -}$  system. In two aerobic steps, xanthine oxidase converts its substrate hypoxanthine to xanthine and subsequently to uric acid, yielding in the production of two  $O_2^{\bullet -}$  molecules. Spermine NONOate spontaneously dissociates in a pH-dependent, first-order process to liberate two molecules of  $\bullet NO$ .

Prior to the determination of ADH activity, the enzyme without  $NAD^+$  was preincubated for 2 h at 37 °C in the presence of 0.5 U/ml xanthine oxidase, 1 mM hypoxanthine and varying concentrations of spermine NONOate. As a control, ADH was kept under the same conditions, but without xanthine oxidase and spermine NONOate.

These results indicate that  $O_2^{\bullet -}$  or  $\bullet NO$  alone is not able to inactivate ADH at physiologically relevant concentrations. However,  $O_2^{\bullet -}$  generation ( $3.0 \pm 0.2$  nM/s) together with an increasing formation of  $\bullet NO$  will lead to an efficient inhibition of ADH (Fig. 5.9). Maximal inhibition was observed between 4 and 6  $\mu M$  spermine NONOate, which corresponds to equal production of both radicals (5  $\mu M$  spermine NONOate will generate  $2.4 \pm 0.1$  nM/s under these conditions). This inactivation is irreversible

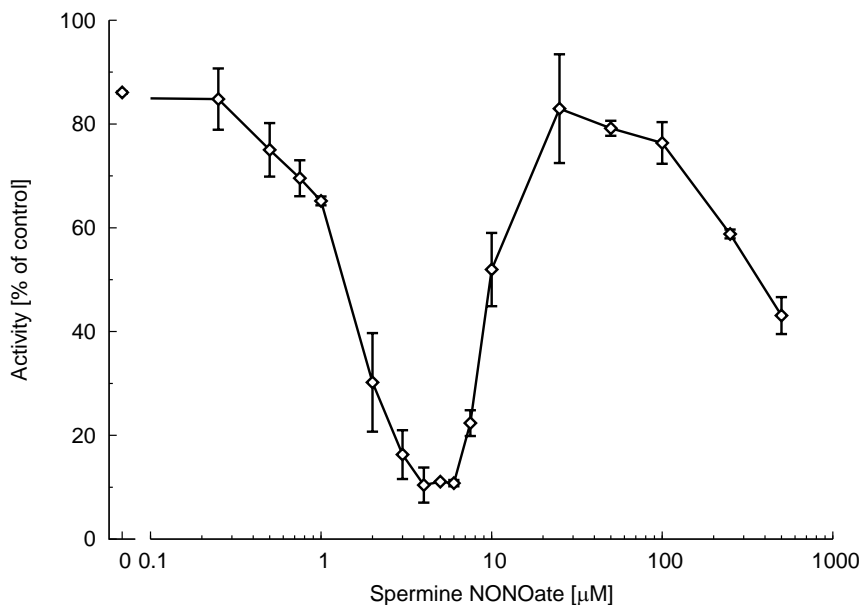


Figure 5.9: **Inactivation of alcohol dehydrogenase (ADH) during simultaneous generation of nitric oxide and superoxide.** The formation of  $\bullet\text{NO}$  and  $\text{O}_2^{\bullet-}$  at equal rates results in 90 % inactivation of ADH. At higher concentrations of  $\bullet\text{NO}$  the oxidizing effects of peroxynitrite are suppressed. Data are mean values  $\pm$  SD;  $n = 3$ . Taken from the author's diploma thesis [251] and published in [51].

in nature; further experiments revealed that inactivation under these conditions will lead to release of one Zn atom per ADH subunit, accompanied with the formation of a disulfide bridge (results not shown, see [51, 251]). The determined  $\text{IC}_{50}$  values for SIN-1 and  $^-\text{OONO}$  were 250 nM and 500 nM, respectively, whereas the  $\text{IC}_{50}$  for  $\bullet\text{NO}$  was three orders of magnitude higher, 200  $\mu\text{M}$  (data not shown, see [51, 251]). The nature as well as the stoichiometry is in line with an oxidative, metal-catalyzed inhibition of ADH by peroxynitrite.

As an unexpected result, conditions in the  $\bullet\text{NO}/\text{O}_2^{\bullet-}$  system where the rate of  $\bullet\text{NO}$  formation exceeds twice that of  $\text{O}_2^{\bullet-}$  did no longer lead to inhibit of ADH activity. At very high concentrations of spermine NONOate in this system (Fig. 5.9), a decrease in ADH activity can be again observed; however, the corresponding  $\bullet\text{NO}$  concentrations are above physiologically relevant levels.

In contrast to GERGEL' and CEDERBAUM [250], we could demonstrate that  $\bullet\text{NO}$  is unable to inactivate ADH under physiologically relevant conditions. Their  $\text{IC}_{50}$  of  $450\ \mu\text{M}$   $\bullet\text{NO}$  is in accordance to the value we found, but these concentrations are too high to play a role in the organism. Likewise, the concentrations of the fast-decomposing  $\bullet\text{NO}$  donor diethylamine NONOate they applied were also too high to be relevant. Concerning the ADH inactivation by SNAP discovered by GERGEL', the *S*-nitrosothiol SNAP was used without taking care for the absence of bivalent metal ions and could have been acted either as a *S*-nitrosothiols or as a  $\bullet\text{NO}$  donor. In addition, GERGEL's data also reveals a rather unspecific oxidation and nitrosation of ADH thiol groups, ruling out a meaningful regulatory mechanism.

From the above results it could be concluded that zinc fingers and therefore transcriptional activity could be affected by  $^-\text{OONO}$  in a similar way. Considering the importance of Zn in diseases, aging and conditions of oxidative stress, our findings could provide a potential mechanism for the increased liberation of Zn in the cell and could as well explain the beneficial effects of Zn under such conditions.

It has to be mentioned that 1 mM GSH is able to protect ADH from  $^-\text{OONO}$  derived oxidations (data not shown). This underlines that an undisturbed cellular redox equilibrium should maintain similar Zn centers in an intact state. Only a shift of cellular redox systems as described in Chapter 3 would allow these oxidations to take place. However, such alterations of redox systems do occur *in vivo* and could also observed *in vitro* and therefore, Zn finger oxidations should be a relevant, but pathophysiological event.

Subsequent results from KRÖNCKE *et al.* revealed that indeed the DNA binding of the Zn finger transcription factors vitamin D receptor and retinoid X receptor will be inhibited by peroxynitrite in an irreversible manner [158]. They determined a relatively high  $\text{IC}_{50}$  of  $300\ \mu\text{M}$   $^-\text{OONO}$ , which is three orders of magnitude higher than the value we observed for ADH. The requirement of high concentrations could

be explained as an artifact due to the bulk additions of peroxynitrite. Bolus additions of peroxynitrite are prone to cause mixing artifacts, but more importantly, there are reports that peroxynitrite from bulk preparations exerts different properties than that *in situ nascendi* [54]. A re-examination of the  $IC_{50}$  value for these Zn fingers with *in situ* formed peroxynitrite would be required to prove the biological relevance of these results. However, they claim that in addition to inhibition by  $^-OONO$ ,  $\bullet NO$  itself is able to inhibit DNA binding of the investigated transcription factors. This  $\bullet NO$ -mediated inhibition revealed a different mechanism, contrary to oxidation by peroxynitrite, dithiothreitol is able to reverse the inactivation. Besides the interesting implications of this observation, these results are diametrically opposed to our findings on ADH as a model for Zn finger proteins. The main discrepancy in their work are the high concentrations of  $\bullet NO$ ; an  $IC_{50}$  of 500  $\mu M$  MAHMA NONOate was necessary to inhibit or release DNA binding. The fast decomposition of the  $\bullet NO$  donor MAHMA NONOate with an half-life of about 2 min results in very high steady-state levels of  $\bullet NO$  during their experiments. Due to the higher stability of  $\bullet NO$  compared to  $^-OONO$ , the achieved  $\bullet NO$  concentrations should be significant higher than those of  $^-OONO$  and far beyond conditions found in a living cell. Taking this into account, these results cannot transferred to the organism, which is a main objective of the herein presented experiments.

Not only Zn fingers are affected by such oxidations; ZOU *et al.* were able to demonstrate that NOS-3 as well can be oxidized in a similar way [252]. The  $ZnCys_4$  center of NOS, located at the dimer interface, stabilizes the dimer;  $^-OONO$  leads to Zn release and weakening of the dimers. In consequence,  $\bullet NO$  synthesis by NOS-3 will be disturbed and an increased uncoupling, leading to  $O_2^{\bullet -}$  formation, was observed. This was discussed in context of diabetic complications, where NOS-3 uncoupling would lead to an increase in vascular dysfunction.

Besides the inhibition of ADH by  $^-OONO$ , the most striking result from the experiment shown in Fig. 5.9 is the effect of a slight excess of  $\bullet NO$  over  $O_2^{\bullet -}$ . If the formation

of  $\bullet\text{NO}$  by spermine NONOate is twice as high as those of  $\text{O}_2^{\bullet-}$ , inhibition of ADH is already half-maximal and higher concentrations completely abolish the inhibitory effects of peroxynitrite. This is in so far surprising as the fast reaction of  $\text{O}_2^{\bullet-}$  and  $\bullet\text{NO}$  to form  $^-\text{OONO}$  cannot be affected by an excess of one of the substrates and therefore peroxynitrite decomposition has to be increased by orders of magnitudes to prevent its reaction with ADH. The only meaningful explanation would be a shift of the reaction pattern in the  $\bullet\text{NO}/\text{O}_2^{\bullet-}$  system from  $^-\text{OONO}$  to a different intermediate, but current knowledge offers no explanation for this phenomenon and lead us to further investigation of the reaction in question. However, this results clearly shows that despite the very fast reaction of  $\bullet\text{NO}$  with  $\text{O}_2^{\bullet-}$  to yield  $^-\text{OONO}$  an excess of  $\bullet\text{NO}$  is a very effective scavenger for  $^-\text{OONO}$  and prevents  $^-\text{OONO}$ -mediated oxidations under physiological conditions. This is of high biological significance, since this implies that oxidations by  $^-\text{OONO}$  *in vivo* can only occur if  $\text{O}_2^{\bullet-}$  levels are in the same region or higher as those of  $\bullet\text{NO}$ .

Based on this result we assume that  $\bullet\text{NO}$  could be able to react with peroxynitrite *in statu nascendi*, more precisely with its acid HOONO. There are clear indications that  $^-\text{OONO}$  is not able to react with  $\bullet\text{NO}$ , as was demonstrated by MERENYI and LIND at pH 12 [253], but in the case of HOONO no experimental data exist in literature. Furthermore, in most of the existing studies regarding the reactivities of peroxynitrite only bolus additions from concentrated alkaline solutions were analyzed, but recent results indicate that under these conditions the formation of an adduct between the peroxynitrite anion and its acid will prevent further reactions (R. KISSNER, personal communication). The investigation of the mechanism of the effect of  $\bullet\text{NO}$  on peroxynitrite decomposition is one subject of this work.

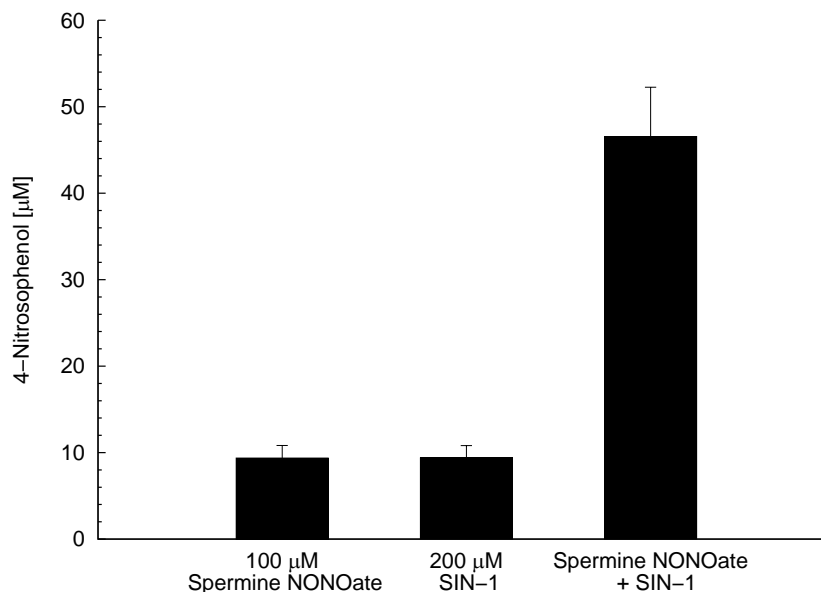


Figure 5.10: **C-Nitrosation of phenol by  $\bullet$ NO from spermine NONOate, peroxyntirite from SIN-1, and both together.** The reaction of 100  $\mu$ M spermine NONOate or 200  $\mu$ M SIN-1, or both together with phenol results in the formation of 4-nitrosophenol. Data are mean values  $\pm$  SD;  $n = 3$ .

### 5.2.1 C-Nitrosation of Phenol by Nitric Oxide from Spermine NONOate, Peroxyntirite from SIN-1, and Both Together

One of the possible explanations of the observed reaction of an excess of  $\bullet$ NO with  $\text{O}_2^{\bullet-}$ , which prevents oxidations by peroxyntirite, would be a reaction of  $\bullet$ NO with HOONO, which in consequence could lead to other RNS. And indeed, PFEIFFER *et al.* observed a fast reaction of peroxyntirite with  $\bullet$ NO at pH 7.4 [254], but this was discussed as the reaction of the peroxyntirite anion with  $\bullet$ NO. But such a reaction should be negligible, as subsequent studies by MERENYI and LIND could confirm [253]. In a recent publication by GOLDSTEIN *et al.* the contradictions in literature concerning a possible reaction of  $^-\text{OONO}$  with  $\bullet$ NO were investigated [255] and an  $^-\text{OONO}$ -consuming effect of an excess of  $\bullet$ NO was proposed due to the mostly aerobic formation of  $\bullet$ NO<sub>2</sub> from  $\bullet$ NO at alkaline conditions and a subsequent reaction with  $\bullet$ NO to yield N<sub>2</sub>O<sub>3</sub>. Additionally anaerobic formation of  $\bullet$ NO<sub>2</sub> at neutral conditions

was explained due to the homolysis of HOONO. In consequence,  $\text{N}_2\text{O}_3$  would react quickly with  ${}^-\text{OONO}$  with  $k = 3.1 \times 10^8 \text{ M}^{-1}\text{s}^{-1}$  [255]:



To test the hypothesis that the observed effects could be explained by the formation of  $\text{N}_2\text{O}_3$ , which yields nitrosating properties, the *C*-nitrosation of phenol was determined at comparable conditions to the ADH experiments. The use of phenol as a probe for nitrosations was established by UPPU *et al.* [256] and therefore represents an accepted and appropriate model. The formation of 4-nitrosophenol was monitored spectrophotometrically at 400 *versus* 500 nm over a time period of 2 h, as described by PILICHOWSKI *et al.* [231], whereas the final yield was determined according to an HPLC method previously developed by DAIBER *et al.* [232].

The reaction of phenol with 100  $\mu\text{M}$  spermine NONOate, decomposing to give two molecules of  $\bullet\text{NO}$ , as well as 200  $\mu\text{M}$  SIN-1, decomposing to equimolar parts  $\bullet\text{NO}$  and  $\text{O}_2^{\bullet-}$  and in consequence  ${}^-\text{OONO}$ , leads in both cases to formation of 9.4  $\mu\text{M}$  4-nitrosophenol (Fig. 5.10). At the above concentrations, both donors together result in the formation of 46.6  $\mu\text{M}$  4-nitrosophenol, significantly more than the sum of both donors.

At the given conditions, a 3:1 stoichiometry of  $\bullet\text{NO}$  to  $\text{O}_2^{\bullet-}$  can be expected, leading to 2  $\bullet\text{NO}$  per  ${}^-\text{OONO}$ , but due to the extended incubation time and the differences in half-life of both donors, this stoichiometry is only an approximation. The increase in 4-nitrosophenol formation indicates the involvement of a nitrosating intermediate, possibly also allowing *N*- and *S*-nitrosations. This leads us to the hypothesis that nitrosation could be a regulatory mechanism under conditions of elevated NOS activity and increasing formation of  $\text{O}_2^{\bullet-}$ , whereas a further increase in  $\text{O}_2^{\bullet-}$  production would subsequently lead to  ${}^-\text{OONO}$  formation and could therefore play a role in the cell's preparation to such conditions.

The increased formation of 4-nitrosophenol could possibly be explained by the reactions proposed by GOLDSTEIN [255], but at the same time also supports our hypothesis of a direct reaction of HOONO with  $\bullet\text{NO}$ . Such a reaction was categorically declined by GOLDSTEIN as a conclusion of the lack of reactivity of the peroxyxynitrite anion, but without providing supporting data.

The gained results indicate that indeed a nitrosating intermediate will be formed during the reaction of an excess of  $\bullet\text{NO}$  with  $\text{O}_2^{\bullet-}$ , but neither does explain the mechanism of its formation nor reveal the intermediate in question. Therefore further experiments were required to examine the involvement of a nitrosating species like  $\text{NO}^+$  or  $\text{N}_2\text{O}_3$ .

## 5.3 Mechanism of Nitrosation in the Nitric Oxide/Superoxide System

### 5.3.1 N-Nitrosation of 2,3-Diaminonaphthalene in the Nitric Oxide/Superoxide System

The preceding results revealed the formation of a nitrosating species if an excess of  $\bullet\text{NO}$  reacts with  $\text{O}_2^{\bullet-}$ . The following experiments are aimed at the uncovering of the underlying mechanism since recent literature does not offer an explanation for the observed phenomenon.

*N*-Nitrosation of 2,3-diaminonaphthalene (DAN) leads to an intermediate which will be converted to 2,3-naphthotriazole (NAT, see Fig. 4.2). The accompanied ring closure results in strong fluorescence; therefore DAN is a preferred model for the investigation of nitrosation [234]. Since the observed nitrosation is the sum of different chemical pathways including  $\bullet\text{NO}$  autoxidation, it is necessary to keep the  $\bullet\text{NO}$  formation at a constant rate and to vary  $\text{O}_2^{\bullet-}$  formation. A concentration of 1 mM hypoxanthine is sufficiently high to assume substrate saturation of xanthine oxidase and a linear correlation between enzyme concentration and reaction rate ( $K_M = 1.86 \text{ M}$  for hypoxanthine [257]).

To investigate nitrosation in the  $\bullet\text{NO}/\text{O}_2^{\bullet-}$  system, the formation of NAT from DAN was determined at different conditions. A constant  $\bullet\text{NO}$  release of 3.87 nM/s was provided by the presence of 5  $\mu\text{M}$  spermine NONOate, whereas the concentration of xanthine oxidase was varied. 1 mU/ml xanthine oxidase yields 2.43 nM/s  $\text{O}_2^{\bullet-}$  at the specific experimental conditions. At 1.6 mU/ml xanthine oxidase,  $\text{O}_2^{\bullet-}$  and  $\bullet\text{NO}$  production are equal during the 20 min of incubation at 37 °C. NAT fluorescence, specified in relative light units (RLU), was  $160 \pm 22$  RLU in the absence of  $\text{O}_2^{\bullet-}$  and maximal at 0.53 mU/ml xanthine oxidase (1.3 nM/s  $\text{O}_2^{\bullet-}$ ) with  $417 \pm 17$  RLU. These

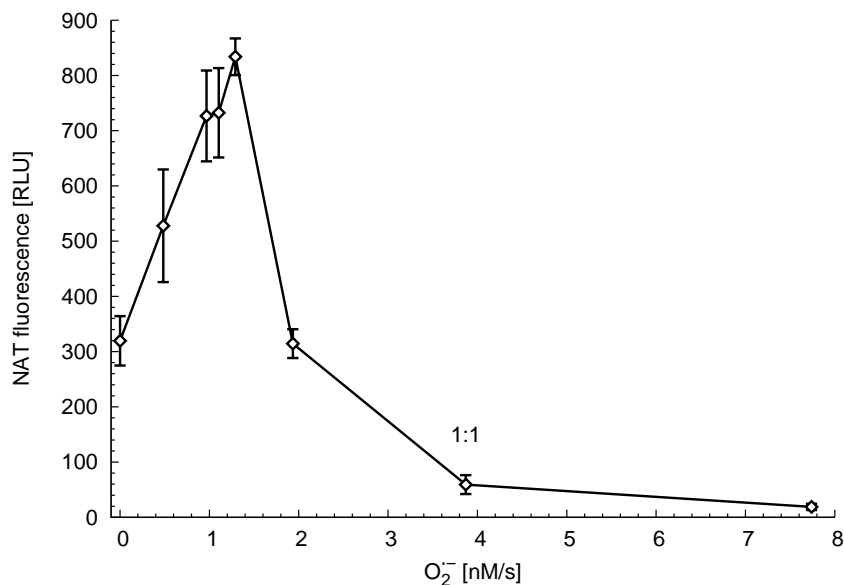


Figure 5.11: ***N*-Nitrosation of DAN in the  $\bullet\text{NO}/O_2^{\bullet-}$ -system.** *N*-Nitrosation of DAN (10  $\mu\text{M}$ ) after incubation with  $\bullet\text{NO}$  from spermine NONOate (5  $\mu\text{M}$ , resulting in 3.87 nM/s  $\bullet\text{NO}$ ) and various rates of superoxide formation (1 mU/ml xanthine oxidase yields 2.43 nM/s  $O_2^{\bullet-}$ ) was determined by measuring NAT fluorescence. At 3.87 nM/s,  $O_2^{\bullet-}$  equals  $\bullet\text{NO}$  formation. Additionally, each sample contained 1 mM hypoxanthine in potassium phosphate buffer (100 mM, pH 7.4) and was incubated for 20 min at 37  $^\circ\text{C}$ . Data are mean values  $\pm$  SD;  $n = 4$ .

results suggest a stoichiometry between 2:1 up to 3:1 of  $\bullet\text{NO}$  to  $O_2^{\bullet-}$ . Rising levels of  $O_2^{\bullet-}$  are leading to a strong decrease of NAT formation. A 1:1 stoichiometry, resulting in peroxynitrite formation, leads to  $30 \pm 9$  RLU, further shifts in stoichiometry revealed a further decrease of fluorescence.

The fact that in the presence of  $O_2^{\bullet-}$  nitrosation can be nearly threefold as high as by  $\bullet\text{NO}$  alone clearly demonstrates that  $\bullet\text{NO}$  alone and the resulting autoxidation during aerobic conditions are not representing the main pathways of nitrosations during physiological conditions. Formation of peroxynitrite at a stoichiometry of 1:1 seems to be faster than other reactions in the system, leading to a strong decrease in nitrosations. This again demonstrates that peroxynitrite is not leading to nitrosations, at least not in the case of DAN.

If one compares DAN nitrosation in the  $\bullet\text{NO}/\text{O}_2^{\bullet-}$  system with the inhibition of ADH (Fig. 5.9), it becomes obvious that conditions of oxidation by peroxynitrite and nitrosation are excluding each other. Conditions of maximal nitrosation exactly correspond to a released ADH inhibition by an excess of  $\bullet\text{NO}$ . In context of the herein discussed physiological relevance of the  $\bullet\text{NO}/\text{O}_2^{\bullet-}$  system as a regulatory mechanism, this indicates distinct and delimited phases of regulatory events during the shift from physiological cellular  $\bullet\text{NO}$  production to finally oxidative stress by  $\text{O}_2^{\bullet-}$ . This results cannot rule out that an increased  $\bullet\text{NO}$  formation can lead to nitrosations, besides specific nitrosylations which only require low levels of  $\bullet\text{NO}$ . However, maximal nitrosation requires a certain level of  $\text{O}_2^{\bullet-}$ , which means activation of sources of  $\text{O}_2^{\bullet-}$  in cellular context. If one assumes conditions which are leading to a cascading activation of cellular  $\text{O}_2^{\bullet-}$  sources as described in Fig. 6.1, conditions of maximal nitrosation should directly precede peroxynitrite formation and oxidative stress. Therefore we hypothesize that one role of cellular nitrosations is the preparation to conditions of imminent oxidative stress.

The experimental results are in principle complying with those from ESPEY *et al.* [52], but in detail some important differences exist. According to their data, between conditions of maximal nitrosation and an 1:1 stoichiometry between  $\bullet\text{NO}$  and  $\text{O}_2^{\bullet-}$  formation, nitrosation only decreases by roughly 25%; our data indicates an decrease of 93%. This is of importance for the interpretation of the physiological relevance of our results; a great overlap of nitrosations and oxidations by peroxynitrite would argue against the discussed model of distinct phases of redoxregulation during the activation of  $\text{O}_2^{\bullet-}$  sources. These differences could be due to variation of xanthine oxidase activity or spermine NONOate decay and their longer incubation time; ESPEY's  $\bullet\text{NO}$  formation rates are only half of ours, despite similar experimental conditions. However, xanthine oxidase activity and spermine NONOate decay were always controlled with the oxyHb and the cytochrome *c* assay prior to the herein described experiments. Another consequence of the discussed difference between Fig. 5.11 and the data published

by ESPEY is the different stoichiometry between  $\bullet\text{NO}$  and  $\text{O}_2^{\bullet-}$  during conditions of maximal *N*-nitrosation of DAN. Our data, both in the absence and presence of  $\text{CO}_2$  (cf. Fig. 5.13), trends toward a ratio of 3:1, whereas their data towards 2:1. The exact determination of the optimal ratio would give a hint about the pathway of nitrosation under these conditions, but until now, neither our data nor data in literature provides unequivocal evidence.

### 5.3.2 Effect of Azide on 2,3-Diaminonaphthalene Nitrosation

Dinitrogen trioxide ( $\text{N}_2\text{O}_3$ ) is an intermediate discussed to play a central role during cellular nitrosations, both in mechanisms via autoxidation of  $\bullet\text{NO}$  and  $\text{CO}_2$ -mediated pathways. With the already discussed mechanism proposed by GOLDSTEIN [255] (cf. 5.2.1),  $\text{N}_2\text{O}_3$  would represent the central nitrosating intermediate in the  $\bullet\text{NO}/\text{O}_2^{\bullet-}$  system, whereas the proposed reaction of  $\bullet\text{NO}$  with  $\text{HOONO}$  could also lead to  $\text{N}_2\text{O}_3$ , but via a different pathway. To test the hypothesis that  $\text{N}_2\text{O}_3$  could be the nitrosating intermediate in the  $\bullet\text{NO}/\text{O}_2^{\bullet-}$  system, azide as a specific scavenger for  $\text{N}_2\text{O}_3$  [73] was added to trap  $\text{N}_2\text{O}_3$  at conditions of maximal nitrosation. Xanthine oxidase would be inhibited by azide, therefore SIN-1 together with spermine NONOate was used to comply with conditions of maximal nitrosation during continuous formation of the relevant intermediates, conforming a 4:1 ratio between  $\bullet\text{NO}$  and  $\text{O}_2^{\bullet-}$  formation.

At the given conditions (Fig. 5.12),  $3.75\ \mu\text{M}$  spermine NONOate yields  $2.90\ \text{nM/s}$   $\bullet\text{NO}$ , whereas  $7\ \mu\text{M}$  SIN-1 should correspond  $0.97\ \text{nM/s}$   $\bullet\text{NO}$  and  $\text{O}_2^{\bullet-}$  each. In the presence of  $1\ \text{mM}$  azide *N*-nitrosation of DAN is only reduced by 11 %. In an additional experiment, nitrosation in the presence of  $25\ \text{mM}$  bicarbonate was investigated, leading to comparable results which will be discussed later in Section 5.4.

The small effect of azide, even smaller as observed by ESPEY *et al.* [52], does not point to  $\text{N}_2\text{O}_3$  as the main nitrosating agent in the  $\bullet\text{NO}/\text{O}_2^{\bullet-}$  system. The existence of an equilibrium between at least four isomers of  $\text{N}_2\text{O}_3$  is discussed in literature [72]

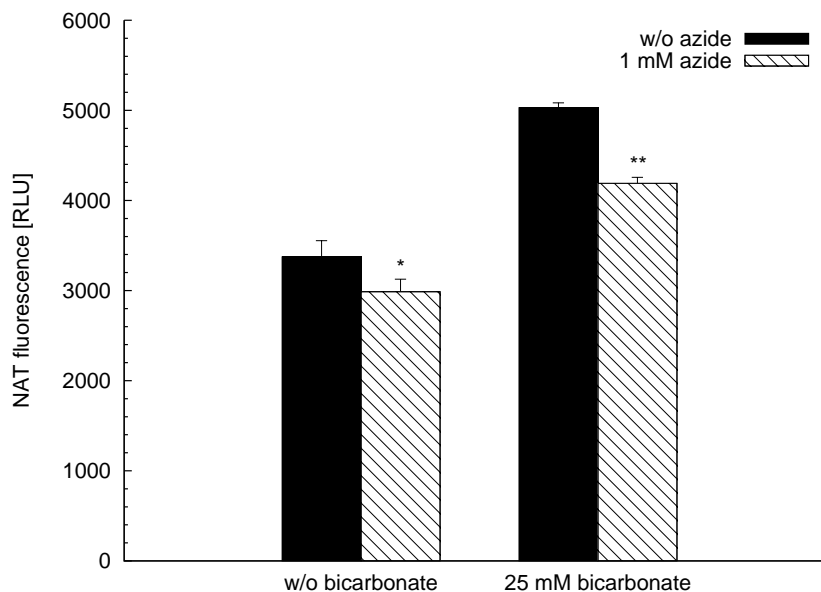


Figure 5.12: **Effect of azide on DAN-nitrosation by the  $\bullet\text{NO}/\text{O}_2^{\bullet-}$  system.** Under conditions of maximal nitrosation ( $7\ \mu\text{M}$  SIN-1 and  $3.75\ \mu\text{M}$  spermine NONOate) only 11 % of DAN-nitrosation can be blocked by sodium azide (1 mM) and 17 % in the presence of bicarbonate/ $\text{CO}_2$  (25 mM potassium hydrogencarbonate). Samples containing  $10\ \mu\text{M}$  DAN and 1 mM hypoxanthine in potassium phosphate buffer (100 mM, pH 7.4) were incubated for 20 min at  $37\ ^\circ\text{C}$ . Data are mean values  $\pm$  SD; \* $P < 0.05$ , \*\* $P < 0.001$ , as compared to the corresponding sample without azide;  $n = 3$ .

and it is not known whether the reaction with azide occurs with all isoforms. This raises the question if azide is an effective scavenger during these conditions, but in literature it is described as the only known specific and effective scavenger. Therefore it has to be assumed that under these conditions  $\text{N}_2\text{O}_3$  is not involved in the observed NAT formation in the  $\bullet\text{NO}/\text{O}_2^{\bullet-}$  system. One cannot exclude the possibility that  $\text{N}_2\text{O}_3$  plays an important role during nitrosations in the absence of peroxynitrite or  $\text{O}_2^{\bullet-}$  and literature provides hints for this thesis. However, the data in this work suggest that nitrosations under physiological conditions should require the presence of  $\text{O}_2^{\bullet-}$ . This supplements the existing data in literature; it is well accepted that formation of *S*-nitrosothiols *in vivo* can be stimulated by activation of  $\text{O}_2^{\bullet-}$  sources in parallel to those of  $\bullet\text{NO}$ . The hypothesis of an involvement of  $\text{N}_2\text{O}_3$  is based on the formal requirement of  $\text{NO}^+$  for *S*-nitrosations, but free  $\text{NO}^+$  itself is elusive at cellular conditions. However,

## 5 Results and Discussion

if  $\text{NO}^+$  would exist as a stabilized adduct within a solvent cage, its half-life could be long enough to lead to *S*-nitrosations in biological systems.

## 5.4 Effect of CO<sub>2</sub> on the Chemistry in the Nitric Oxide/Superoxide System

The reaction of CO<sub>2</sub> with <sup>-</sup>OONO is discussed in recent literature to be responsible for the majority of the reactions in the •NO/O<sub>2</sub><sup>•-</sup> system, or at least referred to if other mechanisms do not provide a reasonable mechanism to explain the observed reactions. Since it is widely accepted that autoxidation of •NO in biological systems cannot account for significant effects, the chemistry of CO<sub>2</sub> in the •NO/O<sub>2</sub><sup>•-</sup> system has to be taken into consideration during investigation concerning this system; especially in context of this work which focuses on reactions involving small, gaseous molecules, the effect of CO<sub>2</sub> has to be considered. Therefore, the relevant experiments in this work were additionally performed in the presence of CO<sub>2</sub>. In blood plasma, the equilibrium between CO<sub>2</sub>, H<sub>2</sub>CO<sub>3</sub> and HCO<sub>3</sub><sup>-</sup> regulates extracellular pH and transports CO<sub>2</sub>. This should provide sufficient concentrations of CO<sub>2</sub> for the discussed reaction with <sup>-</sup>OONO. Commonly, a 25 mM bicarbonate buffer is used for *in vitro* studies of the derived reaction mechanisms. This should provide around 1.3 mM CO<sub>2</sub> in solution [63], assuming that sample volume and time for the experiment does not allow that significant amounts of CO<sub>2</sub> turn over in the gas phase.

In the following, the effect of CO<sub>2</sub> on both oxidations and nitrosations will be investigated, whereas the effect of a simultaneous presence of azide is already shown in Fig. 5.12. In the upper panel of Fig. 5.13, GSH oxidation during different conditions in the •NO/O<sub>2</sub><sup>•-</sup> system was determined by measurement of the remaining reduced GSH with DTNB after 20 min of incubation at 37 °C and pH 7.4. In the absence of O<sub>2</sub><sup>•-</sup>, •NO alone is not able to oxidize GSH, but if levels of O<sub>2</sub><sup>•-</sup> rise to one quarter of those of •NO, a substantial decrease in remaining GSH will occur. From these data it is not possible to differentiate between the possible pathways of GSH oxidation under the distinct conditions. However, considering the results presented in this work, GSH oxidation should occur mainly via GSSG formation and *S*-nitrosation, depending on

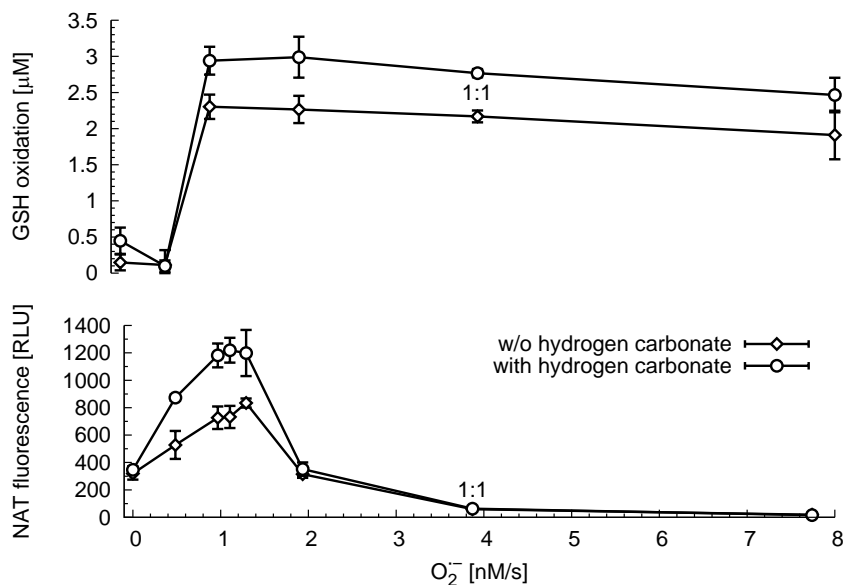


Figure 5.13: **Oxidation of GSH and *N*-Nitrosation of DAN in the  $\bullet\text{NO}/O_2^{\bullet-}$  system in the presence of  $\text{CO}_2$ .** The oxidation of  $5\ \mu\text{M}$  GSH during simultaneous generation of  $\bullet\text{NO}$  by spermine NONOate ( $3.9\ \text{nM/s}$ ) and  $O_2^{\bullet-}$  ( $1.6\ \text{mU/ml}$  xanthine oxidase yields  $3.9\ \text{nM/s}$   $O_2^{\bullet-}$ ) was determined by measuring the decline of GSH with DTNB, whereas the *N*-nitrosation of DAN at the same conditions was determined via NAT fluorescence (see Fig. 5.11). The presence of  $25\ \text{mM}$  bicarbonate increased both oxidation of GSH and DAN nitrosation. Data are mean values  $\pm$  SD;  $n = 4$ .

the ratio between both radicals. Transferred to the cell and the relevant time-frame for such events, Zn finger oxidations, made possible by preceding GSH oxidation, should be a relevant, but pathophysiological event. During the oxidation of GSH, the presence of  $\text{CO}_2$  accounts for an by 30 % increased oxidation which is independent from the stoichiometry between  $\bullet\text{NO}$  and  $O_2^{\bullet-}$  as long as substantial amounts of  $O_2^{\bullet-}$  were formed.

The reaction of  $^-\text{OONO}$  with  $\text{CO}_2$  and its kinetic properties, as described in section 3.4.1, are widely accepted—in contrast to the prediction of its net effect in the cell. This fact manifests itself in the contradictory results of GSH oxidation by DENICOLA and ZHANG *et al.*—both groups reported that  $\text{CO}_2$  inhibits the oxidation of GSH up to 50 % [63, 258] by using comparable bicarbonate concentrations. However, in both publications the concentrations of GSH were two orders of magnitude higher compared

to the above described experiment and GSH oxidation was achieved by bolus addition of  $^-OONO$  in the absence of  $\bullet NO$  or  $O_2^{\bullet -}$  which should be responsible for the different effects of  $CO_2$ . The  $\bullet NO/O_2^{\bullet -}$  system as used in this work enables reactions not possible by  $^-OONO$  alone and the lower concentration of GSH favours these reactions; however, the usage of high concentrations of GSH should capture the oxidizing intermediates in the system. GSH oxidation should occur as the sum of GSSG formation, *S*-nitrosation and other possible oxidative modifications; though formation of GSSG could result in up to two times faster GSH consumption, depending on the relevant mechanism. Therefore, different results within a factor of two should be possible if the parameters are accordingly changed.

During the *N*-nitrosation of DAN,  $CO_2$  has only an effect at conditions of maximal nitrosation, where it increases NAT formation up to two thirds (lower panel of Fig. 5.13). The impact of  $CO_2$  on nitrosations is again a matter of controversial discussions in literature. In most cases, only nitrosations via autoxidation of  $\bullet NO$  in the absence of  $O_2^{\bullet -}$  were investigated [259, 260]. As already discussed, this should not be the relevant mechanism of nitrosations *in vivo*. However, these publications state that nitrosations will be decreased by  $CO_2$ , but in both cases the considerably higher substrate concentrations should be able to quench secondary reactions, giving no indications about the biological direction and relevance of a  $CO_2$ -mediated net effect. Indeed, using comparable conditions in the  $\bullet NO/O_2^{\bullet -}$  system and low substrate concentrations, ESPEY *et al.* reported a profile for nitrosations similar to our results [52].

To estimate the effect of changes in  $CO_2$  concentrations, DAN nitrosation was determined with varying concentrations of bicarbonate. Fig. 5.14 shows the effect of increasing concentrations of bicarbonate on *N*-nitrosation of DAN during conditions of maximal nitrosation. Within the physiological relevant concentration range, NAT formation remains constant; moderate changes in  $CO_2$  concentration should therefore be without consequences for nitrosations occurring *in vivo*.

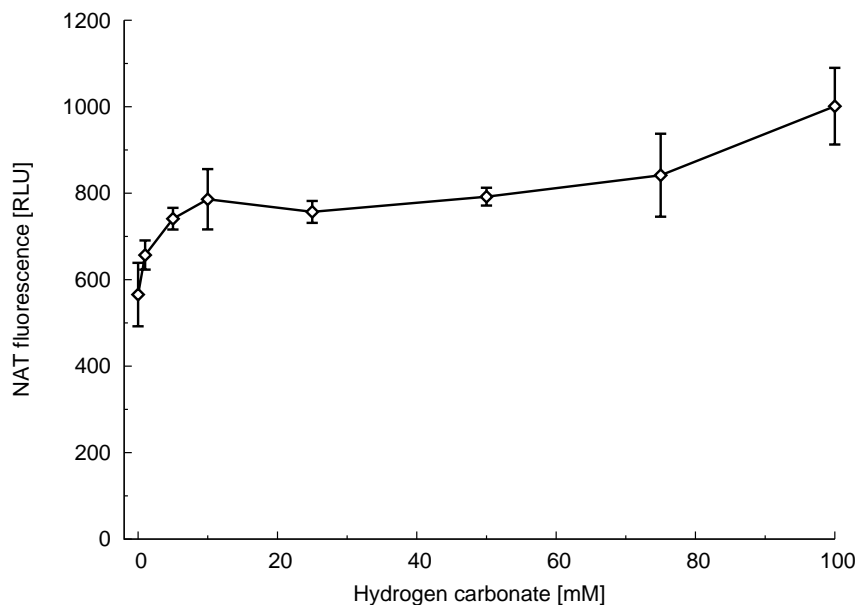


Figure 5.14: ***N*-Nitrosation of DAN at increasing concentrations of hydrogen carbonate.** NAT formation in the  $\bullet\text{NO}/\text{O}_2^{\bullet-}$  formation was determined with increasing concentrations of potassium carbonate. Samples containing 1 mM hypoxanthine, 0.53 mU/ml xanthine oxidase, 5  $\mu\text{M}$  spermine NONOate and 10  $\mu\text{M}$  DAN in 200 mM potassium phosphate buffer, pH 7.4, were incubated for 20 min at 37  $^\circ\text{C}$ . Under these conditions, 3.9 nM/s  $\bullet\text{NO}$  and 1.3 nM/s  $\text{O}_2^{\bullet-}$  will be formed. The pH was adjusted to be constant at all conditions. Data are mean values  $\pm$  SD;  $n = 4$ .

In conclusion, these data suggest that  $\text{CO}_2$  is only to a smaller part responsible for the observed nitrosations and oxidations in the  $\bullet\text{NO}/\text{O}_2^{\bullet-}$  system. At most,  $\text{CO}_2$  is able to intensify nitrosations and oxidations, but only under conditions of already increased rates of nitrosation and oxidation, which is the main insight gained from these experiments.

The same conclusion can be drawn from the effect of azide on DAN nitrosation in the presence of  $\text{CO}_2$  (Fig. 5.12). Under these experimental conditions,  $\text{CO}_2$  is able to elevate NAT formation around 50 %; whereas addition of azide decreases nitrosation by 17 %, compared to 11 % in the absence of  $\text{CO}_2$ . With and without  $\text{CO}_2$ , nitrosations is mostly independent on  $\text{N}_2\text{O}_3$  formation. Together with the unaltered reaction profile during GSH oxidation and *N*-nitrosation of DAN,  $\text{CO}_2$  does not seem to enable a different reaction pathway leading to these modifications.

## 5.5 Nitration and Nitrosation During Freezing of Samples

Since Beckman *et al.* proposed 3-nitrotyrosine (3-NT) as a footprint for peroxynitrite formation *in vivo* [50] and the development of potent antibodies directly against 3-NT, the determination of 3-NT with techniques such as immunofluorescence, optical and electrochemical HPLC or MS methods is a very common step during investigations in the broad field of oxidative stress. During such investigations the samples are usually frozen until measurement of 3-NT, especially since 3-NT is a very stable—to current knowledge irreversible in biological context—covalent protein modification. Together with ANDREAS DAIBER<sup>5</sup> we discovered that after freezing of biological samples one can measure high levels of 3-NT, which were not present before freezing of the samples.

Therefore, the freezing of samples can be a common source for false-positive results regarding •NO-dependent covalent protein modifications. Especially the pattern of protein nitration will change since under physiological conditions only a few proteins can be nitrated and this only happens in a metal-catalyzed manner, whereas tyrosine nitration during freezing is an unspecific process. We determined three key factors which lead to this artificial protein nitration: sodium phosphate (e.g. as buffer medium), nitrite and slow freezing of the samples [261, 262]. In addition to nitration, I discovered high amounts of nitrosation at the same conditions.

### 5.5.1 S-Nitrosation of Albumin

My first indication of the appearance of nitrosative conditions in addition to nitrations during freezing with nitrite in sodium phosphate buffer was by freezing (−20 °C) of metal-free solutions of albumin (25 µM BSA) with or without 10 mM nitrite in sodium

---

<sup>5</sup>Universitätsklinikum Hamburg-Eppendorf, Hamburg, Germany, now at the Klinikum der Johannes Gutenberg-Universität, Mainz, Germany.

or potassium phosphate buffer, followed by determination of *S*-nitrosation. Albumin is known to contain only one accessible cysteine (Cys-34) and this is susceptible to *S*-nitrosation. *S*-Nitrosation of BSA was determined by copper ion driven decomposition of *S*-nitrosothiols and detection of the resulting free  $\bullet\text{NO}$  by DAN fluorescence. In samples which contained nitrite in sodium phosphate buffer and were frozen,  $23.98 \pm 5.93 \mu\text{M}$  nitrosothiols were detected, whereas in all other samples the concentration was below  $1 \mu\text{M}$ . This nearly complete *S*-nitrosation of thiols from BSA could be prevented by blocking thiol groups with DTNB or iodoacetamide prior to freezing. In this case, nitrosation was decreased by more than 50 % (data not shown, see [261]).

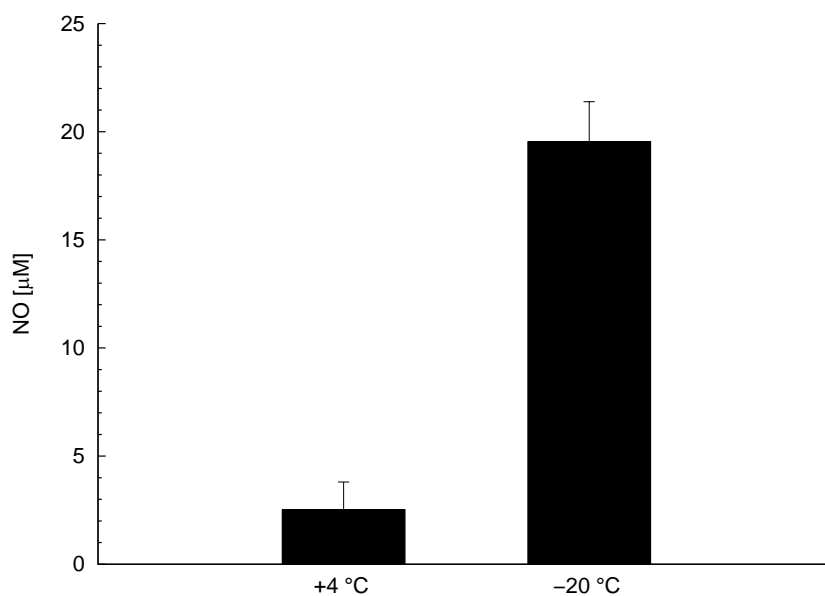


Figure 5.15: ***S*-Nitrosation of albumin during freezing in sodium phosphate buffer.** Samples containing BSA and 1 mM sodium nitrite in 100 mM sodium phosphate buffer (pH 7.4) were stored over night at  $4^\circ\text{C}$  or frozen at  $-20^\circ\text{C}$  prior to determination of *S*-nitrosation. *S*-nitrosation was measured with the oxyHb assay by releasing  $\bullet\text{NO}$  from *S*-nitrosothiols with  $\text{Cu}^{2+}$ . Data are mean values  $\pm$  SD;  $n = 4$ .

Determination of *S*-nitrosation by  $\text{Cu}^{2+}$  and DAN turned out to be not a reliable method, perhaps due to the fact that small traces of nitrite will disturb the assay. Therefore, a similar experiment was done, whereas quantification of nitrosation was performed with a modified oxyHb assay (Fig. 5.15). Although the addition of two-

charged metal ions results in the formation of an insoluble precipitation of potassium salts, which in turn disturbs the optical method, this method provides reliable results. A high level of nitrosation was detected after freezing of the samples, but the  $\bullet\text{NO}$ -signal was lower as in the first experiment; this could be due to the lower concentration of nitrite.

### 5.5.2 N-Nitrosation of 2,3-Diaminonaphthalene

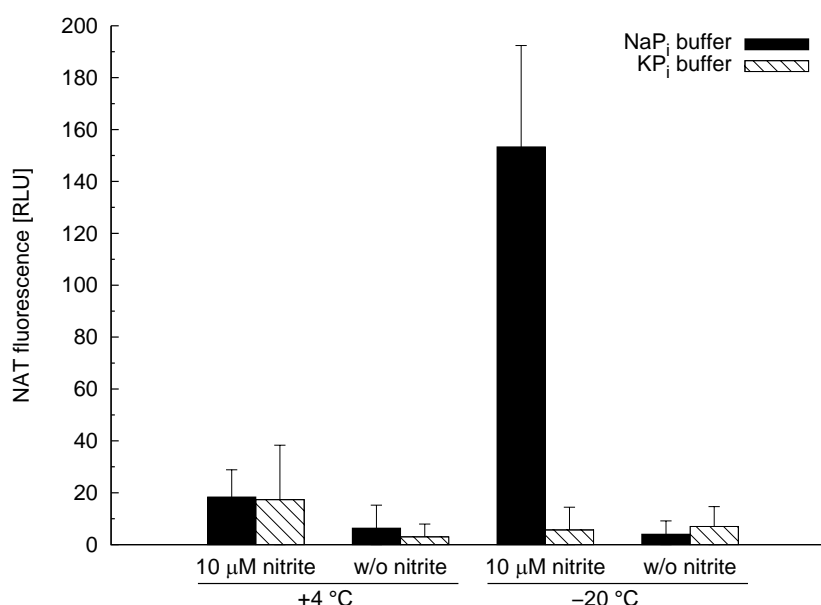


Figure 5.16: **N-Nitrosation of DAN during freezing in sodium phosphate buffer.** Upon storage of samples containing sodium phosphate (100 mM, pH 7.4), nitrite (10  $\mu\text{M}$ ) and DAN (30  $\mu\text{M}$ ) for 2.5 h at  $-20\text{ }^\circ\text{C}$ , a fluorescence signal was observed, whereas in the absence of nitrite or in samples containing potassium instead of sodium phosphate no significant formation of NAT was detectable. In addition, only background fluorescence was observed in samples which were kept at  $4\text{ }^\circ\text{C}$  for the same time. Data are mean values  $\pm$  SD;  $n = 3$ .

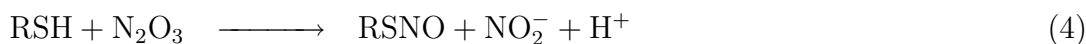
In a third experiment *N*-nitrosation was directly investigated using DAN as a substrate for nitrosation during freezing (Fig. 5.16). This direct nitrosation of DAN results in higher sensitivity and lower error values. Therefore, it was possible to investigate the effects of lower concentrations of nitrite and the used concentration of 10  $\mu\text{M}$  matches

the physiological cytosolic concentration. Upon storage of samples containing sodium phosphate, nitrite and DAN at  $-20\text{ }^{\circ}\text{C}$  a high fluorescence signal of NAT was observed, whereas in the absence of nitrite and/or sodium or in samples which were kept at  $+4\text{ }^{\circ}\text{C}$  only basal fluorescence was detected. These results show that in addition to *S*-nitrosation also *N*-nitrosation is likely to occur during freezing of samples in sodium phosphate buffer and the presence of micromolar concentrations of nitrite is sufficient for this.

Physiological levels of nitrite in cell culture media are around  $0.5\text{ }\mu\text{M}$  and even  $10\text{ }\mu\text{M}$  in the cytosol but can reach up to  $80\text{ }\mu\text{M}$  in media containing cells or tissue with induced NOS. In our experiments  $1\text{ }\mu\text{M}$  nitrite was sufficient to see covalent protein modifications [261, 262]. Depending on the temperature, we observed different levels of nitration and nitrosation. Storage at  $-20\text{ }^{\circ}\text{C}$  results in the highest yield of sample modification, at  $-70\text{ }^{\circ}\text{C}$  the effects were significantly lower and even lower during freezing in liquid nitrogen ( $-196\text{ }^{\circ}\text{C}$ ). But longer storage at these temperatures does not result in higher yields of nitration and nitrosation. Therefore, we determined the velocity of freezing as a key factor, in addition to the presence of sodium phosphate and nitrite. Slow freezing respectively freezing at higher temperatures results in prolongation of the conditions where a solid and a liquid phase is present in the samples.

That freezing of sodium phosphate buffered solutions leads to unexpected results was first demonstrated by GOMEZ *et al.* [263]. During the freezing process, the more acidic  $\text{H}_2\text{PO}_4^-$  anion will accumulate in the liquid phase, whereas sodium salts of the alkaline anions  $\text{HPO}_4^{2-}$  and  $\text{PO}_4^{3-}$  precipitate or co-crystallize with the aqueous phase. This phenomenon will cause a decline in the pH of the liquid phase, even reaching values between 3 and 4. The slower the freezing process, the more distinct the shift in pH will be, in accordance with the fact that sodium phosphate buffer already crystallizes during storage at  $4\text{ }^{\circ}\text{C}$ .

The chemistry behind the nitrosation under such conditions is quite obvious in principle but more complex in detail. During freezing of  $\text{Na}_2\text{HPO}_4/\text{NaH}_2\text{PO}_4$  solutions the pH drops below the  $\text{p}K_a$  of nitrous acid and hence the acidic solution becomes a nitrosating medium, possibly via  $\text{N}_2\text{O}_3$  formation:



The acidification of nitrite solutions represents a common mechanism for synthesis of *S*-nitrosated cysteine, glutathione or albumin [227, 228].

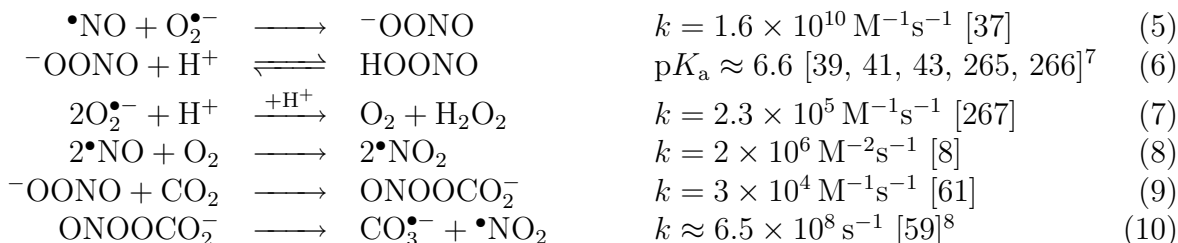
In addition to nitration of proteins during freezing of biological samples, as was investigated by ANDREAS DAIBER, I discovered nitrosation to play a significant role. These nitrosations occur as *S*-nitrosations of biological cysteine residues, as are present in GSH or proteins and also as *N*-nitrosation, as seen with the artificial target DAN. The model of nitration due to a decrease in pH was confirmed by the observation of nitrosation, which is an expected reaction under acidic conditions. The low levels of nitrite which are necessary to yield high levels of nitrosation show that freezing of samples is likely to be a common source of artifacts and since nitrosation is under investigation as a common regulatory mechanism comparable to phosphorylation/dephosphorylation, one has to take care to exclude these artificial nitrosations (and nitrations). In conclusion, an appropriate buffer composition and fast freezing in liquid nitrogen are necessary to avoid these artifacts. Whereas this does not play a role *in vivo*, the newly discovered mechanism of nitrosation is of significant importance for the interpretation of collected data from biological samples.

## 5.6 Kinetic Simulation of the Nitric Oxide/Superoxide System

The large number of reactions possible in the  $\bullet\text{NO}/\text{O}_2^{\bullet-}$  system does not form a linear sequence of reactions but resembles a rather complex network with numerous interactions between the intermediates, cellular targets, and  $\bullet\text{NO}$  and  $\text{O}_2^{\bullet-}$  itself. Despite detailed studies of most of the individual reactions, fundamental questions like the predominant pathway leading to *S*-nitrosations remains unsolved. Simple *in vitro* systems also reveal a different outcome compared to the living cell.

In the following, the complexity of the system will be addressed with the use of computer-assisted kinetic simulations, which should allow to verify completeness of current knowledge and indicate problems within existing models. Therefore, the relevant reactions, as far as they are known and characterized, were used to calculate the pathways and to identify the predominant reactions and intermediates with a special focus on pathways leading to *S*-nitrosation.

Deterministic time course simulations were performed by COPASI, a software application for simulation and analysis of biochemical networks developed by HOOPS, SAHLE *et al.* [235] with the LSODA algorithm [264] for solving the differential equation systems. The following equations were considered within the simulation:<sup>6</sup>

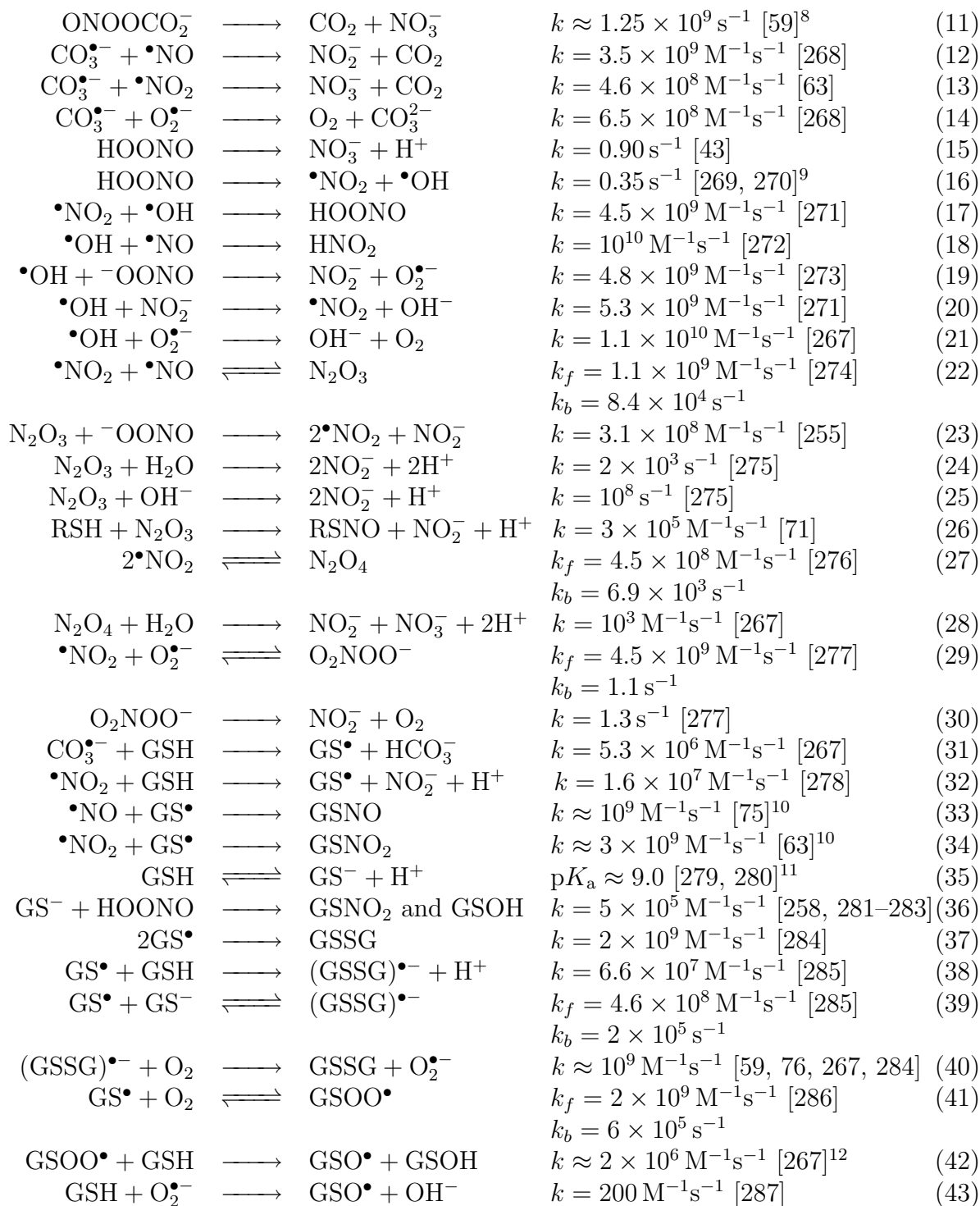


<sup>6</sup>If not otherwise indicated, all pH-dependent rate constants are given at pH 7.4.

<sup>7</sup>Within the simulation, rate constants for protonation and deprotonation of peroxynitrite were calculated from the  $\text{p}K_a$  and the assumption that a typical rate constant for protonation lies in the range of  $1\text{--}10 \times 10^{10} \text{ M}^{-1}\text{s}^{-1}$ .

<sup>8</sup>Kinetic constants for the decomposition of  $\text{ONOOCO}_2^-$  calculated considering  $k = 1.9 \times 10^9 \text{ M}^{-1}\text{s}^{-1}$  [62] and 34% radical yield [59, 63].

## 5 Results and Discussion



<sup>9</sup>The homolysis of HOONO is still a matter of controversy and the main path of HOONO decomposition being a non-radical isomerization could not be excluded [42, 43].

<sup>10</sup>Rate constants for the recombination of  $\bullet\text{NO}$  and  $\bullet\text{NO}_2$  with  $\text{GS}^\bullet$  were estimated to be similar to that of the recombination with the tyrosyl radical [59].

<sup>11</sup>Depending on the buffer composition,  $\text{p}K_a$  lies in the range 8.75–9.4.

<sup>12</sup>Rate constant for the reaction of  $\text{GSOO}^\bullet$  with GSH were assumed to be similar to that of the reaction of 2-mercaptoethanol thiylperoxide with 2-mercaptoethanol [76, 267]; decomposition pathways of  $\text{GSO}^\bullet$  are leading to non-radical products.

## 5 Results and Discussion

The simulation was calculated assuming fixed concentrations of 1.3 mM CO<sub>2</sub>, up to 225 μM O<sub>2</sub> and 5 μM or 5 mM GSH at pH 7.4 with a constant flux of 10 nM/s •NO and varying fluxes of O<sub>2</sub><sup>•-</sup>. A concentration of 1.3 mM CO<sub>2</sub> in the presence of 25 mM hydrogen carbonate is a common assumption for conditions in plasma [63] and were also used for *in vitro* experiments within this work. Glutathione is usually present in the cell around 5 mM up to 10 mM, but decreases with changes in the cellular redox equilibrium. In this model, glutathione as the main cellular reductant acts in addition as the substitute for cellular targets of ROS and RNS; not all pathways of sulfoxidations and its consumption are considered within the simulation, excluding those which do not have an affect on the overall reaction pattern and do not affect *S*-nitrosation of GSH. Therefore, the simulations calculates glutathione oxidation but does not allow to draw conclusions concerning the nature of its ultimate oxidation products. Simulations were calculated for a time-frame of 20 min and final steady-state concentrations of the intermediates were evaluated.

In Fig. 5.17 and 5.18, concentrations of •NO, O<sub>2</sub><sup>•-</sup> and <sup>-</sup>OONO were calculated for aerobic conditions in the •NO/O<sub>2</sub><sup>•-</sup> system. These conditions were modeled to match in principle those of the *in vitro* experiments presented within this work. The flow of •NO was kept constant at 10 nM/s, whereas O<sub>2</sub><sup>•-</sup> formation varied between 0 and 100 nM/s to represent a shift from conditions where •NO is present up to severe oxidative conditions by increased production of O<sub>2</sub><sup>•-</sup>. The left side of Fig. 5.17 with 5 μM GSH corresponds to experiments with low concentrations of targets for RNS and ROS, whereas on the right the concentration of GSH matches its cellular concentration if the cell is in a reduced state.

The calculations reveled that the equilibrium of the steady-state concentrations of •NO and O<sub>2</sub><sup>•-</sup> is shifted to the left, where the flow rates of O<sub>2</sub><sup>•-</sup> are below those of •NO (upper left panel of Fig. 5.17). Steady-state levels of •NO remain constant until O<sub>2</sub><sup>•-</sup> production exceeds half of the rate of the fixed •NO production; afterward no significant free •NO remains. This asymmetric profile of •NO and O<sub>2</sub><sup>•-</sup> levels results

## 5 Results and Discussion

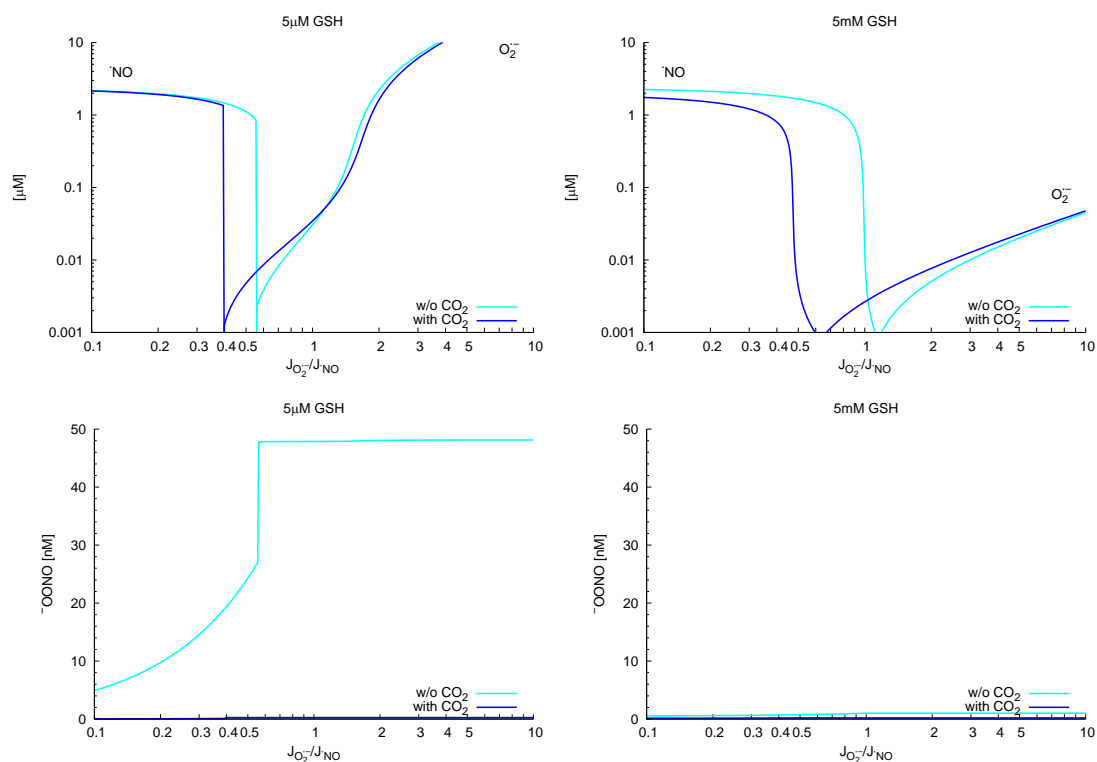


Figure 5.17: Concentrations of  $\text{O}_2^{\bullet-}$ ,  $\bullet\text{NO}$  and  $^-\text{OONO}$  during aerobic conditions, constant formation of  $10 \text{ nM/s}$   $\bullet\text{NO}$  and increasing levels of  $\text{O}_2^{\bullet-}$ . Computer-assisted kinetic simulation of a constant flow of  $10 \text{ nM/s}$   $\bullet\text{NO}$  and  $0\text{--}100 \text{ nM/s}$   $\text{O}_2^{\bullet-}$  in the absence or presence of  $1.3 \text{ mM}$   $\text{CO}_2$ ,  $5 \mu\text{M}$  GSH (left panels) or  $5 \text{ mM}$  GSH (right panels) and  $225 \mu\text{M}$   $\text{O}_2$ , pH 7.4.

from the higher consumption of  $\bullet\text{NO}$  by secondary reactions than that of  $\text{O}_2^{\bullet-}$ . Further increase of  $\text{O}_2^{\bullet-}$  formation leads to high steady-state levels, not limited due to the absence of sufficient antioxidants and SOD. Starting at equal steady-state levels of  $\bullet\text{NO}$  and  $\text{O}_2^{\bullet-}$  up to high levels of  $\text{O}_2^{\bullet-}$ , steady-state concentration of  $^-\text{OONO}$  is maximal (lower left panel). The presence of  $\text{CO}_2$  shifts the steady-state equilibrium of  $\bullet\text{NO}$  and  $\text{O}_2^{\bullet-}$  to the left and effectively prevents formation of significant steady-state levels of  $^-\text{OONO}$  due to the fast reaction between both. If concentrations of GSH are increased to levels existing in the living cell, it will act as antioxidant and lowers steady-state concentrations of  $\text{O}_2^{\bullet-}$  by three orders of magnitude (Fig. 5.17, right panels). At the same time, levels of  $^-\text{OONO}$  are also reduced in the absence of  $\text{CO}_2$ .

## 5 Results and Discussion

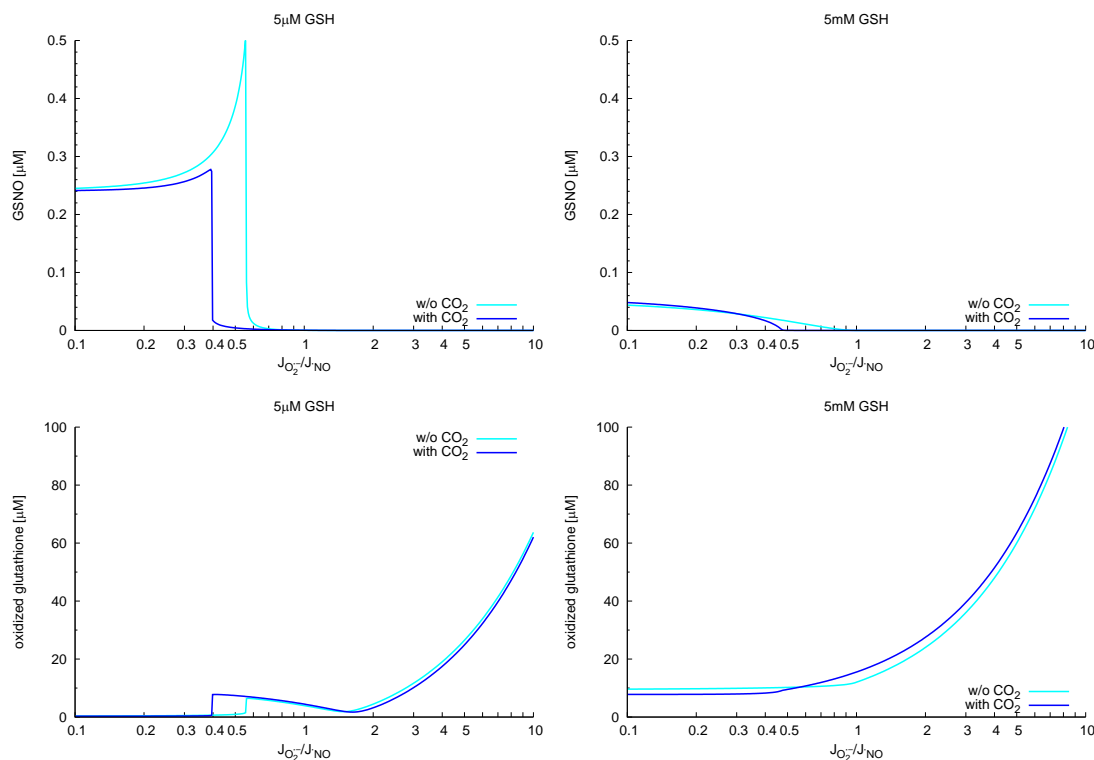


Figure 5.18: **Oxidation of glutathione and formation of *S*-nitrosoglutathione during aerobic conditions, constant formation of 10 nM/s  $\bullet$ NO and increasing levels of  $O_2^{\bullet-}$ .** Computer-assisted kinetic simulation of a constant flow of 10 nM/s  $\bullet$ NO and 0–100 nM/s  $O_2^{\bullet-}$  in the absence or presence of 1.3 mM CO<sub>2</sub>, 5 μM GSH (left panels) or 5 mM GSH (right panels) and 225 μM O<sub>2</sub>, pH 7.4.

Fig. 5.18 shows the fate of GSH within the described model, either as the sum of all oxidized glutathione equivalents (lower panels) or for the special case of its *S*-nitrosation (upper panels). Glutathione oxidation in this model is dependent on the formation of oxidizing intermediates like  $^-OONO$  or derived intermediates as well as high levels of  $O_2^{\bullet-}$ . The formation of *S*-nitrosoglutathione exhibits a dependency either on  $\bullet$ NO sufficient  $\bullet$ NO steady-state levels as well as on a sufficient production of  $O_2^{\bullet-}$ . A high basal *S*-nitrosation is provided by  $\bullet$ NO autooxidation due to sufficient presence of O<sub>2</sub>. As long as free  $\bullet$ NO is present, GSNO increases with  $O_2^{\bullet-}$  formation and becomes maximal during equilibrium of steady-state concentrations of  $\bullet$ NO and  $O_2^{\bullet-}$ ; therefore, CO<sub>2</sub> lowers maximal nitrosation due to earlier steady-state equilibrium of  $\bullet$ NO and  $O_2^{\bullet-}$ . High concentrations of GSH, however, prevent the necessary secondary reactions

leading to nitrosative intermediates at the expense of increased GSH consumption and in consequence GSNO formation decreases.

Besides compartmentation and the presence of numerous antioxidant systems and further targets for RNS and ROS, this model does also not exactly resemble the chemical conditions within the living cell. Further calculations revealed that the intracellular pH of 7.0 does not lead to significant changes in reaction patterns and turnover rates, and since most of the required pH-dependent kinetic constants are only available for pH 7.4, this pH was used for all further studies. The cytosolic concentration of CO<sub>2</sub> should be within the same order of magnitude as in plasma; as can be concluded from Fig. 5.14, its effect should in approximation not depend on its actual concentration. However, it can be assumed that cellular levels of O<sub>2</sub> are significantly below those of an air-saturated solution (225 μM), usually below 40 μM even in well-oxygenated tissues.

Decreasing O<sub>2</sub> concentrations within this model will lead to both an increase in steady-state levels of •NO as well as to a direct correlation between equal •NO and O<sub>2</sub><sup>•-</sup> formation and their respective steady-state levels. This is shown in Fig. 5.19, which is calculated to match anaerobic conditions. In particular the yield of glutathione *S*-nitrosation is affected by changes in O<sub>2</sub> levels, as can be observed in Fig. 5.20 which shows *S*-nitrosoglutathione formation in the •NO/O<sub>2</sub><sup>•-</sup> system from anaerobic conditions up to an air-saturated solution. According to these calculations, *S*-nitrosation due to •NO autoxidation pathways leads to basal GSNO during sufficient steady-state levels of •NO. However, O<sub>2</sub> concentrations below 10 μM are leading to significant higher levels of GSNO and at the same time, nitrosation develops a peak at equimolar •NO and O<sub>2</sub><sup>•-</sup> formation, both with and without CO<sub>2</sub> (left panels). This increased nitrosation during equimolar flux of •NO and O<sub>2</sub><sup>•-</sup> in this model is caused by thiyl radical formation by the reaction of •NO<sub>2</sub> with GSH and, in the presence of CO<sub>2</sub>, also of CO<sub>3</sub><sup>•-</sup> with GSH (Eqs. 32 and 31). *S*-Nitrosation via N<sub>2</sub>O<sub>3</sub> has its maximum during low rates of O<sub>2</sub><sup>•-</sup> formation and requires low GSH levels, but even during optimal

## 5 Results and Discussion

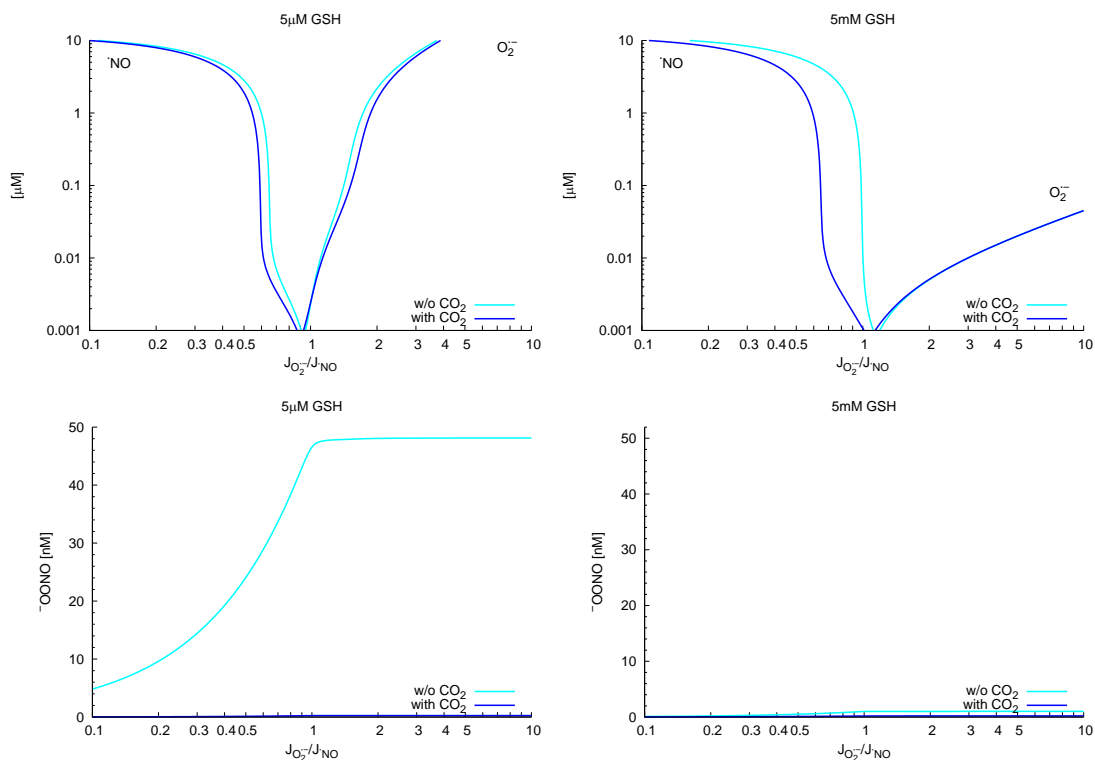


Figure 5.19: **Steady-state concentrations of  $\bullet\text{NO}$ ,  $\text{O}_2^{\bullet-}$  and  $^-\text{OONO}$  during anaerobic conditions and a constant formation of 10 nM/s  $\bullet\text{NO}$  and increasing levels of  $\text{O}_2^{\bullet-}$ .** Computer-assisted kinetic simulation of a constant flow of 10 nM/s  $\bullet\text{NO}$  and 0–100 nM/s  $\text{O}_2^{\bullet-}$  in the absence (upper panels) or presence of 1.3 mM  $\text{CO}_2$  (lower panels), 5  $\mu\text{M}$  GSH (left panels) or 5 mM GSH (right panels) at pH 7.4 in the absence of  $\text{O}_2$ .

conditions does not exceed 5% of total nitrosation. Higher concentrations of GSH (right panels of Fig. 5.20) only results in significant GSNO formation if  $\text{CO}_2$  is present, in equal parts due to  $\text{GS}^\bullet$  formation via Eqs. 32 and 31. The excess of glutathione effectively scavenges peroxynitrite (Eq. 36) which prevents further reactions, but  $\text{CO}_2$ , if present, is able to compete with GSH enabling the necessary subsequent reactions leading to  $\text{GS}^\bullet$ . Contrary to the other conditions,  $\text{CO}_2$  together with 5 mM GSH is leading to significant nitrosations even at anaerobic conditions with only little rates of  $\text{O}_2^{\bullet-}$  formation as a consequence of both effective competition of  $\text{CO}_2$  with GSH for  $^-\text{OONO}$  and increased yield of thiyl radicals during subsequent reactions due to high GSH concentrations (lower left panel of Fig. 5.20). In general, GSNO formation under

## 5 Results and Discussion

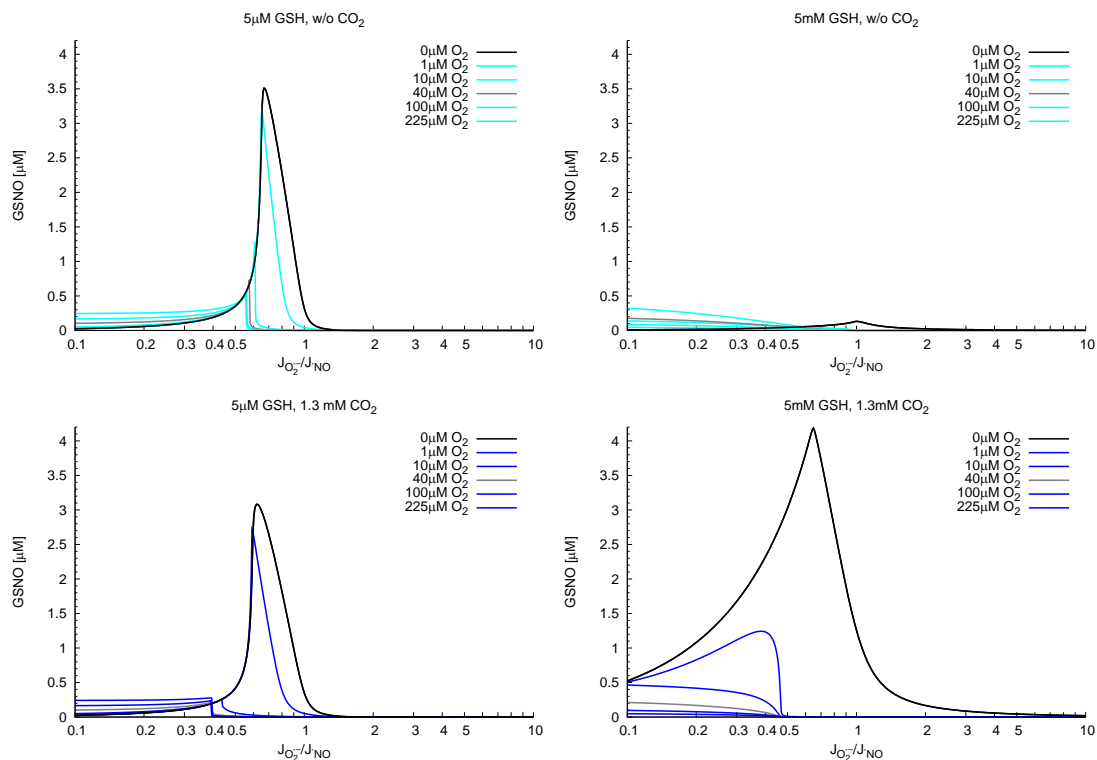


Figure 5.20: **Effect of  $O_2$  on *S*-nitrosoglutathione formation during constant formation of 10 nM/s  $\bullet NO$  and increasing levels of  $O_2^{\bullet -}$ .** Steady-state concentrations of GSNO after 20 min during a computer-assisted kinetic simulation with a constant flow of 10 nM/s  $\bullet NO$  and 0–100 nM/s  $O_2^{\bullet -}$  in the absence (upper panels) or presence of 1.3 mM  $CO_2$  (lower panels), 5  $\mu$ M GSH (left panels) or 5 mM GSH (right panels) and from anaerobic conditions up to 225  $\mu$ M  $O_2$  at pH 7.4.

optimal conditions is provided by the simultaneous formation of both  $\bullet NO_2$  and  $CO_3^{\bullet -}$  and their further reactions within the system.

After the results gained from the simulation mostly correspond to experimental data, the model was modified to resemble the situation in the inside of the cell. The presence of  $CO_2$  was assumed and as well as an  $O_2$  concentration of 40  $\mu$ M, which can be found in tissue with good supply. Due to the reasons discussed above, it was not required to adjust the pH to 7.0. However, mammalian cells contain large amounts of SOD, 4–40  $\mu$ M Cu,Zn-SOD and 1–30  $\mu$ M Mn-SOD are reported to exist in the cytosol and mitochondria [288, 289]. A simplified model of SOD catalysis was added to the simulation and the concentration of SOD was assumed to be 10  $\mu$ M:

## 5 Results and Discussion

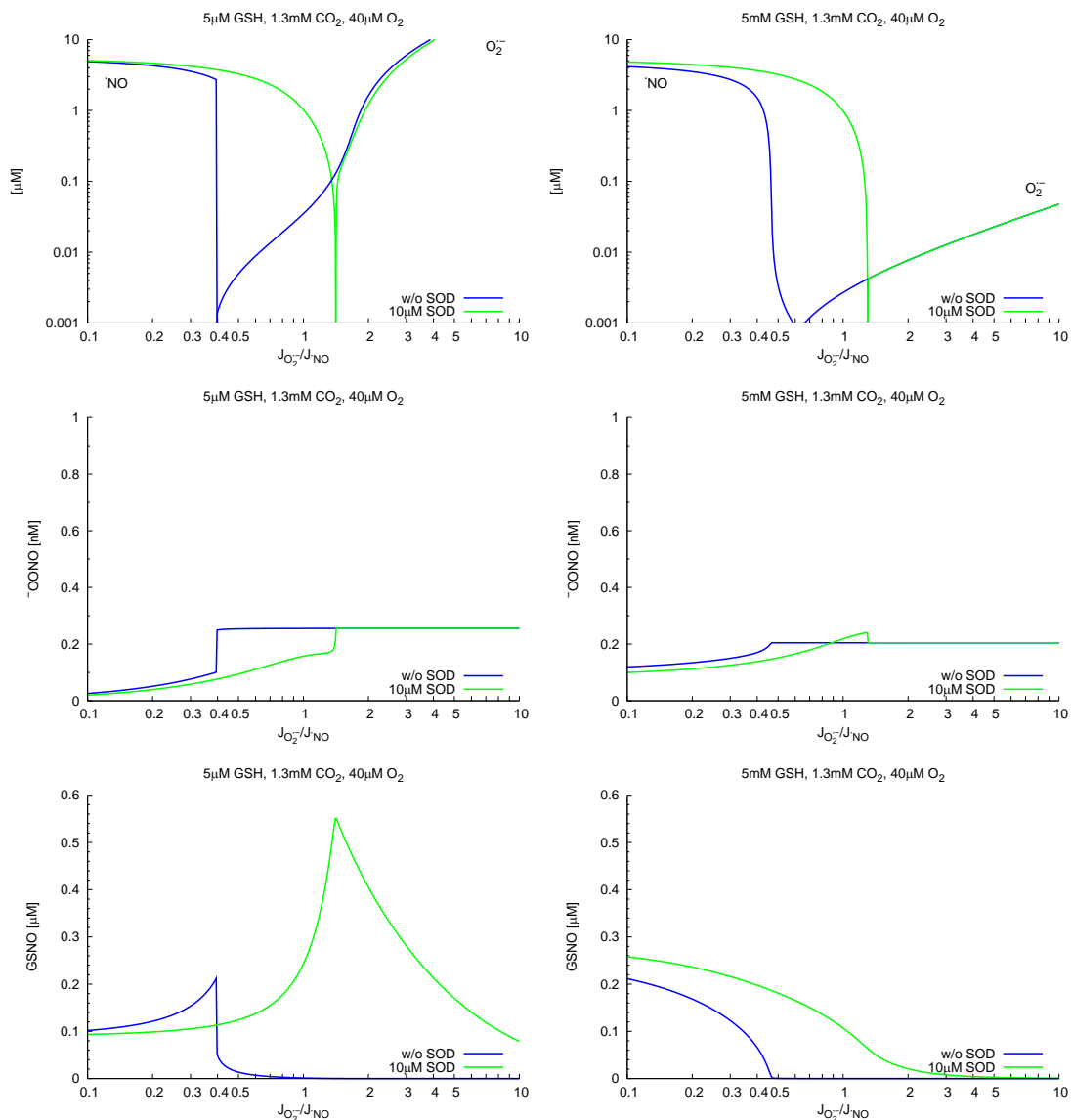
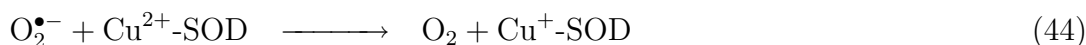


Figure 5.21: **Simulation of the  $\bullet\text{NO}/\text{O}_2^{\bullet-}$  system with intracellular conditions and in the presence of SOD.** Computer-assisted kinetic simulation of a constant flow of 10 nM/s  $\bullet\text{NO}$  and 0–100 nM/s  $\text{O}_2^{\bullet-}$  in the presence of 1.3 mM  $\text{CO}_2$ , 5  $\mu\text{M}$  (left panels) or 5 mM GSH (right panels), 40  $\mu\text{M}$   $\text{O}_2$  and 10  $\mu\text{M}$  SOD, pH 7.4.



Only the rate constant for the rate-limiting step of SOD catalysis is known ( $k = 2 \times 10^9 \text{ M}^{-1}\text{s}^{-1}$  [290]); it was assumed that the second step proceeds at the same rate. The results from this modified model, as shown in Fig. 5.21, reveal higher steady-state levels

of  $\bullet\text{NO}$  during increasing  $\text{O}_2^{\bullet-}$  formation and therefore require significant higher  $\text{O}_2^{\bullet-}$  production to yield significant a steady-state concentration of itself. The attenuation of free  $\text{O}_2^{\bullet-}$  by SOD favors reactions requiring both the formation of  $^-\text{OONO}$  and  $\bullet\text{NO}$ . The fast formation of  $^-\text{OONO}$  from  $\bullet\text{NO}$  and  $\text{O}_2^{\bullet-}$  requires sufficient  $\text{O}_2^{\bullet-}$  production, but only basal steady-state levels, whereas peroxynitrite combined with a subsequent reaction of  $\bullet\text{NO}$  with peroxynitrite or a derived reactive species demands relatively high steady-state levels of  $\bullet\text{NO}$  to compensate the low concentrations of the reactive intermediates. Based on this, SOD not only prevents the formation of elevated levels of  $\text{O}_2^{\bullet-}$ , which would led to cell damage, but at the same time enhances secondary pathways emerging from  $^-\text{OONO}/\text{HOONO}$ . Within this model, this manifests itself by enhanced *S*-nitrosation.

This model clearly favors a radical pathway leading to *S*-nitrosation, even at aerobic conditions and at the same time demonstrates that this pathway is able to provide the required yield of GSNO. This indicates that current knowledge provides a sufficient explanation for *S*-nitrosation under physiological conditions, characterized by reduced concentrations of  $\text{O}_2$ , the presence of  $\text{CO}_2$  and levels of reduced glutathione which depend on cellular redox state. However, these results predict the requirement of an elevated  $\text{O}_2^{\bullet-}$  release as a central assumption within this work. Although the exact mechanism for *S*-nitrosation under cellular conditions must be re-examined as is demonstrated within this work, there is little doubt that  $\text{O}_2^{\bullet-}$  is required.

High levels of GSH in the absence of  $\text{CO}_2$  prevent further RNS formation and thus the various reaction possible in the  $\bullet\text{NO}/\text{O}_2^{\bullet-}$  system. Glutathione gives a sink for most of the reactive intermediates in the system, only steady-state levels of  $\bullet\text{NO}$  itself are not affected. Carbon dioxide is able to transfer the function of  $^-\text{OONO}$  and therefore prevents that  $^-\text{OONO}$  as the central intermediate in the system will be scavenged. These results fit to the nitrosation profile gained from experimental data of DAN nitrosation at aerobic conditions (Fig. 5.11) as well as to its lack of azide sensitivity (Fig. 5.12), but does not provide an explanation for the observed potentiating effect

of  $\text{CO}_2$  (Fig. 5.13). These calculations revealed that maximal nitrosation during these experiments should occur at equal steady-state concentrations of  $\bullet\text{NO}$  and  $\text{O}_2^{\bullet-}$  and does not require an excess of  $\bullet\text{NO}$ , as the graphs suggest. However, due to the differences between DAN and GSH it cannot be concluded that DAN nitrosation could occur via a radical pathway as the simulation suggests.

*S*-Nitrosation via  $\bullet\text{NO}$  autoxidation and  $\text{N}_2\text{O}_3$  exhibits only a minor role within the model, even at optimal conditions. This pathway should be of even lower importance *in vivo*, where levels of both  $\bullet\text{NO}$  as well as  $\text{O}_2$  usually should be lower. Cellular  $\text{O}_2$  concentrations in well-oxygenated tissues can be expected to be between 30 and 40  $\mu\text{M}$ , limiting  $\bullet\text{NO}$  autoxidation and  $\text{GS}\bullet$  consumption. Thiols should represent the main sink for  $\bullet\text{NO}_2$  in the cell, therefore it seems reasonable that thiyl radical formation occurs there via both  $\bullet\text{NO}_2$  and  $\text{CO}_3^{\bullet-}$ , like the simulations suggest. In plasma,  $\bullet\text{NO}_2$  will react with urate with a similar rate constant as with thiols, which therefore represents an effective scavenger of  $\bullet\text{NO}_2$  outside the cell [278] and prevents pathways requiring its presence.

In conclusion, *S*-nitrosation according to this model should occur *in vivo* mainly via thiyl radical formation and subsequent reaction with  $\bullet\text{NO}$  and therefore requires appropriate steady-state levels of  $\bullet\text{NO}$ . However, DUSTIN HOFSTETTER<sup>13</sup> was able to experimentally exclude that *S*-nitrosation is the product of a radical reaction at physiological conditions (unpublished data). The required production of  $\bullet\text{NO}$  is provided by NOS and, at the same time, could also lead to nitrosylations. Due to its high availability, it can be assumed that glutathione represents the only possible target for *S*-nitrosations in the cell and further nitrosations should only occur via transnitrosation. The cellular reductive systems keep levels of peroxyxynitrite below significance and Tyr nitration at these conditions can be excluded. If steady-state levels of  $\text{O}_2^{\bullet-}$  exceed those of  $\bullet\text{NO}$ , *S*-nitrosation is first prevented by the lack of  $\bullet\text{NO}$ , and subsequently, if  $\text{O}_2^{\bullet-}$  production persists, by decreasing levels of reduced glutathione.

---

<sup>13</sup>ETH Zürich, Switzerland.

Such a decrease could yield in significant steady-state concentrations of peroxynitrite, sufficient to nitrate Tyr in PGI<sub>2</sub> synthase and Mn-SOD via metal-catalysis, but no unspecific 3-NT formation will become apparent under these conditions. A further increased O<sub>2</sub><sup>•-</sup> formation together with an inactivated cellular reductive system would then lead to H<sub>2</sub>O<sub>2</sub>, and as soon as catalase fails to handle this situation, to conditions of severe oxidative stress with increasing levels of H<sub>2</sub>O<sub>2</sub> and •OH formation, accompanied by unspecific Tyr-nitration. This unspecific 3-NT formation is discussed to occur analogously to *S*-nitrosation mainly via •NO<sub>2</sub>-mediated tyrosyl radical formation, but due to its subsequent reaction with •NO<sub>2</sub> should not require elevated steady-state levels of •NO. The action of SOD, usually present in micromolar concentrations in the cytosol and mitochondria of mammalian cells, would shift the steady-state equilibrium between •NO and O<sub>2</sub><sup>•-</sup> towards higher rates of O<sub>2</sub><sup>•-</sup> production and therefore leads to prolonged and increased nitrosation during the transition towards oxidative stress, provided that the ongoing oxidations already decreased cellular GSH content.

A reaction of HOONO with •NO, which could be possible, would lead to higher yields of GSNO compared to the predictions by the computed model. Especially if CO<sub>2</sub> is absent, this reaction would multiply overall nitrosation without changing its profile in respect to O<sub>2</sub><sup>•-</sup> production. However, this reaction competes with those of CO<sub>2</sub> with peroxynitrite and the CO<sub>2</sub>-dependent reactions are providing pathways efficiently leading to nitrosation. Assuming accuracy of the model and its kinetic constants, these results support a mechanism involving thiyl radicals for *S*-nitrosations at cellular conditions. From a chemical point of view, current knowledge therefore seems to provide a plausible explanation for the mechanism of *S*-nitrosation, but this mechanism is neither transferable to the situation in the cell nor is supported by experimental data.

The focus on a homogeneous system represents a limitation of this model since it does not take the non-homogeneous organization of the cell into account. The transfer to a system resembling a cell first requires validation of the theoretical model with

the observations gained from a homogeneous system. Within the cell, the  $\bullet\text{NO}/\text{O}_2^{\bullet-}$  system will compete with the cell's antioxidant systems; especially SOD and the reductive state of the cell will affect the pathways leading to *S*-nitrosation. In this respect, the subcellular localization of the radical-producing systems should be of increased relevance for the possible targets of redox regulation. Both  $\bullet\text{NO}$  and  $\text{O}_2$  have higher solubilities in lipophilic than in aqueous solvents and their local concentration should be increased in hydrophobic phases such as those within lipid membranes or at hydrophobic interiors of proteins [20]. Thus, it has to be considered that also the local cellular environment is able to determine the reaction pattern of this highly dynamic system.

Similar calculations to predict the reactions within the  $\bullet\text{NO}/\text{O}_2^{\bullet-}$  system with computer-models have been performed by KIRSCH *et al.* and QUIJANO *et al.* [59, 267] and both of these models include pathways resulting from the presence of  $\text{CO}_2$  and GSH. Especially QUIJANO's calculations attempt to model the situation within the living cell by including SOD and by taking diffusion of  $\bullet\text{NO}$  between the cellular compartments into account, but both groups limit their analysis solely to the nitration of Tyr. But at levels of  $^-\text{OONO}$  possible at physiologic conditions, 3-nitrotyrosine formation should occur exclusively via catalysis by metal centers as a mechanism of enzyme regulation, whereas unspecific Tyr-nitration would require significant higher levels of  $^-\text{OONO}$  (see 3.5.3.3).

Even if the mechanism of  $\bullet\text{NO}$  autoxidation to yield  $\bullet\text{NO}_2$  is not completely understood, its kinetics are known and therefore included in the herein presented calculations, in contrast to KIRSCH's and QUIJANO's publication. This exclusion is based on the assumption that  $\text{CO}_2$ -dependent pathways will outcompete all other decay mechanisms, and therefore QUIJANO excludes also  $\text{HOONO}$  and derived reactions in their simulation. But peroxyntrous acid actually exhibits a substantial higher reactivity than  $^-\text{OONO}$  and should be accounted for most of the peroxyntrite-derived oxidations as well for its fast decomposition. Another limitation of these two models

is the focus on high concentrations of reduced glutathione and therefore situations where the cellular redox equilibrium is shifting to its oxidized state are not considered. Therefore, the herein developed model stands out from the existing ones, predicting the transition from a reduced state of the cell up to severe oxidative stress and giving special attention on the until now not fully understood process of *S*-nitrosation.

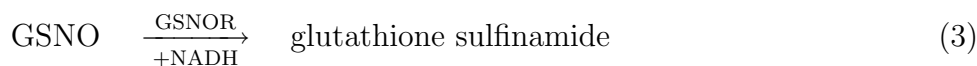
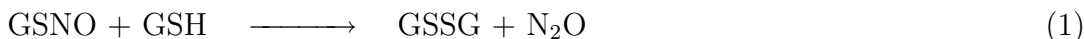
## 6 Conclusions

The results gained within this work imply that *S*-nitrosation under physiological conditions is not the consequence of a direct action of  $\bullet\text{NO}$  or  ${}^-\text{OONO}$ , but rather the result of subsequent reactions within the  $\bullet\text{NO}/\text{O}_2^{\bullet-}$  system. Even if the determination of the predominant mechanism to yield *S*-nitrosation *in vivo* requires further studies, it was shown by *in vitro* and *in silico* experiments that it requires both  $\bullet\text{NO}$ - and  $\text{O}_2^{\bullet-}$ -formation, but steady-state levels of  $\bullet\text{NO}$  have to exceed those of  $\text{O}_2^{\bullet-}$ . Pathways mainly depending on autoxidation of  $\bullet\text{NO}$  could be excluded as well as the requirement of  $\text{N}_2\text{O}_3$  as the nitrosating intermediate. Both the presence of GSH and  $\text{CO}_2$ , which dramatically lowers steady-state levels of  ${}^-\text{OONO}$  and shifts the reaction patterns in the  $\bullet\text{NO}/\text{O}_2^{\bullet-}$  system, could be accommodated within the described model of physiological *S*-nitrosation. Furthermore, these results suggest a sequence of conditions and events leading from a “normal” redox potential via distinct stages to a disturbed redox equilibrium up to conditions of severe oxidative stress.

Starting from reducing conditions in a resting mammalian cell, basal  $\bullet\text{NO}$  production by  $\bullet\text{NO}$  synthase (NOS) will mainly lead to nitrosylation. If  $\bullet\text{NO}$  formation increases and the cellular sources of  $\text{O}_2^{\bullet-}$  are providing basal levels of it, *S*-nitrosation of glutathione will be possible, and via transnitrosation also enzymes will become *S*-nitrosated. In a healthy cell, conditions providing *S*-nitrosations are enabled by  $\bullet\text{NO}$  production by NOS and  $\text{O}_2^{\bullet-}$  from various sources, encouraged by the simultaneous action of superoxide dismutase (SOD), which keeps levels of  $\text{O}_2^{\bullet-}$  below those of  $\bullet\text{NO}$ .

## 6 Conclusions

At these conditions, the cellular GSH/GSSG ratio could be already decreased, but a reductive environment prevails. *S*-Nitrosation will therefore be in equilibrium with the reverse reaction, mainly due to three pathways leading to denitrosation:

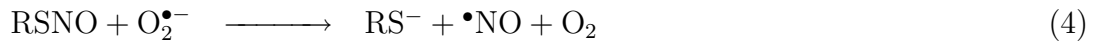


Non-enzymatic denitrosation by GSH itself seems to lead to oxidized glutathione and  $\text{N}_2\text{O}$  after an intermediate step [110]. The enzymatic denitrosation activity by Cu,Zn-SOD first requires a reduction of the enzyme-bound copper to  $\text{Cu}^+$  by GSH [99, 100]; GSNO reductase (GSNOR) depends on NADH and to a lesser extend on NADPH as cofactors and yields glutathione sulfinamide [96].

During transition towards oxidizing conditions by increased  $\text{O}_2^{\bullet-}$  formation, the pathways of denitrosation will be blocked due to the lack of reduction equivalents; at the same time, these are conditions of maximal *S*-nitrosation. In consequence, *S*-nitrosation-mediated enzyme regulation will affect cellular energy metabolism and various other pathways. As will be later shown, this can be interpreted as a regulation to prevent the development of oxidative stress within the cell.

Further transitions towards an oxidized state of the cell will first result in an equilibrium between  $\bullet\text{NO}$  and  $\text{O}_2^{\bullet-}$ , enabling metal-catalyzed Tyr nitration and oxidations by HOONO and derived reactive species. Peroxynitrite's physiologic functions are probably performed at levels between 50 and 500 nM with levels in pathophysiological situations reaching 5  $\mu\text{M}$ , as can be approximated from bolus administration. Unspecific 3-nitrotyrosine (3-NT) formation, however, should require further increases in both  $\bullet\text{NO}$  and  $\text{O}_2^{\bullet-}$  production, which does not necessarily has to occur within this scenario. At these conditions, aconitase will get oxidized, which will have extensive consequences for the cell.

If the cell's protective measures are not able to prevent further  $\text{O}_2^{\bullet-}$  formation, its levels may exceed those of  $\bullet\text{NO}$  and conditions of severe oxidative stress and activation of further  $\text{O}_2^{\bullet-}$ -sources will be the consequence (see Fig. 6.1). This will lead to  $\text{H}_2\text{O}_2$  and  $\bullet\text{OH}$  formation via Haber-Weiss and Fenton chemistry and to irreversible cell damage. Lipid peroxidation resulting from the peroxidative destruction of cellular membranes will have cell death as its ultimate consequence. *S*-Nitrosation cannot occur under these oxidative conditions due to the lack of the required steady-state concentrations of  $\bullet\text{NO}$ , and furthermore the excess of  $\text{O}_2^{\bullet-}$  itself is able to reverse *S*-nitrosation [107]:



Based on this postulated sequence of events during the transition towards oxidative stress, *S*-nitrosation could be considered as a cellular mechanism to suppress further  $\text{O}_2^{\bullet-}$  formation, mainly via depletion of cellular NADPH/NADH and related redox equivalents. This hypothesis will be discussed in the following.

## 6.1 A Model for Redox Regulation by *S*-Nitrosation in the Cell

*S*-Nitrosation regulates the activity of a set of key enzymes within the cell, some enzymes increase their activity while others are inhibited by this posttranslational modification. Some of these regulated enzymes are essential in cellular energy metabolism and maintenance of cellular redox equilibrium, while others are transcription factors or related to apoptosis. A large group of regulated enzymes (see table on page 39f.) are associated with NOS activity, mainly via changes in cellular Arg metabolism. The pattern of enzymes regulated by *S*-nitrosation suggests that those enzyme are regulated in concert and *S*-nitrosation should therefore represent a general mechanism to adapt the cell to changes of its redox equilibrium. Within this context, *S*-nitrosation

## 6 Conclusions

could represent either a preparation to imminent conditions of oxidative stress, or a mechanism to prevent the arising of such a severe situation.

Under physiological conditions vessel endothelium shows a continuous release of  $\bullet\text{NO}$  by the shear-stress activated NOS-3, which characterizes a resting state. Considering that NOS-1 is present in many different cell types and, after activation, is able to contribute to cellular  $\bullet\text{NO}$  production at significantly higher rates than NOS-3, as well as the possibility of a mitochondrial NOS, there should exist  $\bullet\text{NO}$  sources in many, if not even all cell types.

NADPH oxidase, the source for  $\text{O}_2^{\bullet-}$  in phagocytes, is also present in all layers of the vessel wall, in endothelium, media and adventitia. These vascular NAD(P)H oxidases (NOX1–5) are low-output systems; their activation require translocation of their cytosolic subunits to the membrane and subsequent assembly of cytosolic and membrane-bound subunits to become fully active. The activation of the constitutive vascular NAD(P)H oxidases is triggered by agonist stimulation. Protein kinase C (PKC) is an important activator and acts through phosphorylation of NOX subunits; therefore NOX activation occurs in response to angiotensin II, platelet-derived growth factor (PDGF) or tumor necrosis factor- $\alpha$  (TNF- $\alpha$ ). The small G protein Rac is another important activator of the oxidase and lipid metabolites derived from phospholipase D (PLD) and phospholipase A<sub>2</sub> (PLA<sub>2</sub>), especially arachidonic acid, contribute to NOX activation [291]. Thus, agonist-mediated activation of vascular cells in the presence of NADPH or NADH leads to  $\text{O}_2^{\bullet-}$  production at low rates and  $\text{O}_2^{\bullet-}$  as an antagonist to  $\bullet\text{NO}$  will contribute to cellular redox signaling.

Contrary to NOX, mitochondria can be abundant sources for  $\text{O}_2^{\bullet-}$ , but this seems to happen in a controlled process involving  $\text{Ca}^{2+}$ , ROS and structural changes triggered by the opening of the permeability transition pore (PTP) [292]. Reduction of  $\text{O}_2$  to  $\text{O}_2^{\bullet-}$  may occur by autoxidation of redox components in complex I or III. A counter-regulation by uncoupling proteins exist [293] and the combined activity of Mn-SOD

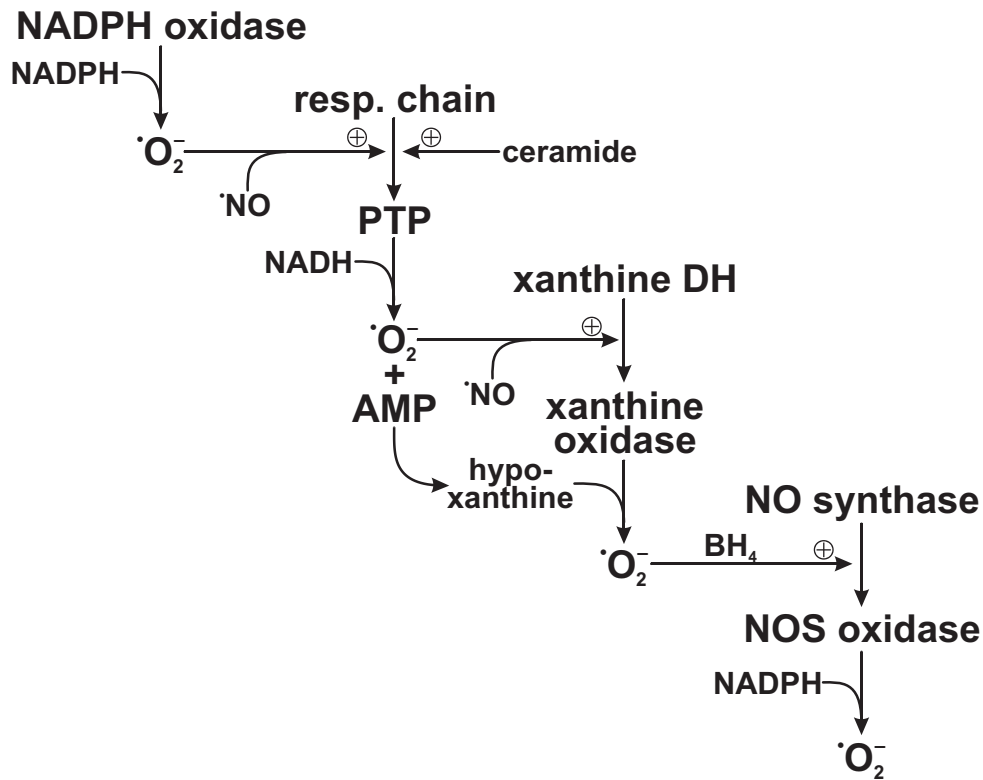


Figure 6.1: **The consecutive model of superoxide release.** Following assembly of the NADPH oxidase complex, elevated superoxide concentrations are leading to peroxynitrite and therefore, mitochondrial permeability transition pores (PTP) can be opened, resulting in an uncoupling of the respiratory chain. As a consequence, additional superoxide is released by complex I and ubiquinone, cellular  $\text{Ca}^{2+}$  levels are increased and ATP formation declines. At this point, the activations of superoxide sources should still be reversible, but further steps in this activation cascade are unlikely to be. Liver-derived xanthine oxidase or oxidation of xanthine dehydrogenase by peroxynitrite provides another source of superoxide and breakdown of cellular ATP finally yields in hypoxanthine, which serves as substrate of xanthine oxidase. Oxidation of tetrahydrobiopterin ( $\text{BH}_4$ ) converts NOS-3 to an oxidase, which acts as a fourth cellular source of  $\text{O}_2^{\bullet-}$ . If the levels of  $\text{O}_2^{\bullet-}$  exceed those required for redox regulation,  $\text{H}_2\text{O}_2$  and  $\bullet\text{OH}$  formation accompanied with severe cell damage will be the consequence. (published in [1])

and GSH peroxidase reduces mitochondrial  $\text{O}_2^{\bullet-}$  to water. Oxidative inactivation of Mn-SOD and GSH depletion eventually would cause  $\text{O}_2^{\bullet-}$  to leave the mitochondrial space and to contribute to cytosolic  $\text{O}_2^{\bullet-}$ . As these levels of  $\text{O}_2^{\bullet-}$  can be much higher than those originating from NOX, this may have severe consequences for the redox

## 6 Conclusions

state of cytosolic components. Subsequently cytosolic GSH will be oxidized, followed by oxidation of the vitamins C and E and tetrahydrobiopterin ( $\text{BH}_4$ ) to  $\text{BH}_2$ .

The accompanied oxidation of  $\text{BH}_4$ , representing an essential redox factor for NOS, will prevent further  $\bullet\text{NO}$  synthesis, and instead  $\text{O}_2^{\bullet-}$  will be produced by NOS, also under consumption of NADPH [294]. Direct oxidation of NOS by peroxynitrite is another possibility and in the case of NOS-3, oxidation of its zinc-thiolate cluster, located at the dimer interface, was reported to lead to increased  $\text{O}_2^{\bullet-}$  instead of  $\bullet\text{NO}$  production [252]. These mechanisms lead to depletion of  $\bullet\text{NO}$ , and since it acts as an effective suppressor of  $\text{O}_2^{\bullet-}$ , the levels of  $\text{O}_2^{\bullet-}$  could rise sharply, allowing Fenton chemistry with the associated formation of  $\bullet\text{OH}$  radicals. Mitochondrial autoxidations triggered by PTP opening still can be reversible and hence cell death as a consequence will only occur if the rescue mechanisms cannot reverse the process.

Superoxide formation originated from xanthine oxidase requires the conversion of xanthine dehydrogenase to its oxidase form, either by oxidation of thiol groups or by proteolysis [295, 296]. The adenosine monophosphate (AMP) degradation products hypoxanthine and xanthine constitute the substrates of xanthine oxidase and should only appear after a massive disturbance in cellular energy metabolism. The contribution of the four main cellular sources for  $\text{O}_2^{\bullet-}$  to redox regulation up to oxidative stress and a hypothetical cascade of their activation are summarized in Fig. 6.1. If the various mechanisms for posttranslational modifications have taken place, the reversible process of a direct reductive restoration must be initiated. This should be possible at any stage of the oxidative modification unless proteolytic processes are involved, as in the case of the conversion of xanthine oxidase or caspases. It should, however, be noted that the mechanisms for the reductive components of redox regulation, leading back to the resting state of the cell, are far from being understood and no clear delineation between reversible redox regulation and irreversible oxidative stress exists.

## 6 Conclusions

It is essential to consider the interactions of the  $O_2^{\bullet-}$  - and  $\bullet NO$ -synthesizing systems as a physiological signaling network. The main intermediates,  $O_2^{\bullet-}$ ,  $H_2O_2$ ,  $\bullet NO$ ,  $\bullet NO_2$ ,  $[NO^+]$  and  $^-OONO/HOONO$ , are strictly controlled for the purpose of redox regulation. Pathophysiological conditions arise by overpowering the cellular antioxidant systems leading to a vicious circle with  $\bullet OH$  and  $\bullet NO_2$  radicals as radical chain reaction initiators. This situation would require pharmacological intervention and this provides a scenario where antioxidants should be beneficial. Indeed, observations in clinical practice confirm that a supply of antioxidants will assist the reductive phase in a preventive way but certainly is of little effect when the damage by oxidative stress has already been established.

The main strategy of a cell to prevent the formation of oxidative stress under such conditions should be the blockade of further  $O_2^{\bullet-}$  formation. Rising levels of  $O_2^{\bullet-}$  will lead to the formation of  $H_2O_2$ , and, with the involvement of free iron, to  $\bullet OH$  radicals via the Haber-Weiss reaction and Fenton chemistry (cf. 3.1). Free reduced iron is scarce *in vivo* but required for the Fenton reaction. Aconitase itself and aconitase-mediated changes in cellular iron storage together with its reduction by reductants like ascorbate or  $O_2^{\bullet-}$  itself, however, could provide the required amounts of ferrous iron under these conditions. NADPH oxidase activity,  $O_2^{\bullet-}$  formation from uncoupled NOS and mitochondria, derived from the opening of PTP, all require the presence of sufficient amounts of NADPH or NADH. Therefore, depletion of both of the redox equivalents NADPH and NADH would represent a feasible strategy to prevent further ROS formation. This would, however, also suppress the regeneration of GSH, thioredoxin and glutaredoxin and therefore the recovery of cellular redox systems (Fig. 1.1). Such an oxidized cellular environment would be a prerequisite for the formation of sufficient levels of peroxynitrite to nitrate tyrosine residues. Indeed, there are existing reports where an increase of cellular NADPH evoke an increase in oxidative stress, whereas its depletion protects the cell from further damage [297, 298].

## 6 Conclusions

Thus, if NADPH and NADH disappear, xanthine oxidase would be the only remaining source of  $O_2^{\bullet-}$  [179].

An important source for NADPH is NADP<sup>+</sup>-dependent isocitrate dehydrogenase (ICDH), which is reported to be inhibited by *S*-nitrosation [125, 299]. In fact, the main function of cytosolic and mitochondrial ICDH seems to be the control of cytosolic and mitochondrial redox balance and oxidative damage [300, 301]. Hyperglycemia also serves as an important model of severe oxidative stress, leading to cell damage e. g. in patients with diabetes mellitus type 1 or 2. In consequence, glucose-6-phosphate dehydrogenase (G6PDH), representing the second major enzyme providing NADPH and the rate-limiting step of the pentose phosphate pathway, will be inhibited; this seems to occur via phosphorylation in a cAMP/PKA-dependent manner [302]. These two mechanisms of negative feed-back regulation between cellular redox state and redox state-maintaining enzymes could represent a general principle—severe changes in the cellular redox state will lead to down-regulation of central metabolic pathways. Besides these two important sources for the maintenance of cellular redox state, glycolysis can be inhibited by *S*-nitrosation of glyceraldehyde-3-phosphate dehydrogenase (GAPDH) [77, 124]. This prevents NADH formation by GAPDH as well as further NADPH supply by malic enzyme. At the same time, aldose reductase (aldehyde reductase 2, ALR2) will be activated by *S*-nitrosation of Cys-298 [83], driving glucose away from glycolysis towards the polyol pathway. In consequence, consumption of NADPH will increase further and sorbitol will accumulate in the cell due to the simultaneous inhibition of glycolysis at these conditions. Thus, in the case of hyperglycemia this otherwise meaningful regulation results in a massive increase in intracellular sorbitol and depletion of NADPH, likely to contribute to oxidative stress during diabetes mellitus [303–306].

If one assumes that this represents a concerted measure to decrease levels of intracellular NADPH with the aim to decrease the mostly NADPH-dependent  $O_2^{\bullet-}$  formation, it will fit into this concept that thioredoxin (Trx) will be activated through *S*-nitrosation

## 6 Conclusions

of its Cys-69 [127], to some extent compensating the cells loss of reductive power by keeping proteins in their reduced state. According to our results and as well as to recent literature, conditions leading to *S*-nitrosation should occur during increasing formation of  $O_2^{\bullet-}$ , a situation of an imminent switch to conditions of severe oxidative stress. In summary, the above mentioned examples of regulations during such conditions are providing extensive measures to react to these changes. Since this hypothesis of a fight against  $O_2^{\bullet-}$  formation will lead to depletion of cellular reducing equivalents and therefore to both a vicious circle and a situation the cell cannot withstand for a longer period of time, there has to exist a meaningful concept of countermeasures to restore the cell's normal state. Such a reversal of these regulations is partly provided by the reversibility of *S*-nitrosation, but this first requires recovery of the cellular redox state. Further oxidation often leads to transition from *S*-nitrosation to *S*-glutathiolation. For ALR2 and Trx it is known that glutathiolation can occur and is linked to enzyme inhibition [83, 116, 127], whereas in the case of Trx, nitrosation and glutathiolation occurs at different Cys residues. GAPDH and ICDH can also be glutathiolated [77, 307], but without releasing their inhibition. Reduction of these oxidized thiols by glutaredoxin requires a restored cellular redox equilibrium [308].

Persistent  $O_2^{\bullet-}$  formation will lead to oxidations by peroxynitrite and later also by  $O_2^{\bullet-}$  and  $H_2O_2$ . Besides other consequences, this results in inhibition of mitochondrial and cytosolic aconitase via oxidation of its  $[Fe_4S_4]^{2+}$  cluster by both HOONO or  $O_2^{\bullet-}$  [163–165]. Due to its central role in the tricarboxylic acid cycle, cellular ATP and NADPH regeneration should be blocked in this phase and in addition, oxidation of the iron-sulphur cluster results in release of iron. The cytosolic isoform of aconitase, exhibiting a second function in iron metabolism as iron regulatory protein-1 (IRP-1), can bind after the loss of its iron to the iron response element located within the mRNA of iron-related proteins. Binding of IRP-1 to this motif results in blocking of the translation of iron storage molecules and therefore increasing levels of free iron, contributing to  $\bullet OH$  formation via Fenton chemistry. At the same time, counter-

## 6 Conclusions

regulations by *S*-nitrosation should be reversed due to oxidation of *S*-nitrosothiols by the above explained mechanisms. This sequence of events indicates that if  $O_2^{\bullet-}$  formation increases beyond certain rates the cell can handle, it will switch away from preventing further increase of oxidative stress towards the opposite and heads itself into self-destruction.

The major diseases of the western world, like atherosclerosis, diabetes, stroke, AIDS or neurodegenerative diseases like Alzheimer's disease, amyotrophic lateral sclerosis (ALS) or Parkinson's disease all have a strong component of oxidative stress accompanied by a disturbance in cellular redox equilibrium. The herein described mechanisms of redox regulation should lead to lesions during these diseases and have to be considered for their cure. Thus, these mechanisms require further investigation to understand and to treat these diseases.

The vascular system, especially the endothelium of large vessels, is able to orchestrate vessel function through a variety of redox mechanisms and the circulatory system provides several examples for redox regulation during pathophysiological situations such as atherosclerosis, ischemia/reperfusion, diabetic endothelial dysfunction and inflammatory processes in general. Vasorelaxation is mediated by  $\bullet NO$  from shear-stress activated NOS-3 and by prostaglandin  $I_2$  ( $PGI_2$ , prostacyclin) originating from endothelial cells. Via cGMP and cAMP, both signaling molecules trigger a decline in free intracellular  $Ca^{2+}$  in smooth muscle cells, characterizing a resting state with a tightly closed endothelium, relaxation of smooth muscles and the adherence of platelets or white blood cells is prevented. Many stimuli including angiotensin II, acetylcholine, substance P, thromboxane  $A_2$  or leukotriene  $C_4$  elicit a PI-response by activation of their corresponding receptors. This not only triggers  $Ca^{2+}$  release but also PKC-dependent phosphorylation of the cytosolic NADPH oxidase-subunits, leading to  $O_2^{\bullet-}$  formation at low rates. Under formation of peroxyxynitrite,  $O_2^{\bullet-}$  traps  $\bullet NO$  leading to smooth muscle contraction in synergy with agonists. The contractive phase ceases after several minutes and is replaced by endothelium-dependent relaxation due to

## 6 Conclusions

$\text{Ca}^{2+}$ -triggered  $\bullet\text{NO}$  synthesis and the liberation of arachidonic acid with subsequent conversion to  $\text{PGH}_2$  and  $\text{PGI}_2$ .

A further increase in  $\text{O}_2^{\bullet-}$  formation by stimuli like e. g. endotoxin (lipopolysaccharide, LPS) will lead to activation of the endothelium, and due to its fast reaction with  $\bullet\text{NO}$ ,  $^-\text{OONO}$  will be formed. This can result in nitration and inactivation of  $\text{PGI}_2$  synthase and the accumulation of its substrate  $\text{PGH}_2$ , which possesses opposing properties leading to vasoconstriction, platelet aggregation and leukocyte adhesion [1]. Therefore, the vascular system provides not only an interesting model for redox regulation in the  $\bullet\text{NO}/\text{O}_2^{\bullet-}$  system, but many chronic diseases of the western world interfere with this complex system, leading to a transition towards conditions of oxidative stress, persistent inflammation and cell damage.

Although redox regulation usually evokes an immediate response and in a healthy organism these regulations should only occur over short time periods, it should be noted that these mechanisms are closely connected to transcriptional regulation and therefore responsible for long-term changes of the cell. Especially  $\text{HIF-1}\alpha$ ,  $\text{p53}$  and  $\text{NF}\kappa\text{B}$  and their regulation by *S*-nitrosation were investigated in detail within the last decade, and these transcription factors also play an important role in controlling the expression of the different isoforms of NOS. Regulation of cellular protein levels does not stop at the level of transcription (and translation), but also includes pathways of degradation at the level of ubiquitination and proteasomal targeting [79]. *S*-Nitrosation of the E3 ubiquitin ligase parkin leads to a biphasic change in its activity and since its nitrosation is known to occur during Parkinson's disease, this could contribute to the degenerative process [154–156]. The apurinic/aprimidinic endonuclease/redox factor-1 ( $\text{APE1/ref-1}$ ) exerts a central role in transcriptional activation and DNA base excision repair during situations of oxidative stress. Its translocation to the nucleus stimulates DNA binding of the transcription factors Fos, Jun,  $\text{NF}\kappa\text{B}$ , PAX,  $\text{HIF-1}\alpha$ , HLF,  $\text{p53}$  and AP-1 [309, 310], and in addition, most of them are additionally regulated by *S*-nitrosation. Activation of  $\text{APE1/ref-1}$  by ROS is not completely understood but

## 6 Conclusions

mainly seems to be triggered via phosphorylation by PKC [311], linking its regulation to other central pathways of redox regulation.

Redox regulation is intimately linked to apoptosis, although the interplay between the different signaling pathways and the ultimate consequences for the cell are far from being understood. The inactive procaspases usually exist in a *S*-nitrosated form even at conditions of basal  $\bullet$ NO formation and their activation requires denitrosation of the zymogen in addition to its cleavage [135, 136]. In this context, *S*-nitrosation clearly has anti-apoptotic properties, but since this occurs at resting conditions, it has to occur in a specific way which is not connected with the explained mechanisms of a more widespread *S*-nitrosation. At the same time, *S*-nitrosation seems to mediate survival by activation of thioredoxin and Ras and by inhibition of the pro-apoptotic regulators apoptosis-signal-regulating kinase 1 (ASK1), c-Jun-*N*-terminal kinase (JNK) and NMDA receptor. But at certain conditions *S*-nitrosation of GAPDH, matrix metalloproteinase-9 (MMP-9), I $\kappa$ B kinase  $\beta$  (IKK $\beta$ ), NF $\kappa$ B, p53 and parkin can occur, inducing apoptosis. These nitrosations should not predominate at resting conditions but require exposure to stress.

The example of apoptosis demonstrates that *S*-nitrosation not only acts as a general signal during conditions favoring this covalent modification but the picture is more complicated and further investigations are required. Especially *S*-nitrosation of GAPDH was recently discovered to promote apoptosis in addition to disruption of glycolysis. Its *S*-nitrosation triggers binding to the E3 ubiquitin ligase Siah1 and subsequent translocation to the nucleus, where it targets nuclear proteins for degradation [123]. A further obstacle in the understanding of the interplay between redox regulation and cell death lies in the requirement of a sufficient supply of GSH for apoptosis [312]. In summary, conditions promoting *S*-nitrosations in the cell should favor apoptosis, whereas the significant lower levels of *S*-nitrosation during resting and reduced conditions are preventing cell death.

## 6 Conclusions

Carbon monoxide from heme oxygenase will join the ensemble of signaling molecules during shifts in the cellular redox state. Since our original hypothesis of a direct activation of NOS-1 via release of its autoinhibition could not be proved, it has to be assumed that its effects at physiologically relevant concentrations (3–30  $\mu\text{M}$  [185]) should mainly depend on the activation of big-conductance  $\text{Ca}^{2+}$ -activated  $\text{K}^+$  ( $\text{BK}_{\text{Ca}}$ ) channels. Heme oxygenase-2 is part of the  $\text{BK}_{\text{Ca}}$  channel complex and could serve as an  $\text{O}_2$  sensor [214]. The recently discovered binding of heme to the channel leads to its inhibition and CO seems to interfere with its binding, provided that heme is reduced [215].

Redox regulation by the  $\bullet\text{NO}/\text{O}_2^{\bullet-}$  system affects cellular signaling networks at various targets and will have extensive consequences for the cell. Its ultimate result depends on the persistence of the initial stimulus as well as on the balance of the cells reductive systems. Shifts within this signaling network are contributing to numerous diseases, and for most of these a successful therapy still has to be developed. Signaling in this context depends on both steady-state levels of  $\bullet\text{NO}$  and  $\text{O}_2^{\bullet-}$  and the rates of their formation. Based on the balance between these two radicals, distinct phases of reactivities can be assumed, which elicit a meaningful sequence of regulatory events in the cell, ranging from protective mechanisms up to cell death. Within the sequence of redox regulatory events it has to be emphasized that a slight excess of  $\bullet\text{NO}$  over  $\text{O}_2^{\bullet-}$  provokes a different pattern of reactions as the one expected from  $^-\text{OONO}$  and  $\bullet\text{NO}$  alone. This reaction should represent the key to understand the effects of  $\bullet\text{NO}$  as an antioxidant and *S*-nitrosation as a comprehensive mechanism to regulate main pathways and in consequence to adapt the cell to a changed situation. The basic mechanisms of cellular redox signaling are mainly disclosed, but the interrelation of the regulated pathways clearly requires further investigation.

## 7 Summary

This work tries to establish a chemical basis for redox regulations, i.e. the physiological regulation of enzyme activity by oxidative modifications of regulatory enzymes. Previous work from our group has highlighted the role of nitric oxide ( $\bullet\text{NO}$ ) and superoxide ( $\text{O}_2^{\bullet-}$ ) in the formation of peroxynitrite, which is responsible for tyrosine nitrations and has been well studied as a physiological inhibitory agent for prostacyclin ( $\text{PGI}_2$ ) synthase. In contrast, *S*-nitrosation reaction as another even more frequent posttranslational modification of proteins is still barely understood with regard to its mechanism and significance. The present data contribute to the chemistry of such redox regulations by the following findings:

1. In contrast to literature reports, we find that  $\bullet\text{NO}$  itself is unable to support *S*-nitrosation under physiological conditions. In presence of  $\text{O}_2^{\bullet-}$  the model of *N*-nitrosation of 2,3-diaminonaphthalene (DAN) requires optimal ratios of 2–3:1 of  $\bullet\text{NO}$  to  $\text{O}_2^{\bullet-}$  indicating that either  $\text{N}_2\text{O}_3$  (3:1) or an  $[\text{NO}^+]$  species (2:1) is involved. Since the  $\text{N}_2\text{O}_3$ -specific inhibitor azide is not effective we propose the latter mechanism.
2. Data from experiments with varying ratios of  $\bullet\text{NO}$  to  $\text{O}_2^{\bullet-}$  generation allow us to suggest that  $\bullet\text{NO}$  reacts with peroxynitrous acid ( $\text{HOONO}$ ) to yield the postulated  $[\text{NO}^+]$  species. This applies for *in situ* generated peroxynitrite, whereas different results exist for bulk additions in presence of  $\bullet\text{NO}$ . The latter, however, do not correspond to the physiological situation.

## 7 Summary

3. Literature data on nitrations and nitrosations were shown to contain artifacts if samples were frozen. This enhanced 3-nitrotyrosine and *S*-nitrosothiol formation occurs by pH-lowering during slow freezing in sodium phosphate buffer, allowing nitrous acid to form and cause nitrosations and by air oxidation also nitrated products.
4. We postulate that *S*-nitrosation occurs in the cell as a pre-stage of oxidations and nitrations by peroxynitrite. This is supported by described blocking effects of *S*-nitrosations on NADPH and NADH supply. This would create conditions allowing an accumulation of peroxynitrite since the antioxidant capacity of the cell is down-regulated.
5. The system  $\bullet\text{NO}/\text{O}_2^{\bullet-}$  was subject to kinetic calculations in order to determine steady state concentrations of peroxynitrite. From the data it appeared unlikely that under cellular resting conditions enough peroxynitrite for tyrosine nitrations can accumulate. This strengthens our hypothesis of a switch-off for reducing pathways after which peroxynitrite levels can be build up.
6. Carbon monoxide at submicromolar levels was found to cause tyrosine nitration in brain vessels which may represent the nitration of PGI<sub>2</sub> synthase. For the mechanism involved several possibilities were considered and experimentally investigated without obtaining conclusive results. It remains that CO could either block myoglobin or hemoglobin from binding  $\bullet\text{NO}$ , leaving more  $\bullet\text{NO}$  available. Our data do not yet exclude a stimulation of NOS-1 by CO and also the opening of big-conductance Ca<sup>2+</sup>-activated K<sup>+</sup> (BK<sub>Ca</sub>) channels through a heme-containing subunit serves as a possible target of CO.

Overall, our results have provided more insight into the complex behavior of  $\bullet\text{NO}/\text{O}_2^{\bullet-}$  interactions and have provided a new basis of redox regulation.

## 8 Zusammenfassung

Diese Arbeit untersucht die chemischen Grundlagen der Redox-Regulation, d.h. die physiologische Regulation der Enzymaktivität durch oxidative Modifikationen von regulatorischen Enzymen. Durch vorausgehende Arbeiten unserer Arbeitsgruppe konnte die zentrale Funktion von Stickstoffmonoxid ( $\bullet\text{NO}$ ) und Superoxid ( $\text{O}_2^{\bullet-}$ ) bei der Entstehung von Peroxynitrit aufgezeigt werden. Peroxynitrit ist für die Nitrierung von Tyrosin verantwortlich und wurde als ein hemmendes Agens für die Prostazyklinsynthase ausgiebig untersucht. Im Gegensatz dazu ist der Mechanismus und die Bedeutung der *S*-Nitrosierung als eine deutlich häufigere posttranslationale Proteinmodifikation bisher kaum verstanden. Die vorliegenden Daten leisten einen Beitrag zum Verständnis der Chemie solcher Redox-Regulationen, insbesondere durch folgende Ergebnisse:

1. Im Gegensatz zu Berichten in der Literatur stellten wir fest, dass  $\bullet\text{NO}$  alleine nicht zu *S*-Nitrosierung unter physiologischen Bedingungen führen kann. Im Modell der *N*-Nitrosierung von 2,3-Diaminonaphthalen (DAN) ist die Gegenwart von  $\text{O}_2^{\bullet-}$  mit einem optimalen Verhältnis von 2–3:1 von  $\bullet\text{NO}$  zu  $\text{O}_2^{\bullet-}$  erforderlich, was darauf hinweist, dass entweder  $\text{N}_2\text{O}_3$  (3:1) oder eine  $[\text{NO}^+]$ -Spezies (2:1) beteiligt ist. Da der  $\text{N}_2\text{O}_3$ -spezifische Inhibitor Azid keinen Effekt zeigte, schlagen wir den letzteren Mechanismus vor.
2. Aufgrund von Versuchen mit variierenden Verhältnissen zwischen  $\bullet\text{NO}$ - und  $\text{O}_2^{\bullet-}$ -Bildung nehmen wir an, dass  $\bullet\text{NO}$  mit Peroxysalpetriger Säure ( $\text{HOONO}$ ) reagiert und so zur Bildung des postulierten  $[\text{NO}^+]$ -Spezies führt. Dieses gilt für

- in situ* gebildetes Peroxynitrit, während für die schnelle Zugabe großer Mengen in Gegenwart von  $\bullet\text{NO}$  andere Ergebnisse bekannt sind. Allerdings entspricht letzteres jedoch nicht den physiologischen Bedingungen.
3. Es konnte gezeigt werden, dass unter der Verwendung von eingefrorenen Proben erhaltene Daten aus der Literatur über Nitrierungen und Nitrosierungen Artefakte aufweisen. Diese erhöhte Bildung von 3-Nitrotyrosin und *S*-Nitrosothiolen beruht auf dem Absinken des pH-Werts während des langsamen Einfrierens in der Gegenwart von Natriumphosphatpuffer. Dadurch wird die Bildung von Salpetriger Säure ermöglicht, welche Nitrosierungen, und durch aerobe Oxidation, auch die Bildung von nitrierten Produkten erlaubt.
  4. Wir postulieren, dass *S*-Nitrosierungen in der Zelle als eine Vorphase für Oxidationen und Nitrierungen durch Peroxynitrit auftreten. Dieses wird unterstützt durch die beschriebene Blockierung der NADPH- und NADH-Versorgung durch *S*-Nitrosierungen. Da so die antioxidative Kapazität der Zelle sinkt, würden die entstehenden Bedingungen eine Akkumulation von Peroxynitrit erlauben.
  5. Durch kinetische Berechnungen wurde das System  $\bullet\text{NO}/\text{O}_2^{\bullet-}$  mit dem Ziel der Bestimmung der steady-state Konzentrationen von Peroxynitrit untersucht. Ausgehend von den erhaltenen Daten erscheint es unwahrscheinlich, dass sich unter Ruhebedingungen in der Zelle ausreichende Konzentrationen an Peroxynitrit zur Nitrierung von Tyrosin bilden können. Dieses stützt unsere Hypothese eines vorausgehenden Ausschaltens reduktiver Mechanismen, welches erst die Bildung relevanter Konzentrationen von Peroxynitrit ermöglicht.
  6. Submikromolare Konzentrationen von Kohlenmonoxid führen zur Tyrosin-Nitrierung, wahrscheinlich der Prostazyklinsynthese, in Gefäßen des Gehirns. Für den verantwortlichen Mechanismus wurden mehrere Möglichkeiten in Betracht gezogen und experimentell untersucht, jedoch ohne abschließende Ergebnisse zu erhalten. Eine andere Möglichkeit wäre, dass CO die Bindung von  $\bullet\text{NO}$

## 8 Zusammenfassung

an Myoglobin oder Hämoglobin blockiert und daher die Verfügbarkeit von  $\bullet\text{NO}$  erhöht. Allerdings können unsere Daten eine Stimulation der NOS-1 durch CO nicht ausschließen und ein Öffnen von  $\text{Ca}^{2+}$ -aktivierten  $\text{K}^+$ -Kanälen vom BK-Typ über eine Häm-assoziierte Untereinheit könnte ein anderes mögliches Target von CO darstellen.

Unsere Ergebnisse haben so einen tieferen Einblick in das komplexe Zusammenspiel von  $\bullet\text{NO}$  und  $\text{O}_2^{\bullet-}$  ermöglicht und liefern daher eine neue Grundlage für das Verständnis der Redox-Regulation.

# References

- [1] D. Frein, S. Schildknecht, M. Bachschmid, and V. Ullrich. Redox regulation: A new challenge for pharmacology. *Biochem Pharmacol*, 70(6):811–823, 2005.
- [2] J. Nordberg and E.S. Arner. Reactive oxygen species, antioxidants, and the mammalian thioredoxin system. *Free Radic Biol Med*, 31(11):1287–1312, 2001.
- [3] H. Sies. *Oxidative Stress*, chapter Oxidative Stress: Introductory Remarks, 1–8. Academic Press, London, 1985.
- [4] L.M. Landino, B.C. Crews, M.D. Timmons, J.D. Morrow, and L.J. Marnett. Peroxynitrite, the coupling product of nitric oxide and superoxide, activates prostaglandin biosynthesis. *Proc Natl Acad Sci U S A*, 93(26):15069–15074, 1996.
- [5] D. Namgaladze, H.W. Hofer, and V. Ullrich. Redox control of calcineurin by targeting the binuclear  $\text{Fe}^{2+}$ - $\text{Zn}^{2+}$  center at the enzyme active site. *J Biol Chem*, 277(8):5962–5969, 2002.
- [6] B. Brüne, K.U. Schmidt, and V. Ullrich. Activation of soluble guanylate cyclase by carbon monoxide and inhibition by superoxide anion. *Eur J Biochem*, 192(3):683–688, 1990.
- [7] V. Pelmeshnikov and P.E. Siegbahn. Copper-zinc superoxide dismutase: theoretical insights into the catalytic mechanism. *Inorg Chem*, 44(9):3311–3320, 2005.
- [8] J.S. Beckman and W.H. Koppenol. Nitric oxide, superoxide, and peroxynitrite: the good, the bad, and ugly. *Am J Physiol*, 271(5 Pt 1):C1424–C1437, 1996.
- [9] R.M. Lebovitz, H. Zhang, H. Vogel, J. Cartwright, Jr, L. Dionne, N. Lu, S. Huang, and M.M. Matzuk. Neurodegeneration, myocardial injury, and perinatal death in mitochondrial superoxide dismutase-deficient mice. *Proc Natl Acad Sci U S A*, 93(18):9782–9787, 1996.
- [10] Y. Li, T.T. Huang, E.J. Carlson, S. Melov, P.C. Ursell, J.L. Olson, L.J. Noble, M.P. Yoshimura, C. Berger, P.H. Chan, D.C. Wallace, and C.J. Epstein. Dilated cardiomyopathy and neonatal lethality in mutant mice lacking manganese superoxide dismutase. *Nat Genet*, 11(4):376–381, 1995.
- [11] M. Yamamoto, J.D. Clark, J.V. Pastor, P. Gurnani, A. Nandi, H. Kurosu, M. Miyoshi, Y. Ogawa, D.H. Castrillon, K.P. Rosenblatt, and M. Kuro-O. Regulation of Oxidative Stress by the Anti-aging Hormone Klotho. *J Biol Chem*, 280(45):38029–38034, 2005.

## References

- [12] Y.S. Ho, M. Gargano, J. Cao, R.T. Bronson, I. Heimler, and R.J. Hutz. Reduced fertility in female mice lacking copper-zinc superoxide dismutase. *J Biol Chem*, 273(13):7765–7769, 1998.
- [13] D.R. Rosen, T. Siddique, D. Patterson, D.A. Figlewicz, P. Sapp, A. Hentati, D. Donaldson, J. Goto, J.P. O'Regan, H.X. Deng, and et al. Mutations in Cu/Zn superoxide dismutase gene are associated with familial amyotrophic lateral sclerosis. *Nature*, 362(6415):59–62, 1993.
- [14] P.B. Stathopoulos, J.A. Rumfeldt, G.A. Scholz, R.A. Irani, H.E. Frey, R.A. Hallewell, J.R. Lepock, and E.M. Meiering. Cu/Zn superoxide dismutase mutants associated with amyotrophic lateral sclerosis show enhanced formation of aggregates in vitro. *Proc Natl Acad Sci U S A*, 100(12):7021–7026, 2003.
- [15] W.P. Arnold, C.K. Mittal, S. Katsuki, and F. Murad. Nitric oxide activates guanylate cyclase and increases guanosine 3':5'-cyclic monophosphate levels in various tissue preparations. *Proc Natl Acad Sci U S A*, 74(8):3203–3207, 1977.
- [16] R.F. Furchgott and J.V. Zawadzki. The obligatory role of endothelial cells in the relaxation of arterial smooth muscle by acetylcholine. *Nature*, 288(5789):373–376, 1980.
- [17] L.J. Ignarro, G.M. Buga, K.S. Wood, R.E. Byrns, and G. Chaudhuri. Endothelium-derived relaxing factor produced and released from artery and vein is nitric oxide. *Proc Natl Acad Sci U S A*, 84(24):9265–9269, 1987.
- [18] M. Kahn and R. Furchgott. *Pharmacology*, chapter Additional evidence that endothelium-derived relaxing factor is nitric oxide. Elsevier, Amsterdam, 1987.
- [19] D.S. Brecht and S.H. Snyder. Isolation of nitric oxide synthetase, a calmodulin-requiring enzyme. *Proc Natl Acad Sci U S A*, 87(2):682–685, 1990.
- [20] A. Nedospasov, R. Rafikov, N. Beda, and E. Nudler. An autocatalytic mechanism of protein nitrosylation. *Proc Natl Acad Sci U S A*, 97(25):13543–13548, 2000.
- [21] S. Schildknecht, M. Bachschmid, K. Weber, D. Maass, and V. Ullrich. Endotoxin elicits nitric oxide release in rat but prostacyclin synthesis in human and bovine vascular smooth muscle cells. *Biochem Biophys Res Commun*, 327(1):43–48, 2005.
- [22] D.J. Stuehr. Mammalian nitric oxide synthases. *Biochim Biophys Acta*, 1411(2-3):217–230, 1999.
- [23] W.K. Alderton, C.E. Cooper, and R.G. Knowles. Nitric oxide synthases: structure, function and inhibition. *Biochem J*, 357(Pt 3):593–615, 2001.
- [24] U. Siddhanta, C. Wu, H.M. Abu-Soud, J. Zhang, D.K. Ghosh, and D.J. Stuehr. Heme iron reduction and catalysis by a nitric oxide synthase heterodimer containing one reductase and two oxygenase domains. *J Biol Chem*, 271(13):7309–7312, 1996.

## References

- [25] U. Siddhanta, A. Presta, B. Fan, D. Wolan, D.L. Rousseau, and D.J. Stuehr. Domain swapping in inducible nitric-oxide synthase. Electron transfer occurs between flavin and heme groups located on adjacent subunits in the dimer. *J Biol Chem*, 273(30):18950–18958, 1998.
- [26] E.D. Garcin, C.M. Bruns, S.J. Lloyd, D.J. Hosfield, M. Tiso, R. Gachhui, D.J. Stuehr, J.A. Tainer, and E.D. Getzoff. Structural basis for isozyme-specific regulation of electron transfer in nitric-oxide synthase. *J Biol Chem*, 279(36):37918–37927, 2004.
- [27] H.M. Abu-Soud, J. Wang, D.L. Rousseau, J.M. Fukuto, L.J. Ignarro, and D.J. Stuehr. Neuronal nitric oxide synthase self-inactivates by forming a ferrous-nitrosyl complex during aerobic catalysis. *J Biol Chem*, 270(39):22997–23006, 1995.
- [28] J.S. Nishimura, R. Narayanasami, R.T. Miller, L.J. Roman, S. Panda, and B.S. Masters. The stimulatory effects of Hofmeister ions on the activities of neuronal nitric-oxide synthase. Apparent substrate inhibition by L-arginine is overcome in the presence of protein-destabilizing agents. *J Biol Chem*, 274(9):5399–5406, 1999.
- [29] S. Adak, C. Crooks, Q. Wang, B.R. Crane, J.A. Tainer, E.D. Getzoff, and D.J. Stuehr. Tryptophan 409 controls the activity of neuronal nitric-oxide synthase by regulating nitric oxide feedback inhibition. *J Biol Chem*, 274(38):26907–26911, 1999.
- [30] J.S. Stamler and G. Meissner. Physiology of nitric oxide in skeletal muscle. *Physiol Rev*, 81(1):209–237, 2001.
- [31] C.E. Sears, E.A. Ashley, and B. Casadei. Nitric oxide control of cardiac function: is neuronal nitric oxide synthase a key component? *Philos Trans R Soc Lond B Biol Sci*, 359(1446):1021–1044, 2004.
- [32] S.L. Elfering, T.M. Sarkela, and C. Giulivi. Biochemistry of mitochondrial nitric-oxide synthase. *J Biol Chem*, 277(41):38079–38086, 2002.
- [33] P.S. Brookes. Mitochondrial nitric oxide synthase. *Mitochondrion*, 3(4):187–204, 2004.
- [34] V. Haynes, S. Elfering, N. Traaseth, and C. Giulivi. Mitochondrial nitric-oxide synthase: enzyme expression, characterization, and regulation. *J Bioenerg Biomembr*, 36(4):341–346, 2004.
- [35] Z. Lacza, E. Pankotai, A. Csordas, . Gero, L. Kiss, E.M. Horvath, M. Kollai, D.W. Busija, and C. Szabo. Mitochondrial NO and reactive nitrogen species production: Does mtNOS exist? *Nitric Oxide*, 2005.
- [36] N.V. Blough and O.C. Zafiriou. Reaction of superoxide with nitric oxide to form peroxynitrite in alkaline solution. *Inorg Chem*, 24(22):3502–3504, 1985.

## References

- [37] T. Nauser and W.H. Koppenol. The rate constant of the reaction of superoxide with nitrogen monoxide: Approaching the diffusion limit. *J Phys Chem A*, 106: 4084–4086, 2002.
- [38] R.E. Huie and S. Padmaja. The reaction of NO with superoxide. *Free Radic Res Commun*, 18(4):195–199, 1993.
- [39] S. Goldstein and G. Czapski. The reaction of  $\bullet\text{NO}$  with  $\text{O}_2^{\bullet-}$  and  $\text{HO}_2\bullet$ : a pulse radiolysis study. *Free Radic Biol Med*, 19(4):505–510, 1995.
- [40] K. Kobayashi, M. Miki, and S. Tagawa. Pulse-radiolysis study of the reaction of nitric oxide with superoxide. *J Chem Soc, Dalton Trans*, (17):2885–2889, 1995.
- [41] R. Kissner, T. Nauser, P. Bugnon, P.G. Lye, and W.H. Koppenol. Formation and properties of peroxynitrite as studied by laser flash photolysis, high-pressure stopped-flow technique, and pulse radiolysis. *Chem Res Toxicol*, 10(11):1285–1292, 1997.
- [42] R. Kissner, T. Nauser, C. Kurz, and W.H. Koppenol. Peroxynitrous acid—where is the hydroxyl radical? *IUBMB Life*, 55(10-11):567–572, 2003.
- [43] S. Goldstein, J. Lind, and G. Merenyi. Chemistry of peroxynitrites as compared to peroxynitrates. *Chem Rev*, 105(6):2457–2470, 2005.
- [44] W.H. Koppenol. The basic chemistry of nitrogen monoxide and peroxynitrite. *Free Radic Biol Med*, 25(4-5):385–391, 1998.
- [45] J. Matthews, A. Sinha, and J.S. Francisco. Relative vibrational overtone intensity of cis-cis and trans-perp peroxynitrous acid. *J Chem Phys*, 120(22): 10543–10553, 2004.
- [46] C.D. Reiter, R.J. Teng, and J.S. Beckman. Superoxide reacts with nitric oxide to nitrate tyrosine at physiological pH via peroxynitrite. *J Biol Chem*, 275(42): 32460–32466, 2000.
- [47] M.C. Symons. Cis- and trans-conformations for peroxynitrite anions. *J Inorg Biochem*, 78(4):299–301, 2000.
- [48] B.D. Bean, A.K. Mollner, S.K. Nizkorodov, G. Nair, M. Okumura, S.P. Sander, K.A. Peterson, and J.S. Francisco. Cavity Ringdown Spectroscopy of cis-cis HOONO and the HOONO/HONO<sub>2</sub> Branching Ratio in the Reaction OH + NO<sub>2</sub> + M. *J Phys Chem A*, 107:6974–6985, 2003.
- [49] D. Jourd’heuil, F.L. Jourd’heuil, P.S. Kutchukian, R.A. Musah, D.A. Wink, and M.B. Grisham. Reaction of superoxide and nitric oxide with peroxynitrite. Implications for peroxynitrite-mediated oxidation reactions in vivo. *J Biol Chem*, 276(31):28799–28805, 2001.
- [50] J.P. Crow and J.S. Beckman. *Reactions between Nitric Oxide, Superoxide, and Peroxynitrite: Footprints of Peroxynitrite in Vivo*, volume 34 of *Advances in Pharmacology*, chapter Chemistry of Nitric Oxide: Biologically Relevant Aspects, 17–43. Academic Press, 1995.

## References

- [51] A. Daiber, D. Frein, D. Namgaladze, and V. Ullrich. Oxidation and nitrosation in the nitrogen monoxide/superoxide system. *J Biol Chem*, 277(14):11882–11888, 2002.
- [52] M.G. Espey, D.D. Thomas, K.M. Miranda, and D.A. Wink. Focusing of nitric oxide mediated nitrosation and oxidative nitrosylation as a consequence of reaction with superoxide. *Proc Natl Acad Sci U S A*, 99(17):11127–11132, 2002.
- [53] A.M. Miles, D.S. Bohle, P.A. Glassbrenner, B. Hansert, D.A. Wink, and M.B. Grisham. Modulation of superoxide-dependent oxidation and hydroxylation reactions by nitric oxide. *J Biol Chem*, 271(1):40–47, 1996.
- [54] S. Goldstein and G. Czapski. Reactivity of peroxynitrite versus simultaneous generation of  $\bullet\text{NO}$  and  $\text{O}_2^{\bullet-}$  toward NADH. *Chem Res Toxicol*, 13(8):736–741, 2000.
- [55] S. Pfeiffer and B. Mayer. Lack of tyrosine nitration by peroxynitrite generated at physiological pH. *J Biol Chem*, 273(42):27280–27285, 1998.
- [56] S. Goldstein, G. Czapski, J. Lind, and G. Merenyi. Tyrosine nitration by simultaneous generation of  $\bullet\text{NO}$  and  $\text{O}_2^{\bullet-}$  under physiological conditions. How the radicals do the job. *J Biol Chem*, 275(5):3031–3036, 2000.
- [57] T. Sawa, T. Akaike, and H. Maeda. Tyrosine nitration by peroxynitrite formed from nitric oxide and superoxide generated by xanthine oxidase. *J Biol Chem*, 275(42):32467–32474, 2000.
- [58] G.R. Hodges, J. Marwaha, T. Paul, and K.U. Ingold. A novel procedure for generating both nitric oxide and superoxide in situ from chemical sources at any chosen mole ratio. First application: tyrosine oxidation and a comparison with preformed peroxynitrite. *Chem Res Toxicol*, 13(12):1287–1293, 2000.
- [59] C. Quijano, N. Romero, and R. Radi. Tyrosine nitration by superoxide and nitric oxide fluxes in biological systems: Modeling the impact of superoxide dismutase and nitric oxide diffusion. *Free Radic Biol Med*, 39(6):728–741, 2005.
- [60] W.G. Keith and R.E. Powell. Kinetics of decomposition of peroxynitrous acid. *J Chem Soc A*, page 90, 1969.
- [61] S.V. Lymer and J.K. Hurst. Rapid reaction between peroxynitrite ion and carbon dioxide: Implications for biological activity. *J Am Chem Soc*, 117(34):8867–8868, 1995.
- [62] G.L. Squadrito and W.A. Pryor. Mapping the reaction of peroxynitrite with  $\text{CO}_2$ : energetics, reactive species, and biological implications. *Chem Res Toxicol*, 15(7):885–895, 2002.
- [63] A. Denicola, B.A. Freeman, M. Trujillo, and R. Radi. Peroxynitrite reaction with carbon dioxide/bicarbonate: kinetics and influence on peroxynitrite-mediated oxidations. *Arch Biochem Biophys*, 333(1):49–58, 1996.

## References

- [64] A. Gow, D. Duran, S.R. Thom, and H. Ischiropoulos. Carbon dioxide enhancement of peroxynitrite-mediated protein tyrosine nitration. *Arch Biochem Biophys*, 333(1):42–48, 1996.
- [65] J.N. Lemercier, S. Padmaja, R. Cueto, G.L. Squadrito, R.M. Uppu, and W.A. Pryor. Carbon dioxide modulation of hydroxylation and nitration of phenol by peroxynitrite. *Arch Biochem Biophys*, 345(1):160–170, 1997.
- [66] R. Radi. Nitric oxide, oxidants, and protein tyrosine nitration. *Proc Natl Acad Sci U S A*, 2004.
- [67] S. Goldstein and G. Czapski. Formation of Peroxynitrate from the Reaction of Peroxynitrite with CO<sub>2</sub>: Evidence for Carbonate Radical Production. *J Am Chem Soc*, 120(14):3458–3463, 1998.
- [68] R. Busse and A. Mulsch. Induction of nitric oxide synthase by cytokines in vascular smooth muscle cells. *FEBS Lett*, 275(1-2):87–90, 1990.
- [69] A. Almeida, P. Ciudad, M. Delgado-Esteban, E. Fernandez, P. Garcia-Nogales, and J.P. Bolanos. Inhibition of mitochondrial respiration by nitric oxide: its role in glucose metabolism and neuroprotection. *J Neurosci Res*, 79(1-2):166–171, 2005.
- [70] M.G. Mason, P. Nicholls, M.T. Wilson, and C.E. Cooper. Nitric oxide inhibition of respiration involves both competitive (heme) and noncompetitive (copper) binding to cytochrome c oxidase. *Proc Natl Acad Sci U S A*, 103(3):708–713, 2006.
- [71] V.G. Kharitonov, A.R. Sundquist, and V.S. Sharma. Kinetics of nitrosation of thiols by nitric oxide in the presence of oxygen. *J Biol Chem*, 270(47):28158–28164, 1995.
- [72] A.A. Nedospasov. Is N<sub>2</sub>O<sub>3</sub> the main nitrosating intermediate in aerated nitric oxide (NO) solutions in vivo? If so, where, when, and which one? *J Biochem Mol Toxicol*, 16(3):109–120, 2002.
- [73] D.A. Wink, J.F. Darbyshire, R.W. Nims, J.E. Saavedra, and P.C. Ford. Reactions of the bioregulatory agent nitric oxide in oxygenated aqueous media: Determination of the kinetics for oxidation and nitrosation by intermediates generated in the nitric oxide/oxygen reaction. *Chem Res Toxicol*, 6(1):23–27, 1993.
- [74] A. Schrammel, A.C. Gorren, K. Schmidt, S. Pfeiffer, and B. Mayer. S-nitrosation of glutathione by nitric oxide, peroxynitrite, and •NO/O<sub>2</sub><sup>•-</sup>. *Free Radic Biol Med*, 34(8):1078–1088, 2003.
- [75] D. Jourd’heuil, F.L. Jourd’heuil, and M. Feelisch. Oxidation and nitrosation of thiols at low micromolar exposure to nitric oxide. Evidence for a free radical mechanism. *J Biol Chem*, 278(18):15720–15726, 2003.

## References

- [76] P. Wardman and C. von Sonntag. Kinetic factors that control the fate of thiyl radicals in cells. *Methods Enzymol*, 251:31–45, 1995.
- [77] S. Mohr, H. Hallak, A. de Boitte, E.G. Lapetina, and B. Brüne. Nitric oxide-induced S-glutathionylation and inactivation of glyceraldehyde-3-phosphate dehydrogenase. *J Biol Chem*, 274(14):9427–9430, 1999.
- [78] J.S. Stamler, E.J. Toone, S.A. Lipton, and N.J. Sucher. (S)NO signals: translocation, regulation, and a consensus motif. *Neuron*, 18(5):691–696, 1997.
- [79] D.T. Hess, A. Matsumoto, S.O. Kim, H.E. Marshall, and J.S. Stamler. Protein S-nitrosylation: purview and parameters. *Nat Rev Mol Cell Biol*, 6(2):150–166, 2005.
- [80] P. Ascenzi, M. Colasanti, T. Persichini, M. Muolo, F. Polticelli, G. Venturini, D. Bordo, and M. Bolognesi. Re-evaluation of amino acid sequence and structural consensus rules for cysteine-nitric oxide reactivity. *Biol Chem*, 381(7):623–627, 2000.
- [81] J.M. Petrash, T.M. Harter, C.S. Devine, P.O. Olins, A. Bhatnagar, S. Liu, and S.K. Srivastava. Involvement of cysteine residues in catalysis and inhibition of human aldose reductase. Site-directed mutagenesis of Cys-80, -298, and -303. *J Biol Chem*, 267(34):24833–24840, 1992.
- [82] B.L. Dixit, G.K. Balendiran, S.J. Watowich, S. Srivastava, K.V. Ramana, J.M. Petrash, A. Bhatnagar, and S.K. Srivastava. Kinetic and structural characterization of the glutathione-binding site of aldose reductase. *J Biol Chem*, 275(28):21587–21595, 2000.
- [83] S.K. Srivastava, K.V. Ramana, D. Chandra, S. Srivastava, and A. Bhatnagar. Regulation of aldose reductase and the polyol pathway activity by nitric oxide. *Chem Biol Interact*, 143-144:333–340, 2003.
- [84] M. Feelisch, T. Rassaf, S. Mnaimneh, N. Singh, N.S. Bryan, D. Jourdeheuil, and M. Kelm. Concomitant S-, N-, and heme-nitros(yl)ation in biological tissues and fluids: implications for the fate of NO in vivo. *FASEB J*, 16(13):1775–1785, 2002.
- [85] N.S. Bryan, T. Rassaf, R.E. Maloney, C.M. Rodriguez, F. Saijo, J.R. Rodriguez, and M. Feelisch. Cellular targets and mechanisms of nitros(yl)ation: An insight into their nature and kinetics in vivo. *Proc Natl Acad Sci U S A*, 2004.
- [86] J.S. Stamler, O. Jaraki, J. Osborne, D.I. Simon, J. Keaney, J. Vita, D. Singel, C.R. Valeri, and J. Loscalzo. Nitric oxide circulates in mammalian plasma primarily as an S-nitroso adduct of serum albumin. *Proc Natl Acad Sci U S A*, 89(16):7674–7677, 1992.
- [87] D. Tsikas, J. Sandmann, P. Luessen, A. Savva, S. Rossa, D.O. Stichtenoth, and J.C. Frolich. S-Transnitrosylation of albumin in human plasma and blood in vitro and in vivo in the rat. *Biochim Biophys Acta*, 1546(2):422–434, 2001.

## References

- [88] L. Jia, C. Bonaventura, J. Bonaventura, and J.S. Stamler. S-nitrosohaemoglobin: a dynamic activity of blood involved in vascular control. *Nature*, 380(6571):221–226, 1996.
- [89] A. Doctor, R. Platt, M.L. Sheram, A. Eischeid, T. McMahon, T. Maxey, J. Doherty, M. Axelrod, J. Kline, M. Gurka, A. Gow, and B. Gaston. Hemoglobin conformation couples erythrocyte S-nitrosothiol content to O<sub>2</sub> gradients. *Proc Natl Acad Sci U S A*, 102(16):5709–5714, 2005.
- [90] Y. Zhang and N. Hogg. S-nitrosohemoglobin: a biochemical perspective. *Free Radic Biol Med*, 36(8):947–958, 2004.
- [91] M.W. Radomski, D.D. Rees, A. Dutra, and S. Moncada. S-nitroso-glutathione inhibits platelet activation in vitro and in vivo. *Br J Pharmacol*, 107(3):745–749, 1992.
- [92] Y. Zhang and N. Hogg. S-Nitrosothiols: cellular formation and transport. *Free Radic Biol Med*, 38(7):831–838, 2005.
- [93] D.J. Meyer, H. Kramer, N. Ozer, B. Coles, and B. Ketterer. Kinetics and equilibria of S-nitrosothiol-thiol exchange between glutathione, cysteine, penicillamines and serum albumin. *FEBS Lett*, 345(2-3):177–180, 1994.
- [94] D.E. Jensen, G.K. Belka, and G.C. Du Bois. S-Nitrosoglutathione is a substrate for rat alcohol dehydrogenase class III isoenzyme. *Biochem J*, 331 ( Pt 2):659–668, 1998.
- [95] L. Liu, A. Hausladen, M. Zeng, L. Que, J. Heitman, and J.S. Stamler. A metabolic enzyme for S-nitrosothiol conserved from bacteria to humans. *Nature*, 410(6827):490–494, 2001.
- [96] J.J. Hedberg, W.J. Griffiths, S.J. Nilsson, and J.O. Hoog. Reduction of S-nitrosoglutathione by human alcohol dehydrogenase 3 is an irreversible reaction as analysed by electrospray mass spectrometry. *Eur J Biochem*, 270(6):1249–1256, 2003.
- [97] M.R. Fernandez, J.A. Biosca, and X. Pares. S-nitrosoglutathione reductase activity of human and yeast glutathione-dependent formaldehyde dehydrogenase and its nuclear and cytoplasmic localisation. *Cell Mol Life Sci*, 60(5):1013–1018, 2003.
- [98] D. Jourdeuil, F.S. Laroux, A.M. Miles, D.A. Wink, and M.B. Grisham. Effect of superoxide dismutase on the stability of S-nitrosothiols. *Arch Biochem Biophys*, 361(2):323–330, 1999.
- [99] A.P. Dicks and D.L. Williams. Generation of nitric oxide from S-nitrosothiols using protein-bound Cu<sup>2+</sup> sources. *Chem Biol*, 3(8):655–659, 1996.
- [100] R.J. Singh, N. Hogg, J. Joseph, and B. Kalyanaraman. Mechanism of nitric oxide release from S-nitrosothiols. *J Biol Chem*, 271(31):18596–18603, 1996.

## References

- [101] C.M. Schonhoff, M. Matsuoka, H. Tummala, M.A. Johnson, A.G. Estevez, R. Wu, A. Kamaid, K.C. Ricart, Y. Hashimoto, B. Gaston, T.L. Macdonald, Z. Xu, and J.B. Mannick. S-nitrosothiol depletion in amyotrophic lateral sclerosis. *Proc Natl Acad Sci U S A*, 103(7):2404–2409, 2006.
- [102] J.E. Freedman, B. Frei, G.N. Welch, and J. Loscalzo. Glutathione peroxidase potentiates the inhibition of platelet function by S-nitrosothiols. *J Clin Invest*, 96(1):394–400, 1995.
- [103] W.N. Kuo and J.M. Kocis. Nitration/S-nitrosation of proteins by peroxynitrite-treatment and subsequent modification by glutathione S-transferase and glutathione peroxidase. *Mol Cell Biochem*, 233(1-2):57–63, 2002.
- [104] D. Nikitovic and A. Holmgren. S-nitrosoglutathione is cleaved by the thioredoxin system with liberation of glutathione and redox regulating nitric oxide. *J Biol Chem*, 271(32):19180–19185, 1996.
- [105] N. Ramachandran, P. Root, X.M. Jiang, P.J. Hogg, and B. Mutus. Mechanism of transfer of NO from extracellular S-nitrosothiols into the cytosol by cell-surface protein disulfide isomerase. *Proc Natl Acad Sci U S A*, 98(17):9539–9544, 2001.
- [106] N. Hogg, R.J. Singh, E. Konorev, J. Joseph, and B. Kalyanaraman. S-Nitrosoglutathione as a substrate for  $\gamma$ -glutamyl transpeptidase. *Biochem J*, 323 ( Pt 2):477–481, 1997.
- [107] M. Trujillo, M.N. Alvarez, G. Peluffo, B.A. Freeman, and R. Radi. Xanthine oxidase-mediated decomposition of S-nitrosothiols. *J Biol Chem*, 273(14):7828–7834, 1998.
- [108] G. Scorza, D. Pietraforte, and M. Minetti. Role of ascorbate and protein thiols in the release of nitric oxide from S-nitroso-albumin and S-nitroso-glutathione in human plasma. *Free Radic Biol Med*, 22(4):633–642, 1997.
- [109] A.J. Holmes and D.L.H. Williams. Reaction of S-nitrosothiols with ascorbate: clear evidence of two reactions. *Chem Commun*, 1998:1711–1712, 1998.
- [110] S.P. Singh, J.S. Wishnok, M. Keshive, W.M. Deen, and S.R. Tannenbaum. The chemistry of the S-nitrosoglutathione/glutathione system. *Proc Natl Acad Sci U S A*, 93(25):14428–14433, 1996.
- [111] K.D. Kröncke. Nitrosative stress and transcription. *Biol Chem*, 384(10-11):1365–1377, 2003.
- [112] L.A. Ridnour, D.D. Thomas, D. Mancardi, M.G. Espey, K.M. Miranda, N. Paolucci, M. Feelisch, J. Fukuto, and D.A. Wink. The chemistry of nitrosative stress induced by nitric oxide and reactive nitrogen oxide species. Putting perspective on stressful biological situations. *Biol Chem*, 385(1):1–10, 2004.
- [113] C.A. O’Brian and F. Chu. Post-translational disulfide modifications in cell signaling—role of inter-protein, intra-protein, S-glutathionyl, and S-cysteaminyll disulfide modifications in signal transmission. *Free Radic Res*, 39(5):471–480, 2005.

## References

- [114] E.A. Konorev, B. Kalyanaraman, and N. Hogg. Modification of creatine kinase by S-nitrosothiols: S-nitrosation vs. S-thiolation. *Free Radic Biol Med*, 28(11):1671–1678, 2000.
- [115] B. Zech, M. Wilm, R. van Eldik, and B. Brüne. Mass spectrometric analysis of nitric oxide-modified caspase-3. *J Biol Chem*, 274(30):20931–20936, 1999.
- [116] A. Chandra, S. Srivastava, J.M. Petrash, A. Bhatnagar, and S.K. Srivastava. Modification of aldose reductase by S-nitrosoglutathione. *Biochemistry*, 36(50):15801–15809, 1997.
- [117] A. Martinez-Ruiz and S. Lamas. Detection and proteomic identification of s-nitrosylated proteins in endothelial cells. *Arch Biochem Biophys*, 423(1):192–199, 2004.
- [118] S.R. Jaffrey and S.H. Snyder. The biotin switch method for the detection of S-nitrosylated proteins. *Sci STKE*, 2001(86):PL1, 2001.
- [119] M.W. Foster and J.S. Stamler. New insights into protein S-nitrosylation: Mitochondria as a model system. *J Biol Chem*, 2004.
- [120] Y. Zhang, A. Keszler, K.A. Broniowska, and N. Hogg. Characterization and application of the biotin-switch assay for the identification of S-nitrosated proteins. *Free Radic Biol Med*, 38(7):874–881, 2005.
- [121] Y. Yang and J. Loscalzo. S-nitrosoprotein formation and localization in endothelial cells. *Proc Natl Acad Sci U S A*, 102(1):117–122, 2005.
- [122] L.M. Landino, M.T. Koumas, C.E. Mason, and J.A. Alston. Ascorbic acid reduction of microtubule protein disulfides and its relevance to protein S-nitrosylation assays. *Biochem Biophys Res Commun*, 340(2):347–352, 2006.
- [123] M.R. Hara, N. Agrawal, S.F. Kim, M.B. Cascio, M. Fujimuro, Y. Ozeki, M. Takahashi, J.H. Cheah, S.K. Tankou, L.D. Hester, C.D. Ferris, S.D. Hayward, S.H. Snyder, and A. Sawa. S-nitrosylated GAPDH initiates apoptotic cell death by nuclear translocation following Siah1 binding. *Nat Cell Biol*, 7(7):665–674, 2005.
- [124] J.M. Souza and R. Radi. Glyceraldehyde-3-phosphate dehydrogenase inactivation by peroxynitrite. *Arch Biochem Biophys*, 360(2):187–194, 1998.
- [125] J.H. Lee, E.S. Yang, and J.W. Park. Inactivation of NADP<sup>+</sup>-dependent isocitrate dehydrogenase by peroxynitrite. Implications for cytotoxicity and alcohol-induced liver injury. *J Biol Chem*, 278(51):51360–51371, 2003.
- [126] J. Haendeler, J. Hoffmann, V. Tischler, B.C. Berk, A.M. Zeiher, and S. Dimmeler. Redox regulatory and anti-apoptotic functions of thioredoxin depend on S-nitrosylation at cysteine 69. *Nat Cell Biol*, 4(10):743–749, 2002.
- [127] H. Yamawaki, J. Haendeler, and B.C. Berk. Thioredoxin: a key regulator of cardiovascular homeostasis. *Circ Res*, 93(11):1029–1033, 2003.

## References

- [128] J. Hoffmann, S. Dimmeler, and J. Haendeler. Shear stress increases the amount of S-nitrosylated molecules in endothelial cells: important role for signal transduction. *FEBS Lett*, 551(1-3):153–158, 2003.
- [129] H.E. Marshall and J.S. Stamler. Inhibition of NF- $\kappa$ B by S-nitrosylation. *Biochemistry*, 40(6):1688–1693, 2001.
- [130] H.E. Marshall, D.T. Hess, and J.S. Stamler. S-nitrosylation: physiological regulation of NF- $\kappa$ B. *Proc Natl Acad Sci U S A*, 101(24):8841–8842, 2004.
- [131] N.L. Reynaert, K. Ckless, S.H. Korn, N. Vos, A.S. Guala, E.F. Wouters, A. van der Vliet, and Y.M. Janssen-Heininger. Nitric oxide represses inhibitory  $\kappa$ B kinase through S-nitrosylation. *Proc Natl Acad Sci U S A*, 101(24):8945–8950, 2004.
- [132] D. Nikitovic, A. Holmgren, and G. Spyrou. Inhibition of AP-1 DNA binding by nitric oxide involving conserved cysteine residues in Jun and Fos. *Biochem Biophys Res Commun*, 242(1):109–112, 1998.
- [133] V.V. Sumbayev, A. Budde, J. Zhou, and B. Brüne. HIF-1  $\alpha$  protein as a target for S-nitrosation. *FEBS Lett*, 535(1-3):106–112, 2003.
- [134] S. Dimmeler, J. Haendeler, M. Nehls, and A.M. Zeiher. Suppression of apoptosis by nitric oxide via inhibition of interleukin-1 $\beta$ -converting enzyme (ICE)-like and cysteine protease protein (CPP)-32-like proteases. *J Exp Med*, 185(4):601–607, 1997.
- [135] J. Hoffmann, J. Haendeler, A.M. Zeiher, and S. Dimmeler. TNF $\alpha$  and oxLDL reduce protein S-nitrosylation in endothelial cells. *J Biol Chem*, 276(44):41383–41387, 2001.
- [136] J.B. Mannick, C. Schonhoff, N. Papeta, P. Ghafourifar, M. Szibor, K. Fang, and B. Gaston. S-Nitrosylation of mitochondrial caspases. *J Cell Biol*, 154(6):1111–1116, 2001.
- [137] B. Zech, R. Kohl, A. Von Knethen, and B. Brüne. Nitric oxide donors inhibit formation of the Apaf-1/caspase-9 apoptosome and activation of caspases. *Biochem J*, 371(Pt 3):1055–1064, 2003.
- [138] J.E. Kim and S.R. Tannenbaum. S-Nitrosation regulates the activation of endogenous procaspase-9 in HT-29 human colon carcinoma cells. *J Biol Chem*, 279(11):9758–9764, 2004.
- [139] H.S. Park, J.W. Yu, J.H. Cho, M.S. Kim, S.H. Huh, K. Ryoo, and E.J. Choi. Inhibition of apoptosis signal-regulating kinase 1 by nitric oxide through a thiol redox mechanism. *J Biol Chem*, 279(9):7584–7590, 2004.
- [140] K. Ckless, N.L. Reynaert, D.J. Taatjes, K.M. Lounsbury, A. van der Vliet, and Y. Janssen-Heininger. In situ detection and visualization of S-nitrosylated proteins following chemical derivatization: identification of Ran GTPase as a target for S-nitrosylation. *Nitric Oxide*, 11(3):216–227, 2004.

## References

- [141] S.R. Jaffrey, M. Fang, and S.H. Snyder. Nitrosopeptide mapping. A novel methodology reveals s-nitrosylation of dexas1 on a single cysteine residue. *Chem Biol*, 9(12):1329–1335, 2002.
- [142] G. Hao, L. Xie, and S.S. Gross. Argininosuccinate synthetase is reversibly inactivated by S-nitrosylation in vitro and in vivo. *J Biol Chem*, 279(35):36192–36200, 2004.
- [143] M. Knipp, O. Braun, P.M. Gehrig, R. Sack, and M. Vasak. Zn(II)-free Dimethylargininase-1 (DDAH-1) Is Inhibited upon Specific Cys-S-Nitrosylation. *J Biol Chem*, 278(5):3410–3416, 2003.
- [144] A. Martinez-Ruiz, L. Villanueva, C. Gonzalez de Orduna, D. Lopez-Ferrer, M.A. Higuera, C. Tarin, I. Rodriguez-Crespo, J. Vazquez, and S. Lamas. S-nitrosylation of Hsp90 promotes the inhibition of its ATPase and endothelial nitric oxide synthase regulatory activities. *Proc Natl Acad Sci U S A*, 102(24):8525–8530, 2005.
- [145] Y.B. Choi, L. Tzeneti, D.A. Le, J. Ortiz, G. Bai, H.S. Chen, and S.A. Lipton. Molecular basis of NMDA receptor-coupled ion channel modulation by S-nitrosylation. *Nat Neurosci*, 3(1):15–21, 2000.
- [146] S. Lipton, Y. Choi, H. Takahashi, D. Zhang, W. Li, A. Godzik, and L. Bankston. Cysteine regulation of protein function - as exemplified by NMDA-receptor modulation. *Trends Neurosci*, 25(9):474, 2002.
- [147] S. Miersch and B. Mutus. Protein S-nitrosation: Biochemistry and characterization of protein thiol-NO interactions as cellular signals. *Clin Biochem*, 38(9):777–791, 2005.
- [148] I. Dalle-Donne, A. Milzani, D. Giustarini, P. Di Simplicio, R. Colombo, and R. Rossi. S-NO-actin: S-nitrosylation kinetics and the effect on isolated vascular smooth muscle. *J Muscle Res Cell Motil*, 21(2):171–181, 2000.
- [149] T. Yasukawa, E. Tokunaga, H. Ota, H. Sugita, J.A. Martyn, and M. Kaneki. S-nitrosylation-dependent inactivation of Akt/protein kinase B in insulin resistance. *J Biol Chem*, 280(9):7511–7518, 2005.
- [150] M.A. Carvalho-Filho, M. Ueno, S.M. Hirabara, A.B. Seabra, J.B. Carvalheira, M.G. de Oliveira, L.A. Velloso, R. Curi, and M.J. Saad. S-nitrosation of the insulin receptor, insulin receptor substrate 1, and protein kinase B/Akt: a novel mechanism of insulin resistance. *Diabetes*, 54(4):959–967, 2005.
- [151] M.A. Rizzo and D.W. Piston. Regulation of  $\beta$  cell glucokinase by S-nitrosylation and association with nitric oxide synthase. *J Cell Biol*, 161(2):243–248, 2003.
- [152] J. Sun, C. Xin, J.P. Eu, J.S. Stamler, and G. Meissner. Cysteine-3635 is responsible for skeletal muscle ryanodine receptor modulation by NO. *Proc Natl Acad Sci U S A*, 98(20):11158–11162, 2001.

## References

- [153] L. Liu, E. Enright, P. Sun, S.Y. Tsai, P. Mehta, D.L. Beckman, and D.M. Terrian. Inactivation of annexin II tetramer by S-nitrosoglutathione. *Eur J Biochem*, 269(17):4277–4286, 2002.
- [154] K.K. Chung, B. Thomas, X. Li, O. Pletnikova, J.C. Troncoso, L. Marsh, V.L. Dawson, and T.M. Dawson. S-nitrosylation of parkin regulates ubiquitination and compromises parkin’s protective function. *Science*, 304(5675):1328–1331, 2004.
- [155] D. Yao, Z. Gu, T. Nakamura, Z.Q. Shi, Y. Ma, B. Gaston, L.A. Palmer, E.M. Rockenstein, Z. Zhang, E. Masliah, T. Uehara, and S.A. Lipton. Nitrosative stress linked to sporadic Parkinson’s disease: S-nitrosylation of parkin regulates its E3 ubiquitin ligase activity. *Proc Natl Acad Sci U S A*, 101(29):10810–10814, 2004.
- [156] K.K. Chung, V.L. Dawson, and T.M. Dawson. Response to Comment on ”S-Nitrosylation of Parkin Regulates Ubiquitination and Compromises Parkin’s Protective Function”. *Science*, 308(5730):1870c, 2005.
- [157] J.P. Crow, J.S. Beckman, and J.M. McCord. Sensitivity of the essential zinc-thiolate moiety of yeast alcohol dehydrogenase to hypochlorite and peroxyxynitrite. *Biochemistry*, 34(11):3544–3552, 1995.
- [158] K.D. Kröncke, L.O. Klotz, C.V. Suschek, and H. Sies. Comparing nitrosative versus oxidative stress towards zinc finger-dependent transcription: Unique role for NO. *J Biol Chem*, 277(15):13294–13301, 2002.
- [159] S. Rajagopalan, X.P. Meng, S. Ramasamy, D.G. Harrison, and Z.S. Galis. Reactive oxygen species produced by macrophage-derived foam cells regulate the activity of vascular matrix metalloproteinases in vitro. Implications for atherosclerotic plaque stability. *J Clin Invest*, 98(11):2572–2579, 1996.
- [160] T. Okamoto, T. Akaike, T. Nagano, S. Miyajima, M. Suga, M. Ando, K. Ichimori, and H. Maeda. Activation of human neutrophil procollagenase by nitrogen dioxide and peroxyxynitrite: a novel mechanism for procollagenase activation involving nitric oxide. *Arch Biochem Biophys*, 342(2):261–274, 1997.
- [161] W. Wang, G. Sawicki, and R. Schulz. Peroxyxynitrite-induced myocardial injury is mediated through matrix metalloproteinase-2. *Cardiovasc Res*, 53(1):165–174, 2002.
- [162] Y. Ben-Yosef, N. Lahat, S. Shapiro, H. Bitterman, and A. Miller. Regulation of endothelial matrix metalloproteinase-2 by hypoxia/reoxygenation. *Circ Res*, 90(7):784–791, 2002.
- [163] A. Hausladen and I. Fridovich. Superoxide and peroxyxynitrite inactivate aconitases, but nitric oxide does not. *J Biol Chem*, 269(47):29405–29408, 1994.
- [164] L. Castro, M. Rodriguez, and R. Radi. Aconitase is readily inactivated by peroxyxynitrite, but not by its precursor, nitric oxide. *J Biol Chem*, 269(47):29409–29415, 1994.

## References

- [165] D. Han, R. Canali, J. Garcia, R. Aguilera, T.K. Gallaher, and E. Cadenas. Sites and Mechanisms of Aconitase Inactivation by Peroxynitrite: Modulation by Citrate and Glutathione. *Biochemistry*, 44(36):11986–11996, 2005.
- [166] W. Vogt. Oxidation of methionyl residues in proteins: tools, targets, and reversal. *Free Radic Biol Med*, 18(1):93–105, 1995.
- [167] B. Alvarez and R. Radi. Peroxynitrite reactivity with amino acids and proteins. *Amino Acids*, 25(3-4):295–311, 2003.
- [168] M.W. Swaim and S.V. Pizzo. Methionine sulfoxide and the oxidative regulation of plasma proteinase inhibitors. *J Leukoc Biol*, 43(4):365–379, 1988.
- [169] J.S. Beckman, H. Ischiropoulos, L. Zhu, M. van der Woerd, C. Smith, J. Chen, J. Harrison, J.C. Martin, and M. Tsai. Kinetics of superoxide dismutase- and iron-catalyzed nitration of phenolics by peroxynitrite. *Arch Biochem Biophys*, 298(2):438–445, 1992.
- [170] H. Ischiropoulos, L. Zhu, J. Chen, M. Tsai, J.C. Martin, C.D. Smith, and J.S. Beckman. Peroxynitrite-mediated tyrosine nitration catalyzed by superoxide dismutase. *Arch Biochem Biophys*, 298(2):431–437, 1992.
- [171] A. Daiber and V. Ullrich. Peroxynitrite reactions with heme and heme-thiolate (P450) proteins. *Methods Enzymol*, 359:379–389, 2002.
- [172] D.D. Thomas, M.G. Espey, M.P. Vitek, K.M. Miranda, and D.A. Wink. Protein nitration is mediated by heme and free metals through Fenton-type chemistry: an alternative to the  $\bullet\text{NO}/\text{O}_2^{\bullet-}$  reaction. *Proc Natl Acad Sci U S A*, 99(20):12691–12696, 2002.
- [173] L.A. MacMillan-Crow and J.A. Thompson. Tyrosine modifications and inactivation of active site manganese superoxide dismutase mutant (Y34F) by peroxynitrite. *Arch Biochem Biophys*, 366(1):82–88, 1999.
- [174] F. Yamakura, H. Taka, T. Fujimura, and K. Murayama. Inactivation of human manganese-superoxide dismutase by peroxynitrite is caused by exclusive nitration of tyrosine 34 to 3-nitrotyrosine. *J Biol Chem*, 273(23):14085–14089, 1998.
- [175] K.S. Aulak, T. Koeck, J.W. Crabb, and D.J. Stuehr. Dynamics of protein nitration in cells and mitochondria. *Am J Physiol Heart Circ Physiol*, 286(1):H30–H38, 2004.
- [176] M.H. Zou and V. Ullrich. Peroxynitrite formed by simultaneous generation of nitric oxide and superoxide selectively inhibits bovine aortic prostacyclin synthase. *FEBS Lett*, 382(1-2):101–104, 1996.
- [177] A.J. Kozak, F. Liu, P. Funovics, A. Jacoby, R. Kubant, and T. Malinski. Role of peroxynitrite in the process of vascular tone regulation by nitric oxide and prostanoids—a nanotechnological approach. *Prostaglandins Leukot Essent Fatty Acids*, 72(2):105–113, 2005.

## References

- [178] P. Schmidt, N. Youhnovski, A. Daiber, A. Balan, M. Arsic, M. Bachschmid, M. Przybylski, and V. Ullrich. Specific nitration at tyrosine 430 revealed by high resolution mass spectrometry as basis for redox regulation of bovine prostacyclin synthase. *J Biol Chem*, 278(15):12813–12819, 2003.
- [179] M. Bachschmid, S. Thureau, M.H. Zou, and V. Ullrich. Endothelial cell activation by endotoxin involves superoxide/NO-mediated nitration of prostacyclin synthase and thromboxane receptor stimulation. *FASEB J*, 17(8):914–916, 2003.
- [180] M. Aslan, T.M. Ryan, T.M. Townes, L. Coward, M.C. Kirk, S. Barnes, C.B. Alexander, S.S. Rosenfeld, and B.A. Freeman. Nitric oxide-dependent generation of reactive species in sickle cell disease. Actin tyrosine induces defective cytoskeletal polymerization. *J Biol Chem*, 278(6):4194–4204, 2003.
- [181] V. Ullrich, D. Namgaladze, and D. Frein. Superoxide as inhibitor of calcineurin and mediator of redox regulation. *Toxicol Lett*, 139(2-3):107–110, 2003.
- [182] T. Adachi, D.R. Pimentel, T. Heibeck, X. Hou, Y.J. Lee, B. Jiang, Y. Ido, and R.A. Cohen. S-glutathiolation of Ras mediates redox-sensitive signaling by angiotensin II in vascular smooth muscle cells. *J Biol Chem*, 279(28):29857–29862, 2004.
- [183] P.A. Savitsky and T. Finkel. Redox regulation of Cdc25C. *J Biol Chem*, 277(23):20535–20540, 2002.
- [184] T. van der Wijk, J. Overvoorde, and J. den Hertog. H<sub>2</sub>O<sub>2</sub>-induced intermolecular disulfide bond formation between receptor protein-tyrosine phosphatases. *J Biol Chem*, 279(43):44355–44361, 2004.
- [185] T. Ingi, G. Chiang, and G.V. Ronnett. The regulation of heme turnover and carbon monoxide biosynthesis in cultured primary rat olfactory receptor neurons. *J Neurosci*, 16(18):5621–5628, 1996.
- [186] R. Zakhary, K.D. Poss, S.R. Jaffrey, C.D. Ferris, S. Tonegawa, and S.H. Snyder. Targeted gene deletion of heme oxygenase 2 reveals neural role for carbon monoxide. *Proc Natl Acad Sci U S A*, 94(26):14848–14853, 1997.
- [187] K.M. Ho, L. Ny, G. McMurray, K.E. Andersson, A.F. Brading, and J.G. Noble. Co-localization of carbon monoxide and nitric oxide synthesizing enzymes in the human urethral sphincter. *J Urol*, 161(6):1968–1972, 1999.
- [188] Z. Grozdanovic and C. Goessl. Comparative localization of heme oxygenase-2 and nitric oxide synthase in the autonomic innervation to the human ductus deferens and seminal vesicle. *J Urol*, 162(6):2156–2161, 1999.
- [189] R. Battish, G.Y. Cao, R.B. Lynn, S. Chakder, and S. Rattan. Heme oxygenase-2 distribution in anorectum: colocalization with neuronal nitric oxide synthase. *Am J Physiol Gastrointest Liver Physiol*, 278(1):G148–G155, 2000.
- [190] O. Baum, M. Feussner, H. Richter, and R. Gossrau. Heme oxygenase-2 is present in the sarcolemma region of skeletal muscle fibers and is non-continuously co-localized with nitric oxide synthase-1. *Acta Histochem*, 102(3):281–298, 2000.

## References

- [191] S.M. Miller, D. Reed, M.G. Sarr, G. Farrugia, and J.H. Szurszewski. Haem oxygenase in enteric nervous system of human stomach and jejunum and colocalization with nitric oxide synthase. *Neurogastroenterol Motil*, 13(2):121–131, 2001.
- [192] H.P. Kim, X. Wang, F. Galbiati, S.W. Ryter, and A.M. Choi. Caveolae compartmentalization of heme oxygenase-1 in endothelial cells. *FASEB J*, 18(10):1080–1089, 2004.
- [193] B. Brüne and V. Ullrich. Inhibition of platelet aggregation by carbon monoxide is mediated by activation of guanylate cyclase. *Mol Pharmacol*, 32(4):497–504, 1987.
- [194] J. Utz and V. Ullrich. Carbon monoxide relaxes ileal smooth muscle through activation of guanylate cyclase. *Biochem Pharmacol*, 41(8):1195–1201, 1991.
- [195] L.E. Otterbein, B.S. Zuckerbraun, M. Haga, F. Liu, R. Song, A. Usheva, C. Stachulak, N. Bodyak, R.N. Smith, E. Csizmadia, S. Tyagi, Y. Akamatsu, R.J. Flavell, T.R. Billiar, E. Tzeng, F.H. Bach, A.M. Choi, and M.P. Soares. Carbon monoxide suppresses arteriosclerotic lesions associated with chronic graft rejection and with balloon injury. *Nat Med*, 9(2):183–190, 2003.
- [196] A. Nakao, K. Kimizuka, D.B. Stolz, J.S. Neto, T. Kaizu, A.M. Choi, T. Uchiyama, B.S. Zuckerbraun, M.A. Nalesnik, L.E. Otterbein, and N. Murase. Carbon Monoxide Inhalation Protects Rat Intestinal Grafts from Ischemia/Reperfusion Injury. *Am J Pathol*, 163(4):1587–1598, 2003.
- [197] S. Brouard, L.E. Otterbein, J. Anrather, E. Tobiasch, F.H. Bach, A.M. Choi, and M.P. Soares. Carbon monoxide generated by heme oxygenase 1 suppresses endothelial cell apoptosis. *J Exp Med*, 192(7):1015–1026, 2000.
- [198] S. Brouard, P.O. Berberat, E. Tobiasch, M.P. Seldon, F.H. Bach, and M.P. Soares. Heme oxygenase-1-derived carbon monoxide requires the activation of transcription factor NF- $\kappa$ B to protect endothelial cells from tumor necrosis factor- $\alpha$ -mediated apoptosis. *J Biol Chem*, 277(20):17950–17961, 2002.
- [199] X.M. Liu, G.B. Chapman, K.J. Peyton, A.I. Schafer, and W. Durante. Anti-apoptotic action of carbon monoxide on cultured vascular smooth muscle cells. *Exp Biol Med (Maywood)*, 228(5):572–575, 2003.
- [200] B.S. Zuckerbraun, T.R. Billiar, S.L. Otterbein, P.K. Kim, F. Liu, A.M. Choi, F.H. Bach, and L.E. Otterbein. Carbon Monoxide Protects against Liver Failure through Nitric Oxide-induced Heme Oxygenase 1. *J Exp Med*, 198(11):1707–1716, 2003.
- [201] J.K. Sarady, B.S. Zuckerbraun, M. Bilban, O. Wagner, A. Usheva, F. Liu, E. Ifedigbo, R. Zamora, A.M. Choi, and L.E. Otterbein. Carbon monoxide protection against endotoxic shock involves reciprocal effects on iNOS in the lung and liver. *FASEB J*, 18(7):854–856, 2004.

- [202] T. Fujita, K. Toda, A. Karimova, S.F. Yan, Y. Naka, S.F. Yet, and D.J. Pinsky. Paradoxical rescue from ischemic lung injury by inhaled carbon monoxide driven by derepression of fibrinolysis. *Nat Med*, 7(5):598–604, 2001.
- [203] X. Zhang, P. Shan, J. Alam, R.J. Davis, R.A. Flavell, and P.J. Lee. Carbon monoxide modulates Fas/Fas ligand, caspases, and Bcl-2 family proteins via the p38 $\alpha$  mitogen-activated protein kinase pathway during ischemia-reperfusion lung injury. *J Biol Chem*, 278(24):22061–22070, 2003.
- [204] X. Zhang, P. Shan, L.E. Otterbein, J. Alam, R.A. Flavell, R.J. Davis, A.M. Choi, and P.J. Lee. Carbon monoxide inhibition of apoptosis during ischemia-reperfusion lung injury is dependent on the p38 mitogen-activated protein kinase pathway and involves caspase 3. *J Biol Chem*, 278(2):1248–1258, 2003.
- [205] H. Fujimoto, M. Ohno, S. Ayabe, H. Kobayashi, N. Ishizaka, H. Kimura, K. Yoshida, and R. Nagai. Carbon monoxide protects against cardiac ischemia-reperfusion injury in vivo via MAPK and Akt-eNOS pathways. *Arterioscler Thromb Vasc Biol*, 24(10):1848–1853, 2004.
- [206] R. Motterlini, J.E. Clark, R. Foresti, P. Sarathchandra, B.E. Mann, and C.J. Green. Carbon monoxide-releasing molecules: characterization of biochemical and vascular activities. *Circ Res*, 90(2):E17–E24, 2002.
- [207] R. Foresti, M. Hoque, S. Bains, C.J. Green, and R. Motterlini. Haem and nitric oxide: synergism in the modulation of the endothelial haem oxygenase-1 pathway. *Biochem J*, 372(Pt 2):381–390, 2003.
- [208] M.H. Halperin, R.A. McFarland, J.I. Niven, and F.J. Roughton. The time course of the effects of carbon monoxide on visual thresholds. *J Physiol*, 146(3):583–593, 1959.
- [209] J.R. Stone and M.A. Marletta. Soluble guanylate cyclase from bovine lung: activation with nitric oxide and carbon monoxide and spectral characterization of the ferrous and ferric states. *Biochemistry*, 33(18):5636–5640, 1994.
- [210] A. Friebe and D. Koesling. Mechanism of YC-1-induced activation of soluble guanylyl cyclase. *Mol Pharmacol*, 53(1):123–127, 1998.
- [211] T.R. Johnson, B.E. Mann, J.E. Clark, R. Foresti, C.J. Green, and R. Motterlini. Metal carbonyls: a new class of pharmaceuticals? *Angew Chem Int Ed Engl*, 42(32):3722–3729, 2003.
- [212] R. Wang, Z. Wang, and L. Wu. Carbon monoxide-induced vasorelaxation and the underlying mechanisms. *Br J Pharmacol*, 121(5):927–934, 1997.
- [213] L. Wu, K. Cao, Y. Lu, and R. Wang. Different mechanisms underlying the stimulation of K<sub>ca</sub> channels by nitric oxide and carbon monoxide. *J Clin Invest*, 110(5):691–700, 2002.
- [214] S.E. Williams, P. Wootton, H.S. Mason, J. Bould, D.E. Iles, D. Riccardi, C. Peers, and P.J. Kemp. Hemoxygenase-2 is an oxygen sensor for a calcium-sensitive potassium channel. *Science*, 306(5704):2093–2097, 2004.

## References

- [215] J.H. Jaggar, A. Li, H. Parfenova, J. Liu, E.S. Umstot, A.M. Dopico, and C.W. Leffler. Heme is a carbon monoxide receptor for large-conductance  $\text{Ca}^{2+}$ -activated  $\text{K}^+$  channels. *Circ Res*, 97(8):805–812, 2005.
- [216] H. Ischiropoulos, M.F. Beers, S.T. Ohnishi, D. Fisher, S.E. Garner, and S.R. Thom. Nitric oxide production and perivascular tyrosine nitration in brain after carbon monoxide poisoning in the rat. *J Clin Invest*, 97(10):2260–2267, 1996.
- [217] S.R. Thom, D. Fisher, Y.A. Xu, S. Garner, and H. Ischiropoulos. Role of nitric oxide-derived oxidants in vascular injury from carbon monoxide in the rat. *Am J Physiol*, 276(3 Pt 2):H984–H992, 1999.
- [218] S.R. Thom. Carbon monoxide-mediated brain lipid peroxidation in the rat. *J Appl Physiol*, 68(3):997–1003, 1990.
- [219] C. Thorup, C.L. Jones, S.S. Gross, L.C. Moore, and M.S. Goligorsky. Carbon monoxide induces vasodilation and nitric oxide release but suppresses endothelial NOS. *Am J Physiol*, 277(6 Pt 2):F882–F889, 1999.
- [220] H. Kimura, Y. Nagai, K. Umemura, and Y. Kimura. Physiological roles of hydrogen sulfide: synaptic modulation, neuroprotection, and smooth muscle relaxation. *Antioxid Redox Signal*, 7(5-6):795–803, 2005.
- [221] P. Kamoun. Endogenous production of hydrogen sulfide in mammals. *Amino Acids*, 26(3):243–254, 2004.
- [222] S. Taoka, M. West, and R. Banerjee. Characterization of the heme and pyridoxal phosphate cofactors of human cystathionine  $\beta$ -synthase reveals nonequivalent active sites. *Biochemistry*, 38(9):2738–2744, 1999.
- [223] S. Taoka and R. Banerjee. Characterization of NO binding to human cystathionine  $\beta$ -synthase: possible implications of the effects of CO and NO binding to the human enzyme. *J Inorg Biochem*, 87(4):245–251, 2001.
- [224] M. Puranik, C.L. Weeks, D. Lahaye, O. Kabil, S. Taoka, S.B. Nielsen, J.T. Groves, R. Banerjee, and T.G. Spiro. Dynamics of carbon monoxide binding to cystathionine  $\beta$ -synthase. *J Biol Chem*, 281(19):13433–13438, 2006.
- [225] M. Whiteman, N.S. Cheung, Y.Z. Zhu, S.H. Chu, J.L. Siau, B.S. Wong, J.S. Armstrong, and P.K. Moore. Hydrogen sulphide: a novel inhibitor of hypochlorous acid-mediated oxidative damage in the brain? *Biochem Biophys Res Commun*, 326(4):794–798, 2005.
- [226] B. Geng, L. Chang, C. Pan, Y. Qi, J. Zhao, Y. Pang, J. Du, and C. Tang. Endogenous hydrogen sulfide regulation of myocardial injury induced by isoproterenol. *Biochem Biophys Res Commun*, 318(3):756–763, 2004.
- [227] T.W. Hart. Some observations concerning the S-nitroso and S-phenylsulphonyl derivatives of L-cysteine and glutathione. *Tetrahedron Letters*, 26(16):2013–2016, 1985.

## References

- [228] J.S. Stamler and M. Feelisch. *Methods in Nitric Oxide Research*, chapter 36 Preparation and Detection of S-Nitrosothiols, 521–539. John Wiley & Sons Ltd, 1996.
- [229] V.B. Kumar, A.E. Bernardo, M.M. Alshaher, M. Buddhiraju, R. Purushothaman, and J.E. Morley. Rapid assay for nitric oxide synthase using thin-layer chromatography. *Anal Biochem*, 269(1):17–20, 1999.
- [230] L.C. Green, D.A. Wagner, J. Glogowski, P.L. Skipper, J.S. Wishnok, and S.R. Tannenbaum. Analysis of nitrate, nitrite, and [<sup>15</sup>N]nitrate in biological fluids. *Anal Biochem*, 126(1):131–138, 1982.
- [231] J.F. Pilichowski, P. Boule, and J.P. Billard. Comportement photochimique du 4-nitrosophenol en solution aqueuse. *Can J Chem*, 73:2143–2147, 1995.
- [232] A. Daiber, M. Mehl, and V. Ullrich. New aspects in the reaction mechanism of phenol with peroxynitrite: the role of phenoxy radicals. *Nitric Oxide*, 2(4): 259–269, 1998.
- [233] M. Kelm, R. Dahmann, D. Wink, and M. Feelisch. The nitric oxide/superoxide assay. Insights into the biological chemistry of the  $\bullet\text{NO}/\text{O}_2^{\bullet-}$  interaction. *J Biol Chem*, 272(15):9922–9932, 1997.
- [234] J.A. Cook, S.Y. Kim, D. Teague, M.C. Krishna, R. Pacelli, J.B. Mitchell, Y. Vodovotz, R.W. Nims, D. Christodoulou, A.M. Miles, M.B. Grisham, and D.A. Wink. Convenient colorimetric and fluorometric assays for S-nitrosothiols. *Anal Biochem*, 238(2):150–158, 1996.
- [235] S. Hoops, S. Sahle, R. Gauges, C. Lee, J. Pahle, N. Simus, M. Singhal, L. Xu, P. Mendes, and U. Kummer. COPASI—a COMplex PATHway SIMulator. *Bioinformatics*, 22(24):3067–3074, 2006.
- [236] R.F. Coburn. Mechanisms of carbon monoxide toxicity. *Prev Med*, 8(3):310–322, 1979.
- [237] H. Lin and J.J. McGrath. Carbon monoxide effects on calcium levels in vascular smooth muscle. *Life Sci*, 43(22):1813–1816, 1988.
- [238] T. Graser, Y.P. Vedernikov, and D.S. Li. Study on the mechanism of carbon monoxide induced endothelium-independent relaxation in porcine coronary artery and vein. *Biomed Biochim Acta*, 49(4):293–296, 1990.
- [239] K.S. Ramos, H. Lin, and J.J. McGrath. Modulation of cyclic guanosine monophosphate levels in cultured aortic smooth muscle cells by carbon monoxide. *Biochem Pharmacol*, 38(8):1368–1370, 1989.
- [240] S.J. McFaul and J.J. McGrath. Studies on the mechanism of carbon monoxide-induced vasodilation in the isolated perfused rat heart. *Toxicol Appl Pharmacol*, 87(3):464–473, 1987.

## References

- [241] J.I. Kaide, F. Zhang, Y. Wei, H. Jiang, C. Yu, W.H. Wang, M. Balazy, N.G. Abraham, and A. Nasjletti. Carbon monoxide of vascular origin attenuates the sensitivity of renal arterial vessels to vasoconstrictors. *J Clin Invest*, 107(9):1163–1171, 2001.
- [242] T. Kyokane, S. Norimizu, H. Taniai, T. Yamaguchi, S. Takeoka, E. Tsuchida, M. Naito, Y. Nimura, Y. Ishimura, and M. Suematsu. Carbon monoxide from heme catabolism protects against hepatobiliary dysfunction in endotoxin-treated rat liver. *Gastroenterology*, 120(5):1227–1240, 2001.
- [243] J.S. Naik, T.L. O’Donoghay, and B.R. Walker. Endogenous carbon monoxide is an endothelial-derived vasodilator factor in the mesenteric circulation. *Am J Physiol Heart Circ Physiol*, 284(3):H838–H845, 2003.
- [244] S.R. Thom, Y.A. Xu, and H. Ischiropoulos. Vascular endothelial cells generate peroxynitrite in response to carbon monoxide exposure. *Chem Res Toxicol*, 10(9):1023–1031, 1997.
- [245] T. Malinski and Z. Taha. Nitric oxide release from a single cell measured in situ by a porphyrinic-based microsensor. *Nature*, 358(6388):676–678, 1992.
- [246] S. Mochizuki, N. Himi, T. Miyasaka, H. Nakamoto, M. Takemoto, K. Hirano, K. Tsujioka, Y. Ogasawara, and F. Kajiya. Evaluation of basic performance and applicability of a newly developed in vivo nitric oxide sensor. *Physiol Meas*, 23(2):261–268, 2002.
- [247] R.K. Porter. Mammalian mitochondrial inner membrane cationic and neutral amino acid carriers. *Biochim Biophys Acta*, 1459(2-3):356–362, 2000.
- [248] E.W. Ades, F.J. Candal, R.A. Swerlick, V.G. George, S. Summers, D.C. Bosse, and T.J. Lawley. HMEC-1: establishment of an immortalized human microvascular endothelial cell line. *J Invest Dermatol*, 99(6):683–690, 1992.
- [249] S. Dimmeler and B. Brüne. Nitric oxide preferentially stimulates auto-ADP-ribosylation of glyceraldehyde-3-phosphate dehydrogenase compared to alcohol or lactate dehydrogenase. *FEBS Lett*, 315(1):21–24, 1993.
- [250] D. Gergel and A.I. Cederbaum. Inhibition of the catalytic activity of alcohol dehydrogenase by nitric oxide is associated with S nitrosylation and the release of zinc. *Biochemistry*, 35(50):16186–16194, 1996.
- [251] D. Frein. Nitrating and nitrosating intermediates in the system nitrogen monoxide / superoxide. Diplomarbeit, Universität Konstanz, 2002.
- [252] M.H. Zou, C. Shi, and R.A. Cohen. Oxidation of the zinc-thiolate complex and uncoupling of endothelial nitric oxide synthase by peroxynitrite. *J Clin Invest*, 109(6):817–826, 2002.
- [253] G. Merenyi and J. Lind. Free radical formation in the peroxynitrous acid (ONOOH)/peroxynitrite (ONOO<sup>-</sup>) system. *Chem Res Toxicol*, 11(4):243–246, 1998.

## References

- [254] S. Pfeiffer, A.C. Gorren, K. Schmidt, E.R. Werner, B. Hansert, D.S. Bohle, and B. Mayer. Metabolic fate of peroxynitrite in aqueous solution. Reaction with nitric oxide and pH-dependent decomposition to nitrite and oxygen in a 2:1 stoichiometry. *J Biol Chem*, 272(6):3465–3470, 1997.
- [255] S. Goldstein, G. Czapski, J. Lind, and G. Merenyi. Effect of NO on the decomposition of peroxynitrite: reaction of  $N_2O_3$  with  $ONOO^-$ . *Chem Res Toxicol*, 12(2):132–136, 1999.
- [256] R.M. Uppu, J.N. Lemercier, G.L. Squadrito, H. Zhang, R.M. Bolzan, and W.A. Pryor. Nitrosation by peroxynitrite: use of phenol as a probe. *Arch Biochem Biophys*, 358(1):1–16, 1998.
- [257] J. Escribano, F. Garcia-Canovas, and F. Garcia-Carmona. A kinetic study of hypoxanthine oxidation by milk xanthine oxidase. *Biochem J*, 254(3):829–833, 1988.
- [258] H. Zhang, G.L. Squadrito, R.M. Uppu, J.N. Lemercier, R. Cueto, and W.A. Pryor. Inhibition of peroxynitrite-mediated oxidation of glutathione by carbon dioxide. *Arch Biochem Biophys*, 339(1):183–189, 1997.
- [259] J.L. Caulfield, S.P. Singh, J.S. Wishnok, W.M. Deen, and S.R. Tannenbaum. Bicarbonate inhibits N-nitrosation in oxygenated nitric oxide solutions. *J Biol Chem*, 271(42):25859–25863, 1996.
- [260] D. Jourdeuil, K.M. Miranda, S.M. Kim, M.G. Espey, Y. Vodovotz, S. Laroux, C.T. Mai, A.M. Miles, M.B. Grisham, and D.A. Wink. The oxidative and nitrosative chemistry of the nitric oxide/superoxide reaction in the presence of bicarbonate. *Arch Biochem Biophys*, 365(1):92–100, 1999.
- [261] A. Daiber, M. Bachschmid, C. Kavakli, D. Frein, M. Wendt, V. Ullrich, and T. Munzel. A new pitfall in detecting biological end products of nitric oxide-nitration, nitros(yl)ation and nitrite/nitrate artefacts during freezing. *Nitric Oxide*, 9(1):44–52, 2003.
- [262] A. Daiber, M. Bachschmid, D. Frein, and V. Ullrich. Reply to "Trouble with the analysis of nitrite, nitrate, S-nitrosothiols, and 3-nitrotyrosine: freezing-induced artifacts". *Nitric Oxide*, 11(3):214–215, 2004.
- [263] G. Gomez, M.J. Pikal, and N. Rodriguez-Hornedo. Effect of initial buffer composition on pH changes during far-from-equilibrium freezing of sodium phosphate buffer solutions. *Pharm Res*, 18(1):90–97, 2001.
- [264] L. Petzold. Automatic selection of methods for solving stiff and nonstiff systems of ordinary differential equations. *SIAM J Sci Stat Comput*, 4:136–148, 1983.
- [265] T. Logager and K. Sehested. Formation and decay of peroxynitric acid: a pulse radiolysis study. *J Phys Chem*, 97(39):10047–10052, 1993.
- [266] W.A. Pryor and G.L. Squadrito. The chemistry of peroxynitrite: a product from the reaction of nitric oxide with superoxide. *Am J Physiol*, 268(5 Pt 1):L699–L722, 1995.

## References

- [267] M. Kirsch, M. Lehnig, H.G. Korth, R. Sustmann, and H. de Groot. Inhibition of peroxyxynitrite-induced nitration of tyrosine by glutathione in the presence of carbon dioxide through both radical repair and peroxyxynitrate formation. *Chemistry*, 7(15):3313–3320, 2001.
- [268] A.B. Ross, W.G. Mallard, W.P. Helman, G.V. Buxton, R.E. Huie, and P. Neta. *NDRL/NIST Solution Kinetics Database ver. 3*. Notre Dame Radiation Laboratory, Gaithersburg, MD: Notre Dame, 1998.
- [269] O.V. Gerasimov and S.V. Lyamar. The Yield of Hydroxyl Radical from the Decomposition of Peroxyxynitrous Acid. *Inorg Chem*, 38(19):4317–4321, 1999.
- [270] G.R. Hodges and K.U. Ingold. Cage-Escape of Geminate Radical Pairs Can Produce Peroxyxynitrate from Peroxyxynitrite under a Wide Variety of Experimental Conditions. *J Am Chem Soc*, 121(46):10695–10701, 1999.
- [271] G. Merenyi, J. Lind, S. Goldstein, and G. Czapski. Mechanism and Thermochemistry of Peroxyxynitrite Decomposition in Water. *J Phys Chem A*, 103(29):5685–5691, 1999.
- [272] G.V. Buxton, C.L. Greenstock, W. Phillip, and A.B. Ross. Critical review of rate constants for reactions of hydrated electrons, hydrogen atoms and hydroxyl radicals in aqueous solution. *J Phys Chem Ref Data*, 17:513–886, 1988.
- [273] S. Goldstein, A. Saha, S.V. Lyamar, and G. Czapski. Oxidation of Peroxyxynitrite by Inorganic Radicals: A Pulse Radiolysis Study. *J Am Chem Soc*, 120(22):5549–5554, 1998.
- [274] M. Grätzel, S. Taniguchi, and A. Henglein. Pulse radiolytic investigation of NO oxidation and equilibrium  $\text{N}_2\text{O}_3$   $\text{NO}$   $\text{NO}_2$  in aqueous solution. *Ber Bunsenges Phys Chem*, 74:488–492, 1970.
- [275] A. Treinin and E. Hayon. Absorption spectra and reaction kinetics of  $\text{NO}_2$ ,  $\text{N}_2\text{O}_3$ , and  $\text{N}_2\text{O}_4$  in aqueous solution. *J Am Chem Soc*, 92(20):5821–5828, 1970.
- [276] J.W. Coddington, J.K. Hurst, and S.V. Lyamar. Hydroxyl Radical Formation During Peroxyxynitrous Acid Decomposition. *J Am Chem Soc*, 121(11):2438–2443, 1999.
- [277] S. Goldstein, G. Czapski, J. Lind, and G. Merenyi. Mechanism of Decomposition of Peroxyxynitric Ion ( $\text{O}_2\text{NOO}^-$ ): Evidence for the Formation of  $\text{O}_2^{\bullet-}$  and  $\bullet\text{NO}_2$  Radicals. *Inorg Chem*, 37(16):3943–3947, 1998.
- [278] E. Ford, M.N. Hughes, and P. Wardman. Kinetics of the reactions of nitrogen dioxide with glutathione, cysteine, and uric acid at physiological pH. *Free Radic Biol Med*, 32(12):1314–1323, 2002.
- [279] D.L. Rabenstein. Nuclear magnetic resonance studies of the acid-base chemistry of amino acids and peptides. I. Microscopic ionization constants of glutathione and methylmercury-complexed glutathione. *J Am Chem Soc*, 95:2797–2803, 1973.

## References

- [280] G.D. Fasman, editor. *Handbook of Biochemistry and Molecular Biology, Physical and Chemical Data*, volume 1. CRC Press, Boston, 3rd edition, 1976.
- [281] R. Radi, J.S. Beckman, K.M. Bush, and B.A. Freeman. Peroxynitrite oxidation of sulfhydryls. The cytotoxic potential of superoxide and nitric oxide. *J Biol Chem*, 266(7):4244–4250, 1991.
- [282] W.H. Koppenol, J.J. Moreno, W.A. Pryor, H. Ischiropoulos, and J.S. Beckman. Peroxynitrite, a cloaked oxidant formed by nitric oxide and superoxide. *Chem Res Toxicol*, 5(6):834–842, 1992.
- [283] M. Balazy, P.M. Kaminski, K. Mao, J. Tan, and M.S. Wolin. S-Nitroglutathione, a product of the reaction between peroxynitrite and glutathione that generates nitric oxide. *J Biol Chem*, 273(48):32009–32015, 1998.
- [284] C. Schöneich. Kinetics of thiol reactions. *Methods Enzymol*, 251:45–55, 1995.
- [285] S.P. Mezyk. Rate Constant Determination for the Reaction of Hydroxyl and Glutathione Thiyl Radicals with Glutathione in Aqueous Solution. *J Phys Chem*, 100(21):8861–8866, 1996.
- [286] M. Tamba, G. Simone, and M. Quintiliani. Interactions of thiyl free radicals with oxygen: a pulse radiolysis study. *Int J Radiat Biol Relat Stud Phys Chem Med*, 50(4):595–600, 1986.
- [287] C.M. Jones, A. Lawrence, P. Wardman, and M.J. Burkitt. Electron paramagnetic resonance spin trapping investigation into the kinetics of glutathione oxidation by the superoxide radical: re-evaluation of the rate constant. *Free Radic Biol Med*, 32(10):982–990, 2002.
- [288] B. Halliwell and J.M.C. Gutteridge. *Antioxidant defences. Free radicals in biology and medicine.*, 105–245. Oxford Univ. Press, Oxford, 1999.
- [289] L.Y. Chang, J.W. Slot, H.J. Geuze, and J.D. Crapo. Molecular immunocytochemistry of the CuZn superoxide dismutase in rat hepatocytes. *J Cell Biol*, 107(6 Pt 1):2169–2179, 1988.
- [290] D. Klug-Roth, I. Fridovich, and J. Rabani. Pulse radiolytic investigations of superoxide catalyzed disproportionation. Mechanism for bovine superoxide dismutase. *J Am Chem Soc*, 95(9):2786–2790, 1973.
- [291] B. Lassegue and R.E. Clempus. Vascular NAD(P)H oxidases: specific features, expression, and regulation. *Am J Physiol Regul Integr Comp Physiol*, 285(2):R277–R297, 2003.
- [292] P.S. Brookes, Y. Yoon, J.L. Robotham, M.W. Anders, and S.S. Sheu. Calcium, ATP, and ROS: a mitochondrial love-hate triangle. *Am J Physiol Cell Physiol*, 287(4):C817–C833, 2004.
- [293] M.D. Brand, C. Affourtit, T.C. Esteves, K. Green, A.J. Lambert, S. Miwa, J.L. Pakay, and N. Parker. Mitochondrial superoxide: production, biological effects, and activation of uncoupling proteins. *Free Radic Biol Med*, 37(6):755–767, 2004.

## References

- [294] C.C. Wei, Z.Q. Wang, D. Durra, C. Hemann, R. Hille, E.D. Garcin, E.D. Getzoff, and D.J. Stuehr. The three nitric-oxide synthases differ in their kinetics of tetrahydrobiopterin radical formation, heme-dioxy reduction, and arginine hydroxylation. *J Biol Chem*, 280(10):8929–8935, 2005.
- [295] R. Hille and T. Nishino. Flavoprotein structure and mechanism. 4. Xanthine oxidase and xanthine dehydrogenase. *FASEB J*, 9(11):995–1003, 1995.
- [296] C. Enroth, B.T. Eger, K. Okamoto, T. Nishino, T. Nishino, and E.F. Pai. Crystal structures of bovine milk xanthine dehydrogenase and xanthine oxidase: structure-based mechanism of conversion. *Proc Natl Acad Sci U S A*, 97(20):10723–10728, 2000.
- [297] R. Matsui, S. Xu, K.A. Maitland, R. Mastroianni, J.A. Leopold, D.E. Handy, J. Loscalzo, and R.A. Cohen. Glucose-6-phosphate dehydrogenase deficiency decreases vascular superoxide and atherosclerotic lesions in apolipoprotein E<sup>-/-</sup> mice. *Arterioscler Thromb Vasc Biol*, 26(4):910–916, 2006.
- [298] C.J. Zuurbier, O. Eerbeek, P.T. Goedhart, E.A. Struys, N.M. Verhoeven, C. Jakobs, and C. Ince. Inhibition of the pentose phosphate pathway decreases ischemia-reperfusion-induced creatine kinase release in the heart. *Cardiovasc Res*, 62(1):145–153, 2004.
- [299] E.S. Yang, C. Richter, J.S. Chun, T.L. Huh, S.S. Kang, and J.W. Park. Inactivation of NADP<sup>+</sup>-dependent isocitrate dehydrogenase by nitric oxide. *Free Radic Biol Med*, 33(7):927–937, 2002.
- [300] S.H. Jo, M.K. Son, H.J. Koh, S.M. Lee, I.H. Song, Y.O. Kim, Y.S. Lee, K.S. Jeong, W.B. Kim, J.W. Park, B.J. Song, and T.L. Huh. Control of mitochondrial redox balance and cellular defense against oxidative damage by mitochondrial NADP<sup>+</sup>-dependent isocitrate dehydrogenase. *J Biol Chem*, 276(19):16168–16176, 2001.
- [301] S.M. Lee, H.J. Koh, D.C. Park, B.J. Song, T.L. Huh, and J.W. Park. Cytosolic NADP<sup>+</sup>-dependent isocitrate dehydrogenase status modulates oxidative damage to cells. *Free Radic Biol Med*, 32(11):1185–1196, 2002.
- [302] Z. Zhang, K. Apse, J. Pang, and R.C. Stanton. High glucose inhibits glucose-6-phosphate dehydrogenase via cAMP in aortic endothelial cells. *J Biol Chem*, 275(51):40042–40047, 2000.
- [303] T. Nishikawa, D. Edelstein, X.L. Du, S. Yamagishi, T. Matsumura, Y. Kaneda, M.A. Yorek, D. Beebe, P.J. Oates, H.P. Hammes, I. Giardino, and M. Brownlee. Normalizing mitochondrial superoxide production blocks three pathways of hyperglycaemic damage. *Nature*, 404(6779):787–790, 2000.
- [304] J.L. Evans, I.D. Goldfine, B.A. Maddux, and G.M. Grodsky. Oxidative stress and stress-activated signaling pathways: a unifying hypothesis of type 2 diabetes. *Endocr Rev*, 23(5):599–622, 2002.

## References

- [305] S.S. Chung, E.C. Ho, K.S. Lam, and S.K. Chung. Contribution of polyol pathway to diabetes-induced oxidative stress. *J Am Soc Nephrol*, 14(8 Suppl 3):S233–S236, 2003.
- [306] M.C. Van Zandt, M.L. Jones, D.E. Gunn, L.S. Geraci, J.H. Jones, D.R. Sawicki, J. Sredy, J.L. Jacot, A.T. Diciocco, T. Petrova, A. Mitschler, and A.D. Podjarny. Discovery of 3-[(4,5,7-trifluorobenzothiazol-2-yl)methyl]indole-N-acetic acid (lidorestat) and congeners as highly potent and selective inhibitors of aldose reductase for treatment of chronic diabetic complications. *J Med Chem*, 48(9):3141–3152, 2005.
- [307] I.S. Kil and J.W. Park. Regulation of mitochondrial NADP<sup>+</sup>-dependent isocitrate dehydrogenase activity by glutathionylation. *J Biol Chem*, 280(11):10846–10854, 2005.
- [308] C. Johansson, C.H. Lillig, and A. Holmgren. Human mitochondrial glutaredoxin reduces S-glutathionylated proteins with high affinity accepting electrons from either glutathione or thioredoxin reductase. *J Biol Chem*, 279(9):7537–7543, 2004.
- [309] A.R. Evans, M. Limp-Foster, and M.R. Kelley. Going APE over ref-1. *Mutat Res*, 461(2):83–108, 2000.
- [310] P. Angkeow, S.S. Deshpande, B. Qi, Y.X. Liu, Y.C. Park, B.H. Jeon, M. Ozaki, and K. Irani. Redox factor-1: an extra-nuclear role in the regulation of endothelial oxidative stress and apoptosis. *Cell Death Differ*, 9(7):717–725, 2002.
- [311] M.M. Hsieh, V. Hegde, M.R. Kelley, and W.A. Deutsch. Activation of APE/Ref-1 redox activity is mediated by reactive oxygen species and PKC phosphorylation. *Nucleic Acids Res*, 29(14):3116–3122, 2001.
- [312] H. Hentze, M. Latta, G. Kunstle, R. Lucas, and A. Wendel. Redox control of hepatic cell death. *Toxicol Lett*, 139(2-3):111–118, 2003.